Met Office

Met Office Intercomparison of Vaisala RS92 and RS41 Radiosondes

Camborne, United Kingdom, 7th – 19th November 2013

David Edwards, Graeme Anderson, Tim Oakley, Peter Gault

12/02/14

Vaisala staff launching a 4 radiosonde rig used in this report from the rotating balloon shed at the Met Office site in Camborne.

Contents

Glossary

Accuracy: Measure of closeness of the measured value of a variable to the true value of that variable.

ASCII: American Standard Code for Information Interchange data file format.

Bias: Consistently observed difference in measured value of the same variable by separate systems.

BUFR: Binary Universal Form for the Representation of meteorological data file format.

DigiCORA: Vaisala radiosonde software

GPS: Global Positioning System, US-developed global navigation satellite system.

GUAN: GCOS (Global Climate Observing System) Upper Air Network.

GC25: Vaisala ground check set for RS92 radiosonde.

MW41: Vaisala sounding system.

NWP: Numerical Weather Prediction

Precision: Measure of reproducibility of measured variable under repeated tests.

RI41: Vaisala ground check device for RS41 radiosonde.

RS41: Newly developed Vaisala radiosonde model.

RS41-SG: Version of the RS41 radiosonde model using 400 MHz transmission and GPS wind finding.

RS92: Established Vaisala radiosonde model.

RS92-SGP: Version of the RS92 radiosonde using 400 MHz transmission, GPS wind finding and pressure sensor.

RS92-SGPL: As RS92-SGP with lithium battery.

RSK: Software package for analyzing radiosonde data.

SPS311: Vaisala sounding processing subsystem.

SD: Standard deviation. Also referred to as σ (sigma).

Standard deviation: A measure of the dispersion of a dataset from the mean.

TEMP: Upper air data file format.

WLIST: RSKOMP software module used to import ASCII data to RSKOMP database

WMO: World Meteorological Organization.

WSTAT: RSKOMP software module used for statistical analysis of RSKOMP database

WVIEW: RSKOMP software module used for visual analysis of RSKOMP database

Executive Summary

30 trial ascents were launched during November 2013 from the Met Office radiosonde station in Camborne to compare the performance of RS92 and RS41 radiosondes. Each ascent used 2x RS92 and 2x RS41 radiosondes and was launched by Vaisala staff under Met Office supervision. The RS92 software and model versions were the same as those used in the *WMO Intercomparison of high quality radiosonde systems, Yangjiang, China, 2010*.

All hardware and consumables apart from helium were provided by Vaisala. The design of the trial was agreed by both parties and follows the methodology of WMO intercomparisons (see *Guide to Meteorological Instruments and Methods of Observation).* The Met Office was contracted by Vaisala to provide an independent report from the data produced by the trial. The report and all statistical analysis were completed by Met Office staff.

In previous intercomparisons, synchronising the times of each radiosonde during each ascent had to be completed manually. In this trial, Vaisala used the GPS times for each radiosonde to synchronise all 4 datasets. This is a novel approach and reduces the impact of variability due to time synchronisation errors.

Throughout the trial at Camborne, the RS41 radiosonde performed very similarly to the RS92, but several key differences and improvements were observed.

No significant consistent temperature differences were observed between the RS41 and RS92. The temperature observations of the RS41 are more precise and less susceptible to the problems caused by moisture contamination when exiting cloud than the RS92, including wet-bulb effects. In the wet-bulb events observed during this trial, the RS41 radiosondes demonstrated a significant improvement in performance relative to the RS92.

Some slight consistent differences in humidity were observed between the RS41 and RS92. The humidity measurements of the RS41 are more precise and should be less prone to moisture contamination and solar radiation correction errors than the RS92.

The GPS derived wind speeds and directions calculated by the RS41 are consistent with the performance of the RS92.

The GPS derived heights observed by the RS41 are consistent with the performance of the RS92, but demonstrate greater precision.

Relative to pressure derived heights observed by the RS92, GPS derived heights from both the RS92 and RS41 demonstrate significantly improved precision and potentially greater accuracy. This will have an impact on standard TEMP and BUFR output data files if GPS derived altitudes are used, as pressure is then also calculated from GPS derived altitudes.

Important:

As there was no scientific reference system used in this intercomparison, it was not possible to know which radiosonde model made the most accurate measurements. However, the use of two of each type of radiosonde allowed analysis of their flight-by-flight precision – the consistency of measurement of each radiosonde. Also, the impact of known effects on radiosonde data including those listed below enabled an assessment of relative data quality between the two radiosonde models:

- Evaporative cooling of moisture contamination from temperature sensors (referred to as 'wet-bulbing' or 'the wet-bulb effect')
- Sensor response time changes with temperature
- Contamination of humidity sensors by moisture

Organisation of the intercomparison

Duration, location and experimental design

30 trial ascents were completed between the 7th and 19th of November 2013 at the Met Office radiosonde station at Camborne, England. This site has the WMO station number 03808 and is part of the GUAN network. Met Office operational equipment was not used in the trial, as the radiosonde systems were provided by, set up and staffed by Vaisala. Vaisala also constructed and launched each rig. At least one member of Met Office staff was present throughout the trial period.

20 daytime and 10 night-time trial ascents were completed, and each ascent carried 2 of each type of radiosonde attached to a cross-shaped rig with a parachute and unwinder/dereeler, (it will be called an 'unwinder' in this report). Helium gas was used to lift the balloons to achieve an ascent rate of 6 – 6.5m/s per flight.

Daytime ascents were launched at the times of approximately 0915 and 1330 UTC with the night-time launches at approximately 1900-2130 UTC in order to minimise variation due to solar radiation effects during the day and eliminate them at night-time. As Camborne is an operational radiosonde station, the times were also chosen to minimise the risk of interference from the Met Office operational scheduled radiosonde launches at 1115 and 2315 UTC.

Flight metadata

Flight number	Series	Date	Oktas of C_L or C_M present	Low cloud type	Medium cloud type	High cloud type	Present weather
5	Day	07/11/2013					State of sky on the whole unchanged
6	Day	07/11/2013	7	Cu & Sc	Ac	Ci	State of sky on the whole unchanged
7	Night	07/11/2013	4	Cu & Sc	Ac	None	Shower(s) of rain during the preceding hour but not at the time of observation
8	Night	07/11/2013	1	Sc	None	None	State of sky on the whole unchanged
9	Day	08/11/2013	8	Cb	\	\	Rain, not freezing, continuous, slight at time of ob.
10	Day	08/11/2013	7	Sc	\	Ci	Rain shower(s), slight
11	Night	08/11/2013	3	Sc	None	None	State of sky on the whole unchanged
12	Day	11/11/2013	8	St	\	\	Drizzle, not freezing, continuous, slight at time of ob.
13	Day	11/11/2013	8	St	\	\	Fog or ice fog, sky visible, has begun or has become thicker during preceding hour
14	Night	11/11/2013	8	St	\	\	Fog or ice fog, sky visible, no appreciable change during the past hour
15	Night	11/11/2013	8	St	\	\	Drizzle, not freezing, intermittent, slight at time of ob.
16	Day	12/11/2013	1	Sc	Ac	Ci	Cloud generally dissolving or becoming less developed
17	Day	12/11/2013	2	Sc	Ac / Ac & Ns	Ci	State of sky on the whole unchanged
18	Night	12/11/2013	2	Cu & Sc	\	\	State of sky on the whole unchanged
19	Day	13/11/2013	1	St	None	Ci	State of sky on the whole unchanged
20	Day	13/11/2013	5	Sc	Ac	Ci	State of sky on the whole unchanged
21	Night	13/11/2013	8	Sc	\	\	Rain, not freezing, intermittent, slight at time of ob.
22	Night	13/11/2013	8	Sc	\	\	Rain (not freezing), not falling as showers, during the preceding hour but not at the time of observation
23	Day	14/11/2013	7	Sc	\	\	Shower(s) of rain during the preceding hour but not at the time of observation
25	Night	14/11/2013	7	St	\	Ci	State of sky on the whole unchanged
26	Day	15/11/2013	8	Sc	None	None	State of sky on the whole unchanged
27	Day	15/11/2013	8	Sc	\	\	State of sky on the whole unchanged
28	Night	15/11/2013	7	Sc	\	\	State of sky on the whole unchanged
29	Day	16/11/2013	7	Sc	\	\	State of sky on the whole unchanged
30	Day	16/11/2013	8	Sc	\	\	State of sky on the whole unchanged
31	Day	17/11/2013	8	Sc	\	\	Cloud development not observed or not observable
32	Day	18/11/2013	5	Sc	Ac / Ac & Ns	\	State of sky on the whole unchanged
33	Day	18/11/2013	8	St	\	\	Rain and drizzle, moderate or heavy
34	Day	19/11/2013	4	St	None	None	Precipitation within sight, reaching the ground or the surface of the sea, but distant, i.e. > 5 km from the station
35	Day	19/11/2013	4	Sc	None	Ci	Precipitation within sight, reaching the ground or the surface of the sea, but distant, i.e. > 5 km from the station

Table 1: Flight metadata taken from observations at time of launch. Not included: Test flights 1-4 and flight 24 which failed on launch due to a collision between one radiosonde and the rig.

Description of the systems used

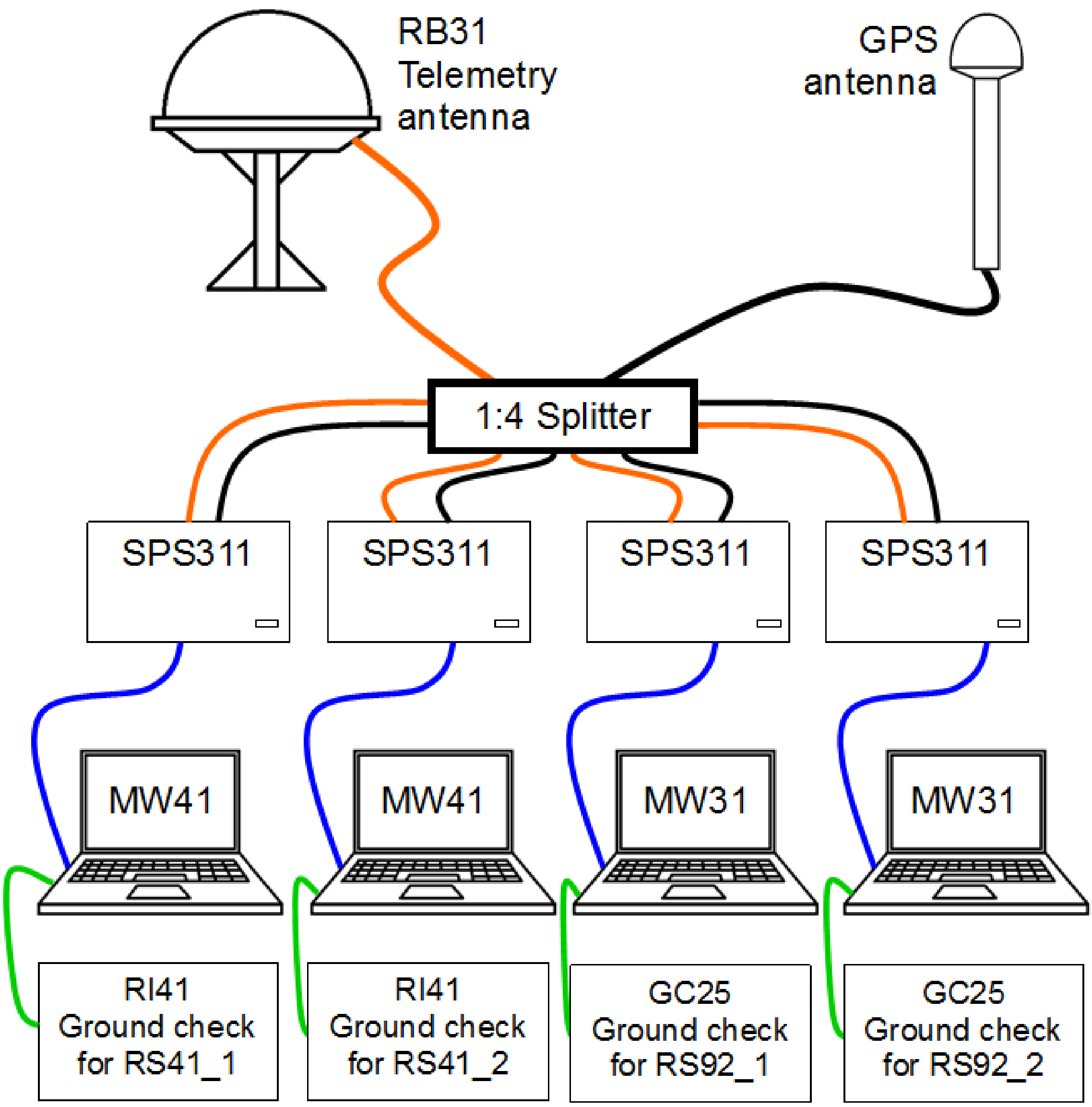

Figure 1 - System diagram showing hardware configuration for all 4 systems being used.

Radiosonde hardware

RS92-SGP

All ascents were completed using RS92-SGPL radiosondes.

Temperature

The RS92 uses a small capacitive wire sensor mounted near the end of the sensor boom between two support struts. The sensor boom is constructed of a thin flexible material coated in a layer of aluminium with an additional hydrophobic coating over the temperature end. The hydrophobic coating is designed to reduce contamination from water when in flight.

Figure 2 – Photograph of Vaisala RS92-SPG series radiosonde.

Humidity

The RS92 uses dual capacitive humidity sensors. Each humidity sensor also contains a heating element. The sensors are swapped periodically when in use and the sensor not in use is heated to remove moisture contamination. This continues until a certain set of temperature or pressure criteria are met. The observed humidity values are corrected for solar radiation in the software based on calculated solar angle.

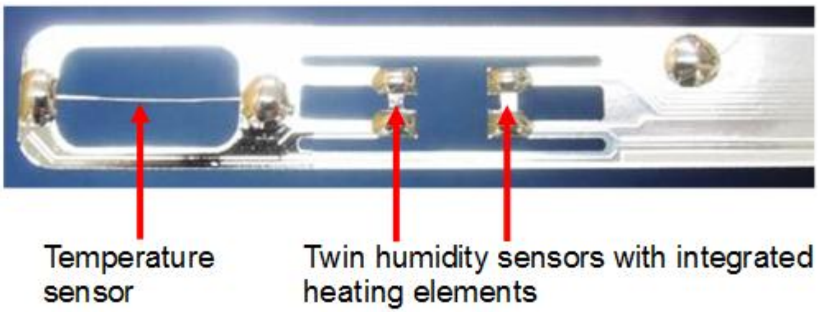

Figure 3 – Photograph demonstrating Vaisala RS92-SGP sensor boom design.

Pressure

The RS92 radiosondes supplied were fitted with silicon wafer pressure sensors, but these were not used in the trial to determine altitude, which was instead derived from differential GPS. However, additional analysis was completed to compare the performance of GPS and pressure sensor derived altitudes, and this analysis is included in this report.

Wind and location

The RS92 uses differential GPS to calculate the radiosonde position relative to the ground station. Wind components are calculated from the GPS signals. The antenna has an external helix design.

Hardware

The hardware used was two GC25 ground check systems and SPS311 radiosonde receivers connected to the shared RB31 and GPS antennas. Due to the different ground check systems, the datasets cannot be combined and are therefore referred to as RS92_1 and RS92_2 in the analysis.

The GC25 ground check allowed the radiosonde temperature sensor to be checked against a calibrated Pt100 sensor. The humidity sensors are first heated up remove any chemical or moisture contamination before they are checked against a 0% humidity environment generated using desiccant. The GC25 is used to apply corrections to the radiosonde. The temperature module requires periodic calibration to ensure that accurate corrections are being applied to the radiosonde. However, even when calibrated, the temperatures observed by these sensors can differ slightly. This can also cause systematic differences between radiosonde systems.

RS41-SG

All ascents were completed using RS41-SG radiosondes.

Figure 4 – Photograph of Vaisala RS41-SG radiosonde.

Temperature

The RS41 uses a small platinum resistive wire sensor mounted near the end of the sensor boom on one side. It replaces part of the support structure. The sensor boom itself is a thin flexible material, coated in a layer of aluminium with a hydrophobic coating to reduce contamination from water when in flight.

Humidity

The RS41 uses a capacitive humidity sensor with an integrated resistive temperature sensor and heating element for active de-icing. The integrated temperature sensor is used to calculate the humidity values with respect to the actual temperature of the sensor. This will account for heating from the element and solar radiation, eliminating the need for a separate solar radiation correction.

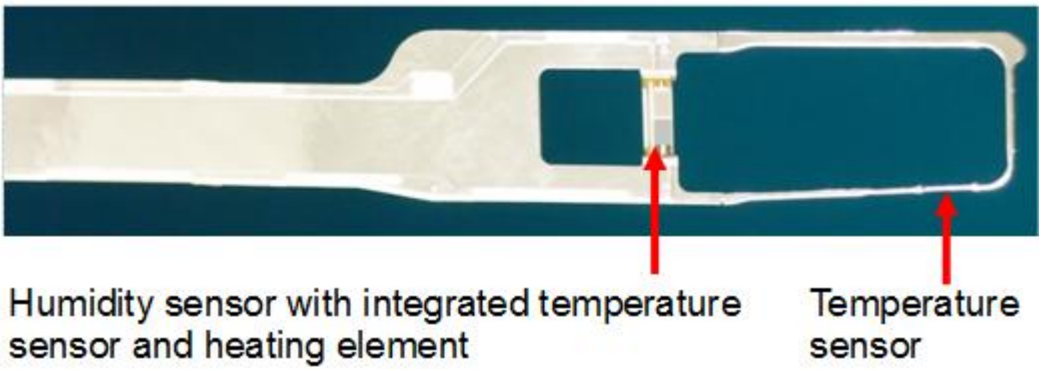

Figure 5 – Photograph demonstrating of Vaisala RS41-SG sensor boom design.

Pressure

The RS41 model supplied did not have a pressure sensor, so pressure could not be used to determine altitude. Altitude was derived from differential GPS. A model with an integrated pressure sensor will be available.

Wind and location

The RS92 uses differential GPS to calculate the radiosonde position relative to the ground station. Wind components are calculated from the GPS signals. The antenna is internal and integrated into the main circuit board of the radiosonde.

Hardware

The hardware used was two RI41 ground check systems and SPS311 radiosonde receivers connected to the shared RB31 and GPS antennas. Due to the different ground check systems used for the RS92 radiosondes, the 2 RS41 systems were also kept separate and are referred to as RS41_1 and RS41_2 in the analysis.

The RI41 ground check enables the radiosonde temperature sensor to be checked for faults and compared to the temperature sensor embedded in the humidity sensor. The humidity sensor is checked and corrected using its internal heating element to generate a 0% humidity environment at the sensor. This also removes any chemical contamination. The RI41 is not used to apply any corrections to the radiosondes. It is only used to check that the radiosonde sensors are working correctly, and that the measured values are within acceptable limits.

Procedures

Radio frequency

Radio frequencies within the 401-406 MHz band were used for this trial. The frequencies were selected to avoid frequencies used at Camborne operationally or at other nearby stations. The launch times were chosen to minimise interference from the operational radiosonde ascents at Camborne. There was some interference identified in the test flights which resulted in periods of missing data. As a result, this interference was studied and suitable frequencies were chosen to avoid this known interference. No similar periods of missing data were seen during the 30 flights during the trial.

Rig design and launch

The rigs were designed by Vaisala. They consisted of a central 8 cm x 8 cm square mounting point. To this, 4 wooden rods (95 cm long) with a rounded rectangular profile (1.5 x 1.0 cm) were attached by small screws in an offset arrangement.

The radiosondes were hung 3 cm from the end of each rod. The total horizontal distance between radiosonde mounting points of approximately 179 cm and the diagonal distance between mounting points was approximately 126.7 cm.

The rig was supported by a central string attached to the unwinder, and support strings from approximately 50cm above the rig to each of the radiosonde mounting points.

Each radiosonde was tied to the radiosonde mounting points using the string normally used to attach it to its own unwinder. The knots were secured with reinforced clear tape.

The length of string between the top of the radiosonde mounting boom and rig was chosen to make the distance between the radiosonde sensor booms and the rig approximately equal for the RS92 and RS41 radiosondes. The similar radiosondes were mounted opposite each other in order to balance the rig.

Totex TX1500 (1500g weight) balloons were used for all ascents.

Totex 160V-05 parachutes were used to minimise the chance of damage upon descent.

Standard RS92 or RS41 unwinders are not suitable for multi-radiosonde launches so were not used in this trial. Graw UW1 unwinders were used to give a steady and reliable string release after launch for these heavier rigs.

The conditions throughout the trial were variable and often windy. This sometimes made launches difficult. The launch temperatures averaged 9.8^{o}C with an average wind speed at launch of 5.3m/s and a maximum of 10.8m/s. Wind directions during the trial were variable, but the rotating balloon shed at Camborne made launches easier. 2 or 3 Vaisala staff were used to launch each balloon and rig.

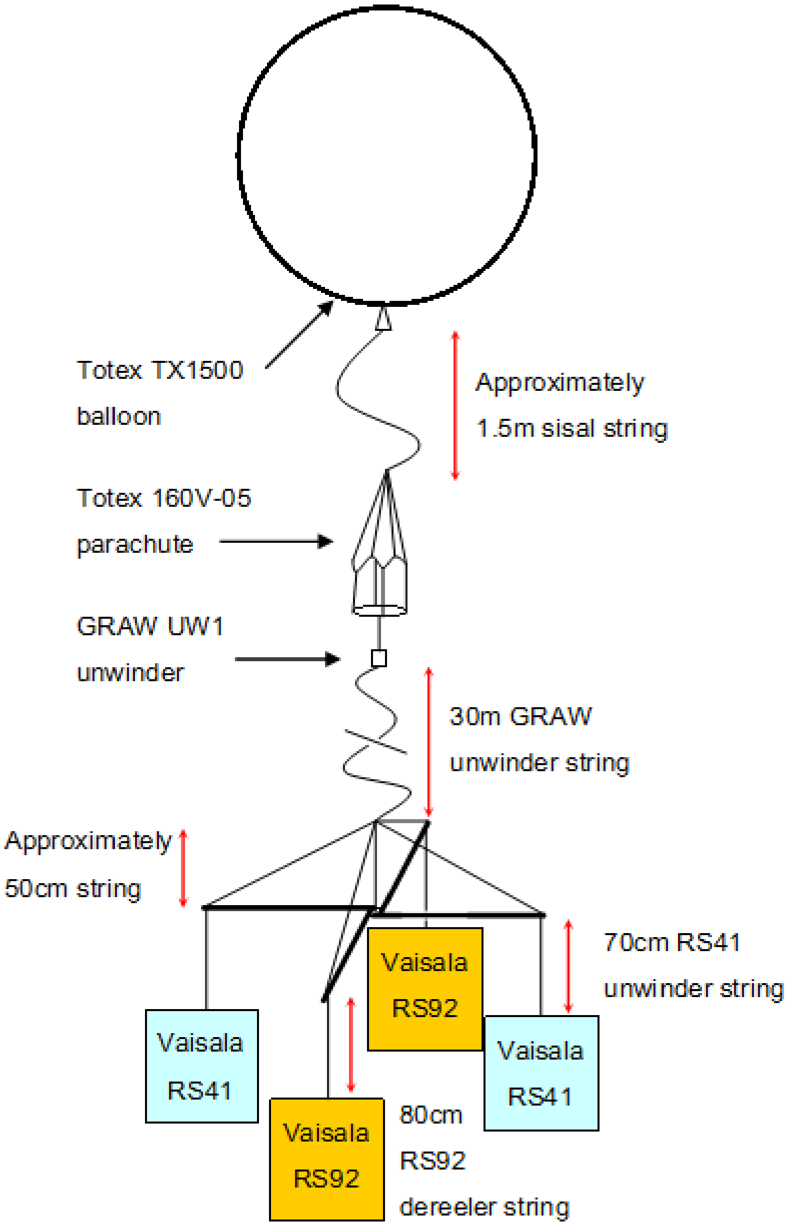

Figure 6 - Example of the balloon train with rig supporting Vaisala RS92 and Vaisala RS41 radiosondes.

Balloon performance

Across all 30 flights, the average ascent rate was 6.3m/s to 12000m. This is within the desired range of ascent rates required by Vaisala to ensure a correct rate of airflow over the sensors. It is also within the typical ascent rates specified in the WMO *Guide to Meteorological Instruments and Methods of Observation.* The average burst height for the 30 flights in this intercomparison was 31810m, with an average first tropopause height of 11315m. This data was taken from the results reported by the RS92_1 system, which is arbitrarily regarded as the reference system throughout this report.

Following 4 test flights, the trials began on flight 5. Flight 24 failed on launch because of a collision between a sonde and the rig in very windy conditions.

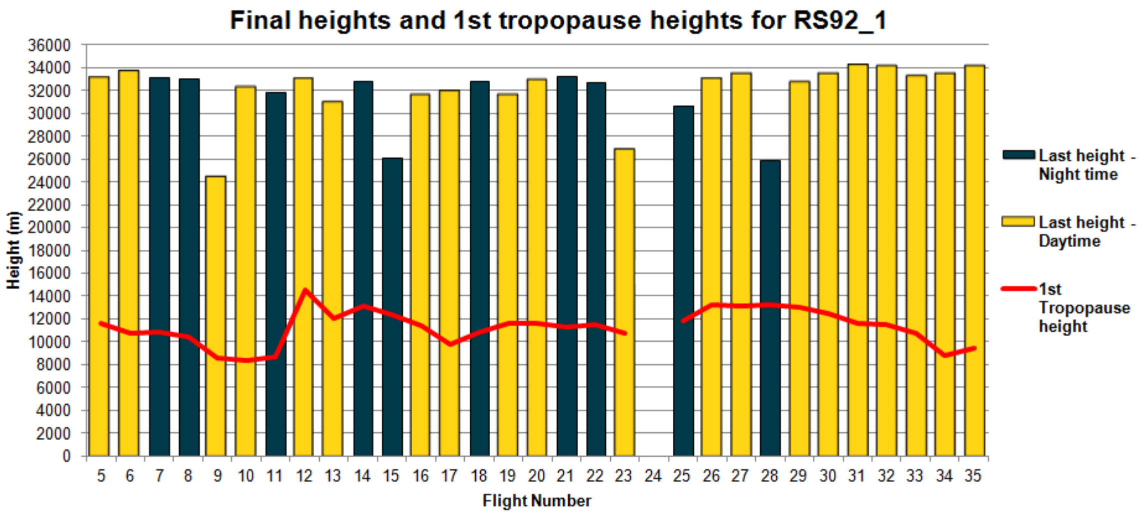

Figure 7 - Balloon performance showing final height observed by system RS92_2.

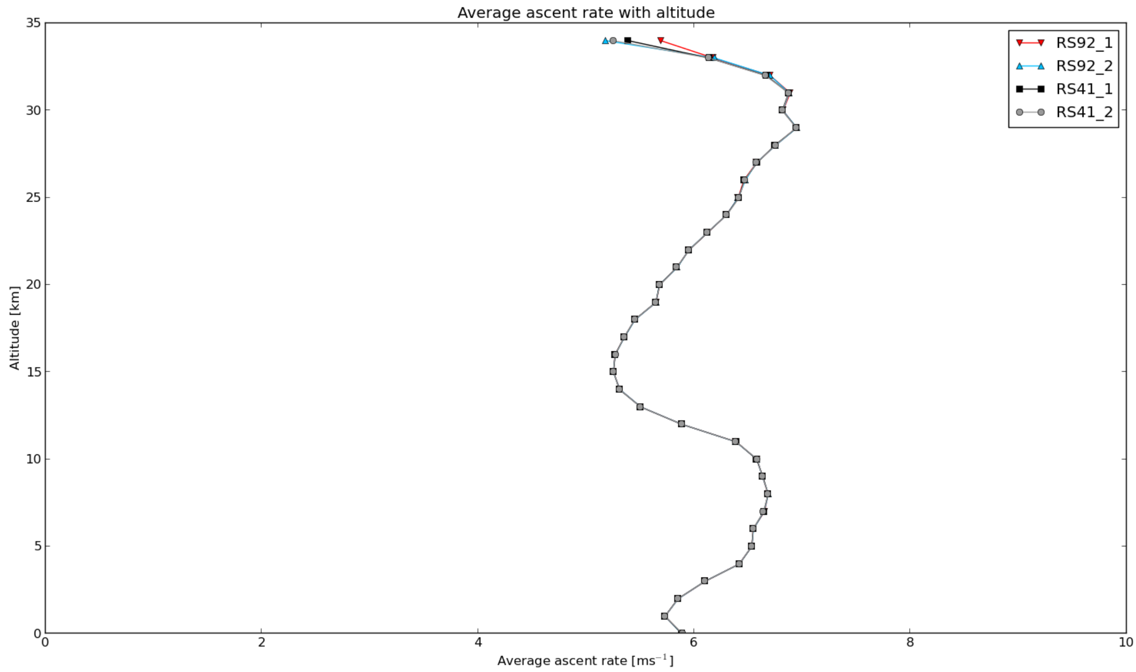

Figure 8 – Average balloon ascent rates as measured by each radiosonde against height across all flights. The final point at 34 km is from a single flight only.

Data collection, processing and editing

Radiosonde software

RS92

All RS92 ascents were processed using Vaisala DigiCORA sounding system MW31 software version 3.64.1. This includes the solar radiation corrections as applied to both the temperature and humidity measurements in the *WMO Intercomparison of high quality radiosonde systems, Yangjiang, China, 2010*. This software creates files containing interpolated data between missing points. This feature was used in this analysis to reflect operational output of the systems.

RS41

All RS41 ascents were processed using Vaisala DigiCORA sounding system MW41 software version 2.0. This includes solar radiation corrections specific to the RS41. This software creates files containing interpolated data between missing points. This feature was used in this analysis to reflect operational output of the systems.

Missing Data

Total missing data per system

During the trial, each radiosonde transmitted data once every second. Occasionally data was lost, possibly caused by interference near the data transmission frequency. In the following analysis, missing data is defined as data points where no temperature/RH values were present in the data for a period of at least one second.

During the test, only the RS92 radiosondes had a loss of data exceeding 1% per flight, occurring in 1 flight out of 30. Figure 9 shows RS92 radiosondes had the largest loss of data per flight, in flight 31. No distinct cause could be found for the loss of data. The RS41 radiosondes generally showed fewer seconds of missing data than the RS92 radiosondes, although there is a possibility that the choice of frequencies for each sonde may have caused this difference.

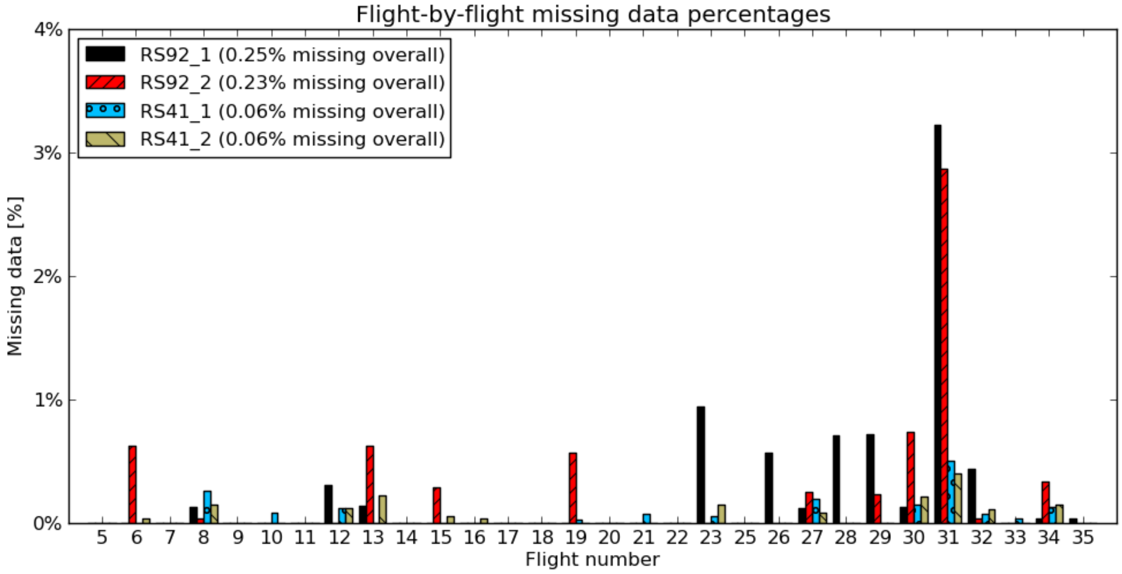

5399	5627	5503	5488	4265	5297	5053	5334	5005	5379	4170	5347	4891	5089	4966	5187	5450	5168	4274	4974	5165	5305	4260	5304	5658	5828	5725	5699	5650	5872
5418	5619	5501	5514	4267	5296	5054	5330	5006	5375	4171	5396	4893	5091	4964	5188	5443	5180	4238	4977	5115	5275	4261	5303	5706	5794	5772	5692	5656	5863
5376	5591	5463	5471	4236	5257	5014	5298	4968	5341	4138	5356	4855	5051	4928	5157	5419	5141	4239	4941	5123	5275	4228	5267	5667	5792	5734	5658	5617	5841
5376	5590	5463	5471	4236	5257	5014	5298	4968	5341	4138	5355	4854	5052	4929	5157	5420	5140	4240	4941	5122	5275	4227	5268	5667	5792	5732	5658	5617	5841

Figure 9 – Missing data quantities for each radiosonde by flight and for each radiosonde system overall (inset). Below is a table of observation totals per flight at 1 second resolution.

Average missing data duration

It was of interest to investigate how long each period of missing data lasted. A single extended period of missing data in the middle of a flight could lead to a key feature in the profile being missed. However, many individual seconds of missing data spread out across the ascent would be unlikely to have much impact.

Figure 10 shows the statistics of missing data from each flight. The duration of missing data was generally on the order of only 2 to 4 seconds when it occurred, with relatively little deviation from this. As such, the impact of missing data, when points were interpolated from surrounding data, was unlikely to impact on the detection of major features.

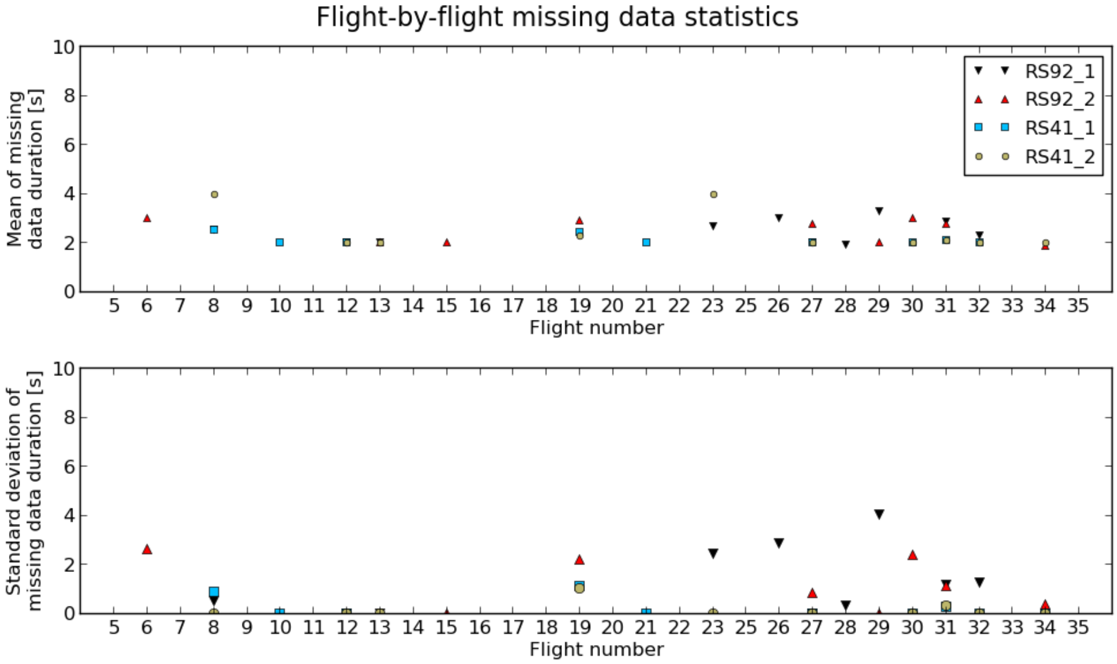

Figure 10 – Total quantities of missing data per flight (top) and standard deviations of missing data duration (bottom).

Sample Size

A total of 30 separate flights were made: 20 during the daytime, 10 at night-time. The majority of flights exceeded 30 km in altitude before the balloon burst. Flight durations ranged from 68 to 117 minutes, sampling at one sample per second, generally giving over 5000 samples per sonde per flight. More data was available at some altitudes compared with others, because of differences in ascent rate. By comparing with Figure 8, it is possible to see that altitude bins with greater sample size tie in with altitudes where the balloon ascended less quickly, and so had more time to take measurements.

Figure 11 shows total number of data points from each sonde in each altitude bin up to 35 km. The plot on the right shows how many of those data points contained no data in the raw data, and so were interpolated in the final data. Only one flight succeeded in taking measurements above 34 km from all four sondes.

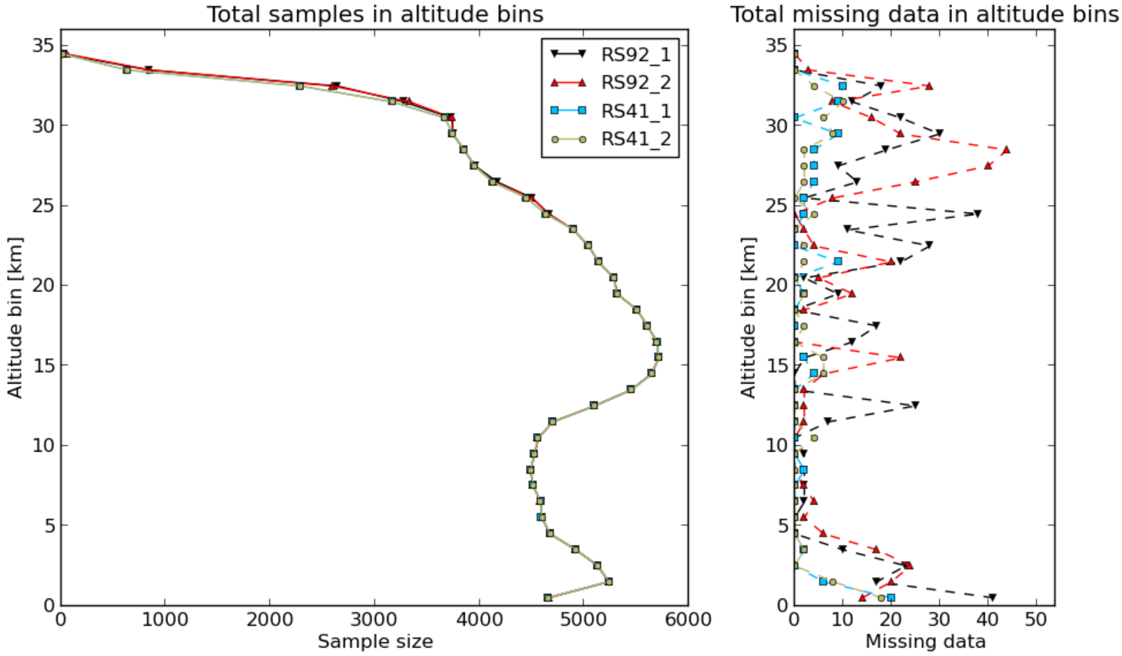

Figure 11 – Total sample sizes against height with missing data quantities in 1 km range bins.

Analysis software and methodology

RSK software version 3.5, comprising WVIEW, WLIST and WSTAT were used to display and analyse the data files in this trial. This is the same version as was used during the *WMO Intercomparison of high quality radiosonde systems, Yangjiang, China, 2010*. All radiosonde analysis compared the processed outputs from the radiosonde software versions being used. While raw data was available and was useful for interpreting certain results, it is not included in this analysis as it does not represent operational output.

WSTAT analysis

The statistical analysis plots generated by WSTAT were produced using 1 second sampling, as provided by the radiosondes themselves. Analysis was either completed over 1 km or 10°C bands, as was the process in the *WMO Intercomparison of high quality radiosonde systems, Yangjiang, China, 2010*.

Where helpful, the WSTAT analysis charts have been replicated between different sections with identical axes making visual comparison of the results of the two radiosonde designs easier. Most plots show average flight-by-flight differences between the radiosondes and the corresponding flight-by-flight standard deviation (SD) plot.

When all 4 radiosondes were compared, the RS92_1 was used as the arbitrary reference radiosonde in all cases to demonstrate the typical deviations from the RS92_1 data that would be expected from either another RS92 flying at the same time, or in comparison with the RS41.

Where only 2 radiosondes of the same model were compared, the results indicate the typical precision of the radiosonde's measurements. Precision is referred to as 'reproducibility in sounding' in the *Vaisala RS92-SGP datasheet* and *Vaisala RS41-SG datasheet*.

When interpreting radiosonde plots comparing 2 radiosondes of the same model, smaller standard deviations indicate higher radiosonde precision. Under a normal distribution, 1 SD accounts for approximately 68% of the data, and is an indicator of typical performance.

For additional information, some average flight-by-flight difference plots also include thinner 2σ (2 sigma, which is equivalent to 2 SD) lines. The 2σ lines show the boundaries of where approximately 95% of the differences in the data fall, representing expected performance for that radiosonde in most cases. Note that the 2σ lines are not for the standard deviation of flight-by-flight differences, but are instead for direct differences due to restrictions within the software and are therefore only to aid visual comparison of the data.

In some circumstances, the datasets are reduced through early bursts or manual restrictions of the dataset by temperature and humidity bands. Data points containing data from fewer than 3 flights were partially masked in grey to give a simple visual assessment of the validity of the result. Full sample size tables are included in annex 4.

To make the analysis by WSTAT and WVIEW more accurate, the individual flight processed data files were converted to ASCII format and time synced by their GPS times by Vaisala. This ensured that all of the data points were accurately mapped across all 4 systems for RSK analysis without the need for the application of manual timing offsets. In order to ensure that the points matched exactly, linear interpolation between data points was used to map to the correct time. RS92_2 was used as the reference time for the purposes of this processing.

Python analysis

New code was developed in the Python programming language to analyse the radiosonde data and statistics. For example, the code for creating the plots in Figures 8 – 11 was developed to directly read the ASCII data files and carry out the required data analysis before plotting the data.

Code was also developed in Python to recreate plots that could be generated using the RSK WSTAT software, but in such a way that the plots could be customized. The mean difference in kilometre bins between the measurements of each radiosonde and a reference sonde were calculated, and averaged across a number of flights, in order to recreate the 'flight-by-flight' difference plots created using WSTAT. The standard deviations of these flight-by-flight differences could then be calculated using the Python NumPy module, allowing for flight-by-flight standard deviations to also be recreated.

The advantage of using Python to create these plots was that the standard deviations of the flight-by-flight differences between the two RS41 radiosondes on each flight and the two RS92 radiosondes on each flight could be directly overlaid. This provided a quick visual comparison of the difference in precision of the measurements of each system.

These plots were found to provide values extremely close to those produced by the RSK software, except in the maximum and minimum altitude bins. This effect was assumed to be caused by different approaches to selecting data at the start and end of each flight, but the exact cause could not be determined. As such, the Python analysis figures of this type have been included, but only in annex 3 as a reference.

Outliers

In previous WMO intercomparisons it was standard practice to mask agreed data which is outside of the typical behaviour of the radiosonde. However, there were no instances of significant deviations from 'normal' behaviour in this intercomparison with either radiosonde.

In flight 6 (Figure 77), the temperature readings from system RS92_1 were approximately +0.3^{o}C above those of the RS92_2 until approximately 3 km. This is a slightly greater difference than was observed in the other ascents. This flight was included in the analysis for two reasons: the values recovered after 3 km to normal differences from the other RS92 system, and the radiosonde passed its ground check, representing what would be seen in an operational situation.

Comparison of simultaneous temperature measurements

RS92 vs. RS41 general performance

On a flight-by flight basis, the temperature observations of the RS41 radiosondes compared to the RS92 radiosondes are very similar. An example from a single typical flight is shown in Figure 12, with the temperature profiles of all 4 radiosondes plotted on top of each other on the left. On the right are the temperature differences seen for the other 3 sondes relative to the RS92_1 radiosonde at 5 m resolution, which are below the tropopause are all within ±0.3°C at any point. These differences are grouped and averaged to generate the overall 'average flight-by-flight' differences and standard deviations seen in the day/night performance and precision in the following sections.

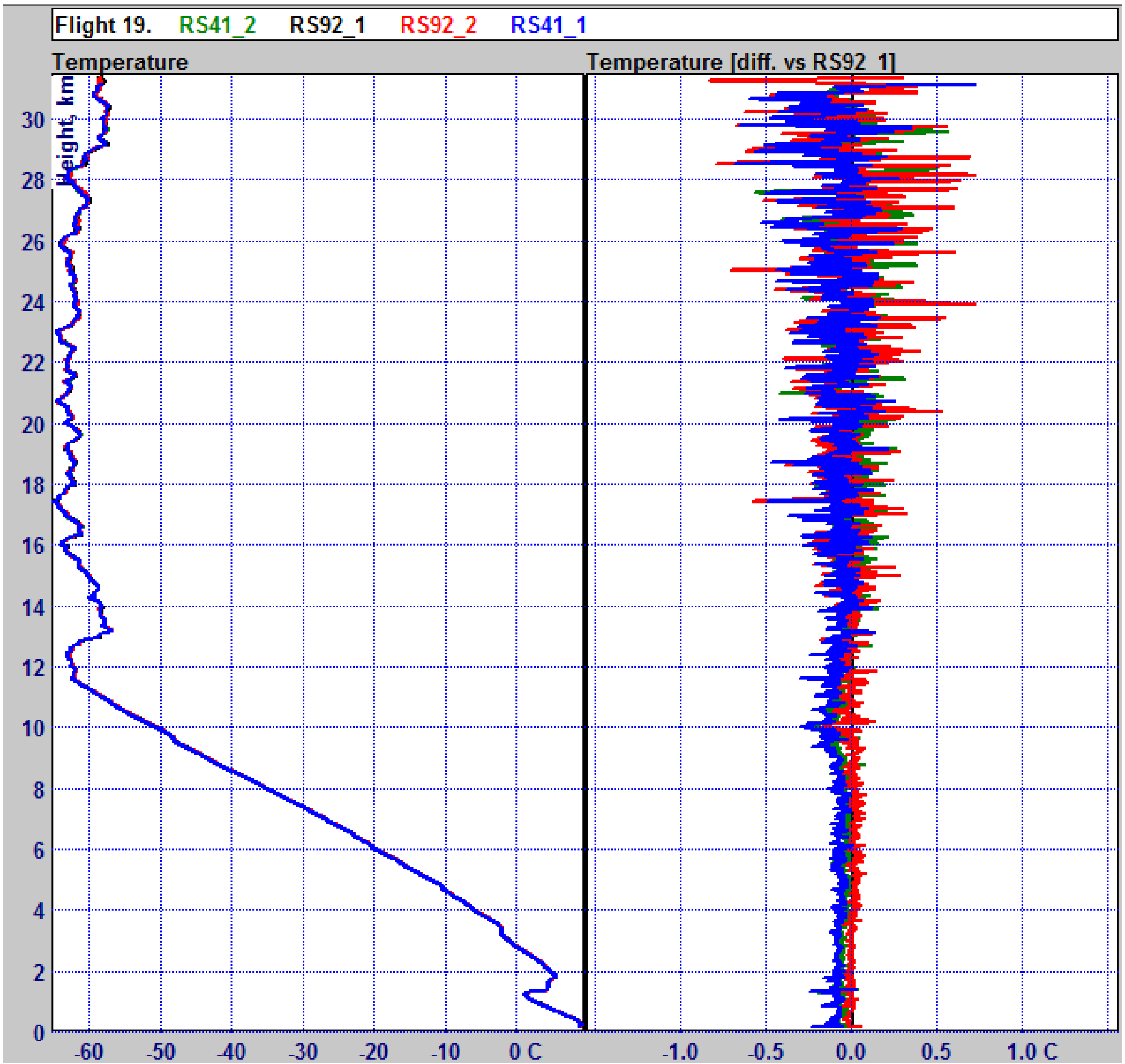

Figure 12 - Flight 19 temperature profile showing the measured temperature profiles (left) and differences of the radiosondes relative to the RS92_1 sonde (right).

The ascent features a sharp inversion which is tracked well by all 4 radiosondes with no notable increase in variability. This behaviour is typical, except in situations involving thick cloud which will be discussed later.

The subsequent images show sections of the ascent from Figure 12 in greater detail, demonstrating how closely the temperature profiles match each other.

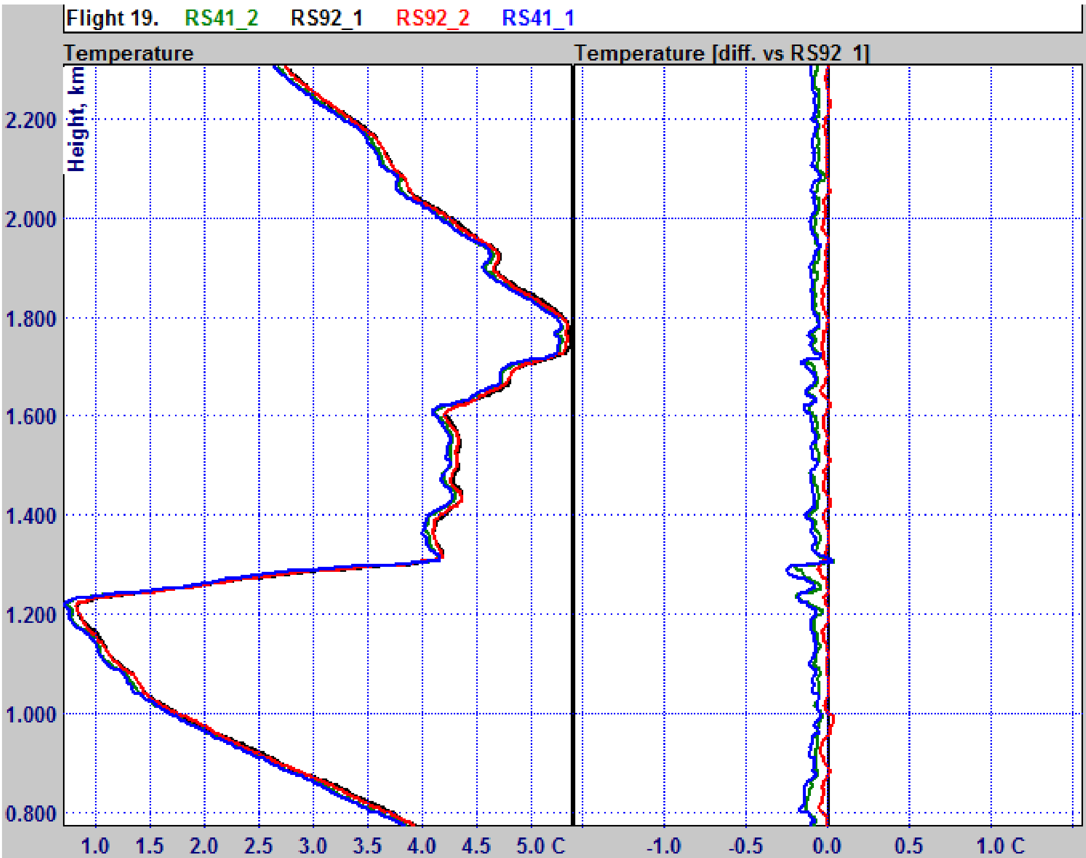

Figure 13 – Example from flight 19 showing the measured temperature differences of the RS41 radiosondes and RS92_2 radiosondes relative to the RS92_1.

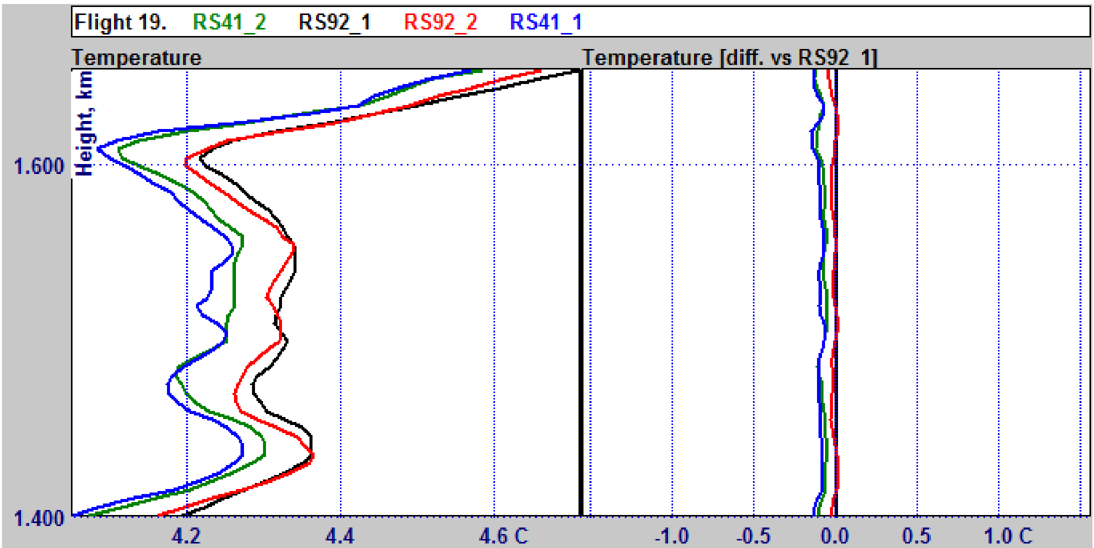

Figure 14 – Detailed section of flight 19 showing the measured temperature differences of the RS41 and RS92_2 radiosondes relative to the RS92_1.

RS92 vs. RS41: Day/night performance

The RS92 and RS41 offer very similar results when compared at night-time, showing general direct differences of less than ±0.1°C except for in the lowest 4 km of ascents (see Figure 15). This variability at this level is largely due to the differences in behaviour around clouds, which will be discussed later.

During the night-time, the RS92 dataset indicates a slight systematic negative temperature bias for the RS92_2 relative to RS92_1. This may be partially due to the differences in the ground check temperature corrections applied to the radiosondes, which was -0.05°C lower for the RS92_2 ground check system on average.

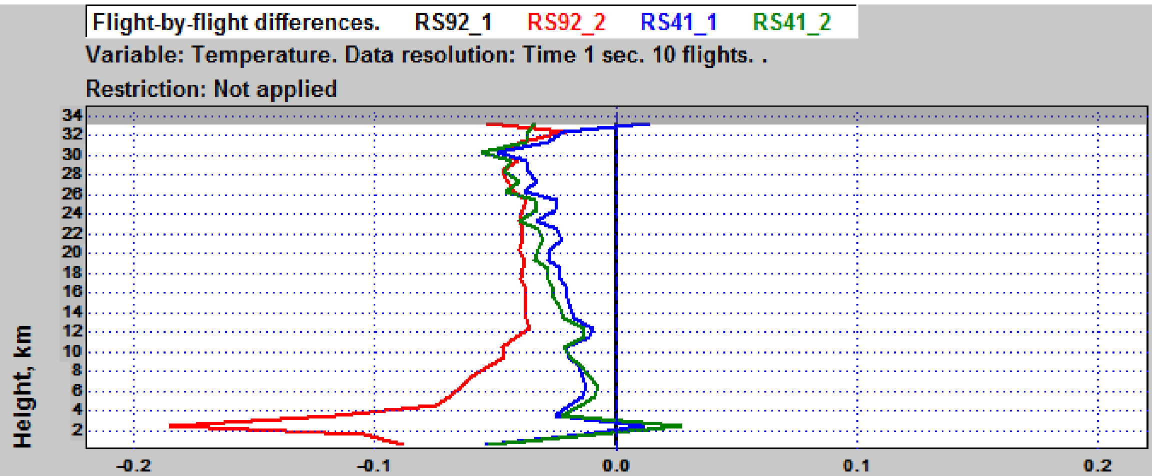

Figure 15 - Night-time temperature comparison between the RS92_1 and the RS92_2 and RS41 radiosondes – flight-by-flight direct differences.

During the daytime, the RS41 radiosondes show some slight consistent differences (within ±0.2^{o}C) relative to the RS92 radiosondes relative to altitude. As discussed below, these consistent differences disappear when viewed against temperature bands (Figure 18), indicating that they are due to altitude-related phenomena rather than temperature.

The result between 34 and 35 km in Figure 16 is a limited sample size, so is not very representative of general performance.

During the daytime the RS92 dataset indicates a smaller systematic negative temperature bias for the RS92_2 relative to RS92_1 than is seen at night-time. However, this data includes the application of solar radiation corrections and have increased uncertainty in the dataset relative to the night-time ascents, as seen in the precision plots for day and night.

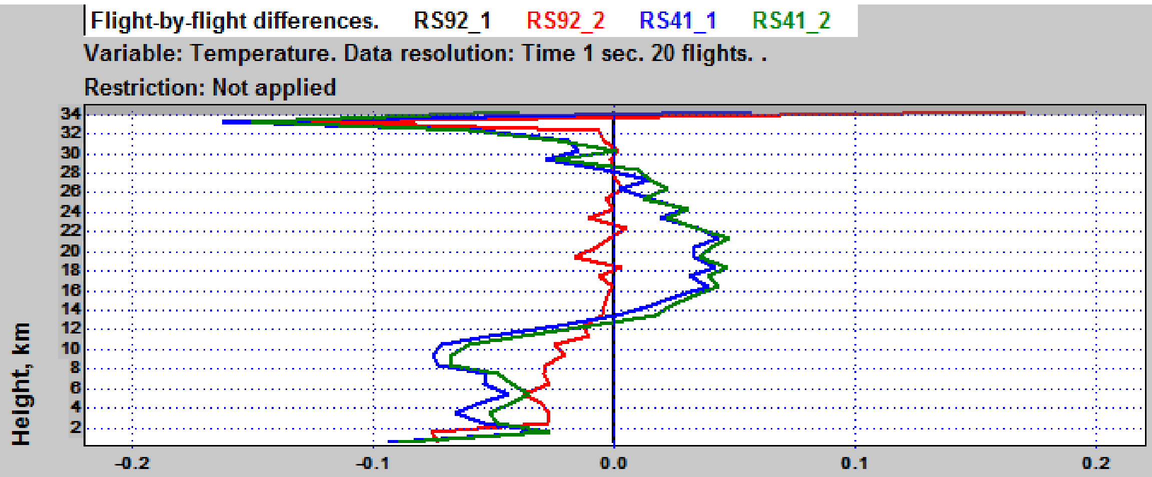

Figure 16 - Daytime temperature comparison between the RS92_1 and the RS92_2 and RS41 radiosondes – flight-by-flight direct differences.

Although presenting the results of this trial against height is useful for the circumstances seen in this trial, it is perhaps more informative from an international perspective to show how the systems' temperature measurements differ as measured over various temperature bands. This will give an indication of how the systems would differ from a climatic perspective in day and night situations.

The key outcome from this analysis is that the temperatures observed by the RS41 relative to the RS92 do not differ much at any temperature range, except in the regions exiting clouds in the lower troposphere during the day. This accounts for the increased difference and variability seen at -5°C at night and 5°C during the day, but at night this variability was approximately equivalent to that seen in the RS92 measurements. As the temperature at which cloud tops occur is highly variable, this exception is therefore only representative of differences seen during this trial.

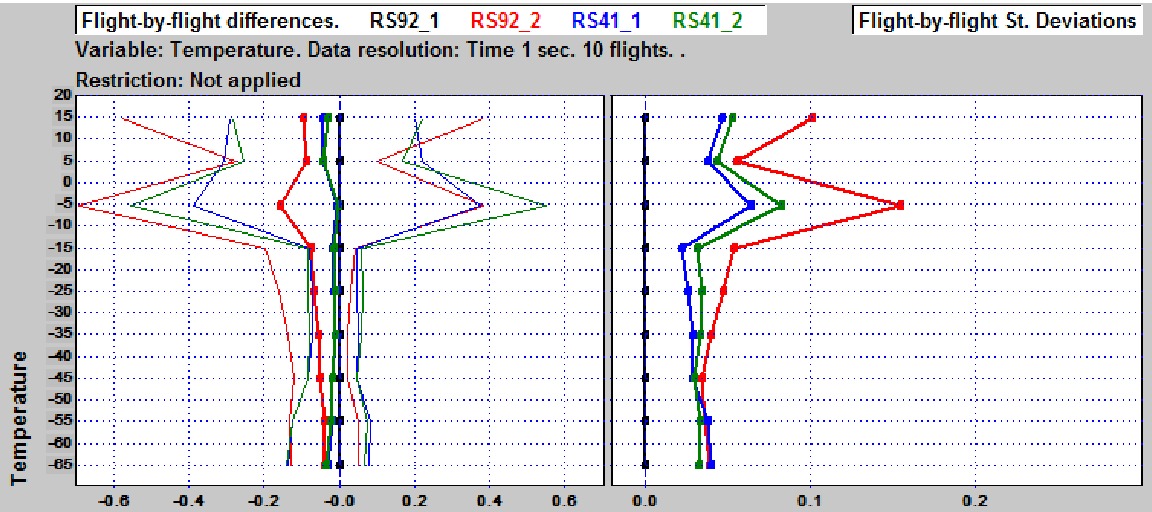

Figure 17 - Night-time temperature comparison between the RS92_1 and the RS92_2 and RS41 radiosondes flight-by-flight differences (left) including direct difference 2σ bands and flight-by-flight standard deviations (right).

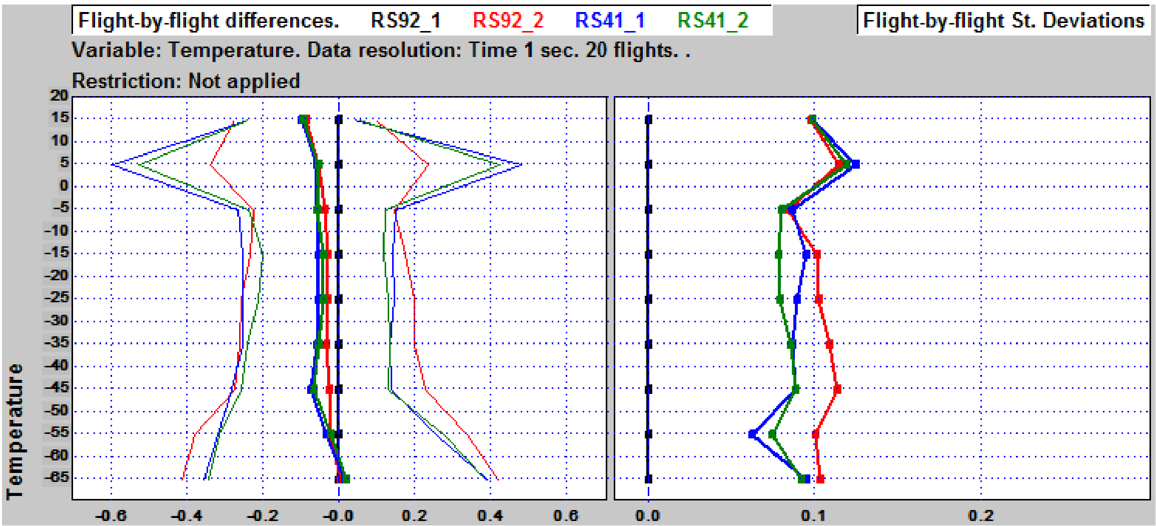

Figure 18 - Daytime temperature comparison between the RS92_1 and the RS92_2 and RS41 radiosondes flight-by-flight differences (left) including direct difference 2σ bands and flight-by-flight standard deviations (right).

The consistent differences seen between the RS41 and RS92 during the daytime (Figure 16) with height were not replicated when compared using temperature bands (Figure 18). This indicates that the consistent differences would not have a large impact over a longer period, as they are linked to the heights of atmospheric phenomena during individual ascents rather than temperature bands.

RS92 precision

The agreement between the systems is generally very high. This is demonstrated by the low standard deviation values in Figure 19. As shown in Figure 15, during the night-time the RS92_2 system indicated a consistent difference in temperature bias to the RS92_1 system of <-0.2°C which may be partially due to the differences in corrections applied by the different ground check systems. This was noted above as -0.05°C.

The increase in variability measured in the lowest 4 km of ascents seen in Figure 19 is related to each of the RS92 sondes behaving slightly differently when interacting with clouds, as discussed later in this section. In general, the RS92_2 system experienced more examples of wet-bulbing than the RS92_1 system and this resulted in the higher variability seen. This is not thought to be a systematic difference, but because of the individual variability in the performance of the RS92 temperature sensors.

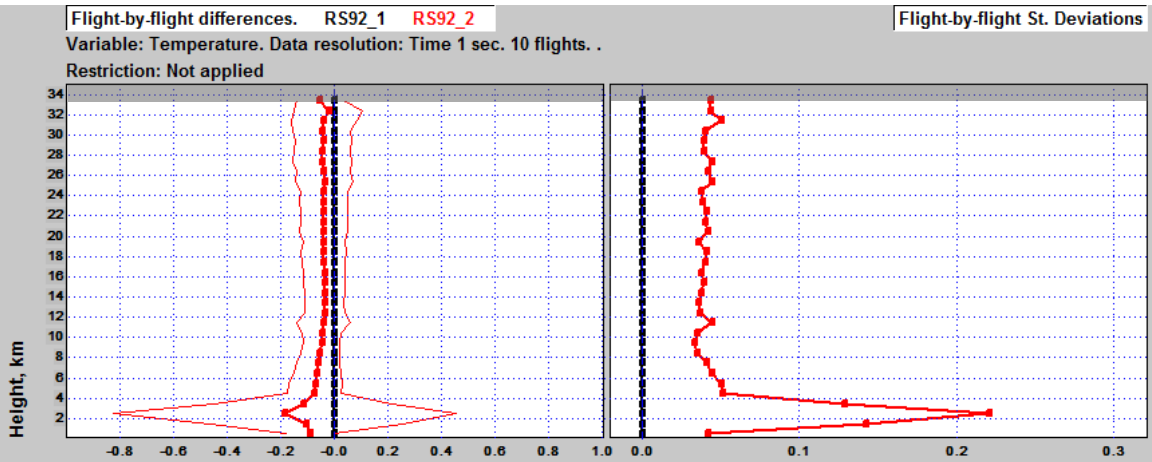

Figure 19 - Night-time temperature - average RS92_1 vs. RS92_2 flight-by-flight differences (left) including direct difference 2σ bands and flight-by-flight standard deviations (right).

Comparing Figure 19 and Figure 20, while the two RS92 systems' flight-by-flight differences appear to agree more closely during the daytime on average than at night-time, the standard deviations are higher. This shows that there is slightly less agreement between the two RS92 systems which is masked in the flight-by-flight differences plot. This is expected to be caused by the application of solar radiation corrections to the measurements, adding additional uncertainty into the results.

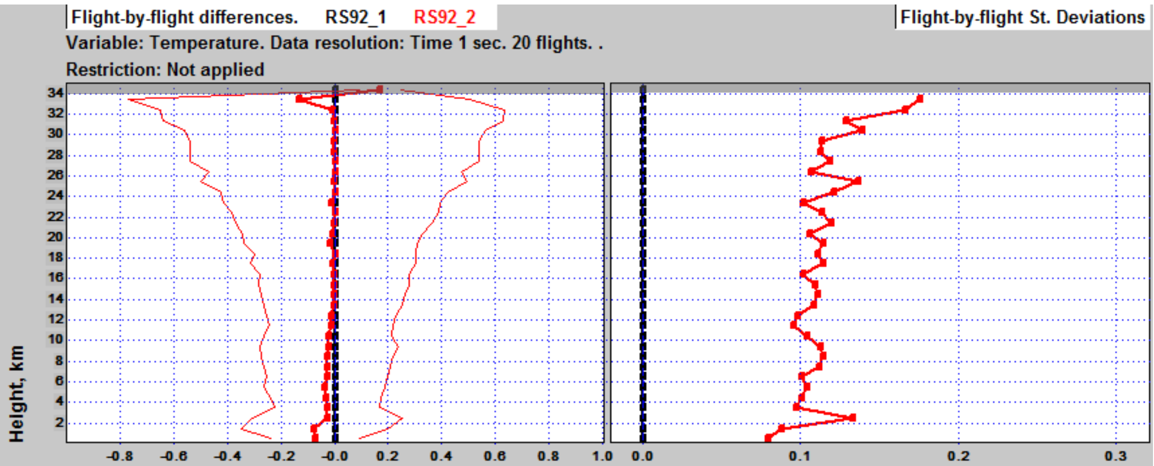

Figure 20 - Daytime temperature - average RS92_1 vs. RS92_2 flight-by-flight differences (left) including direct difference 2σ bands and flight-by-flight standard deviations (right).

The *Vaisala RS92-SGP datasheet* indicates that the reproducibility (precision to 1 SD) of RS92 temperature measurements is ±0.2°C (1080-100hPa), ±0.3°C (100-20hPa) and ±0.5°C (20-3hPa). The flight-by-flight standard deviation results in Figure 19 and Figure 20 are within these boundaries except for the significant deviation during the night-time 2-3 km range, the causes of which are discussed below.

Note that the 2σ lines on the figures are for direct differences rather than flight-by-flight differences, so are only to enable easier visual comparison of the figures. Total uncertainty in temperature measurements is stated as ±0.5°C for the RS92.

RS41 precision

Comparing Figure 19 to Figure 21 and Figure 20 to Figure 22, the RS41 radiosondes show better agreement between the two systems than the RS92 radiosondes. This is observed in daytime and night-time flight-by-flight differences and their respective standard deviations. Overall, this indicates that the RS41 sensors are more precise than the RS92 sensors.

There was a very small increase in variability noticeable in the lowest 4 km of ascents that is most likely caused by each of the RS41 sondes behaving slightly differently when interacting with clouds, as shown in Figure 28. The magnitude of this increase in variability is less than that seen with the RS92 as demonstrated in Figure 24.

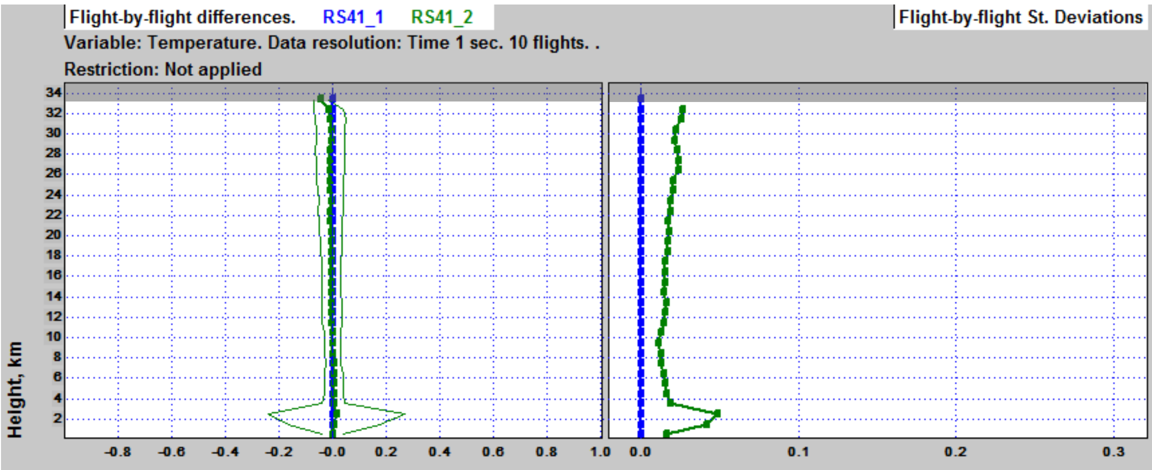

Figure 21 - Night-time temperature - average RS41_1 vs. RS41_2 flight-by-flight differences (left) including direct difference 2σ bands and flight-by-flight standard deviations (right).

The daytime flight-by-flight performance of the two RS41 systems shows similar agreement to the night-time performance, but as with the RS92, the standard deviations are higher. The magnitude of the solar radiation corrections being applied to the raw data increases with height, so the increasing standard deviations with height are likely to be caused by this additional uncertainty.

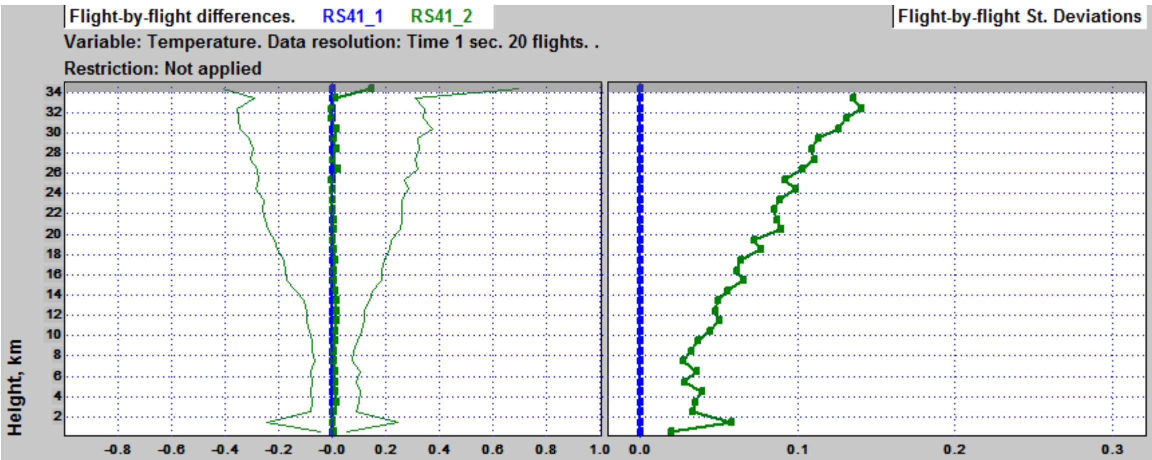

Figure 22 - Daytime temperature - average RS41_1 vs. RS41_2 flight-by-flight differences (left) including direct difference 2σ bands and flight-by-flight standard deviations (right).

The *Vaisala RS41-SG datasheet* indicates that the reproducibility (precision to 1 SD) of RS41 temperature measurements is ±0.15^{o}C (>100hPa) and ±0.3^{o}C (<100hPa). The flight-by-flight standard deviation results in Figure 21 and Figure 22 are within these boundaries at all times.

Note that the 2σ lines on the figures are for direct differences rather than flight-by-flight differences, so are only to enable easier visual comparison of the figures. Total uncertainty in temperature measurements is stated as ±0.3^{o}C (<16 km) and ±0.4^{o}C (>16 km) for the RS41.

RS92 vs. RS41 key differences

RS92 vs. RS41: Behaviour around clouds – wet-bulb effect

Generally, the RS92 and RS41 performed very similarly when measuring temperature throughout the ascents. The main differences occurred as a result of interactions with clouds or suspected cloud layers, usually in the lowest 4 km of the ascents.

The RS92 systems sometimes showed evidence of cooling upon exit from cloud layers or suspected cloud layers (the ‘wet-bulb’ effect), but this was not always consistent for both RS92 radiosondes in the same flight. On several occasions, one system was affected but the other was not, or the magnitude of the effect varied between the two RS92 systems relative to the RS41 radiosondes.

Both radiosonde designs utilise a hydrophobic coating on the temperature sensor to reduce the wet-bulb effect while minimising the impact on temperature measurements, however, it appears that the RS41 sensor design is an improvement on that of the RS92. There were no occasions where the RS41 radiosondes exhibited ‘wet-bulb’ behaviour relative to the RS92 radiosondes, and in general they showed consistently faster temperature response times when exiting cloud or suspected cloud layers relative to the RS92 radiosondes. Please see the metadata table (Table 2, page 79) for further information relating to the number of noted instances of wet-bulb events and slow sensor response times.

Flight 22 demonstrated the largest wet-bulb effect seen in these trials, as demonstrated in Figures 23 - 25, following the transition from thick cloud into a very dry layer.

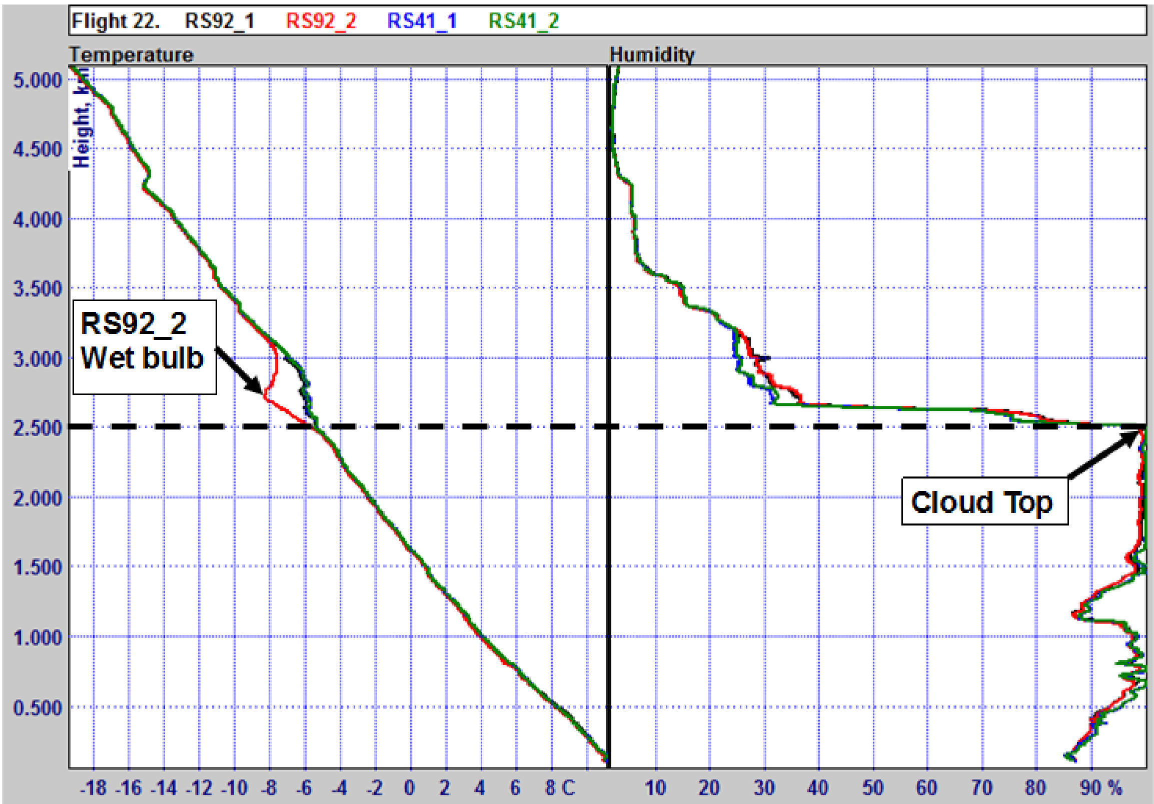

Figure 23 - Example of a cloud exit in flight 22 causing cooling of the RS92_2 temperature sensor relative to the RS41 radiosondes, with the RS92_1 sensor on the same ascent unaffected.

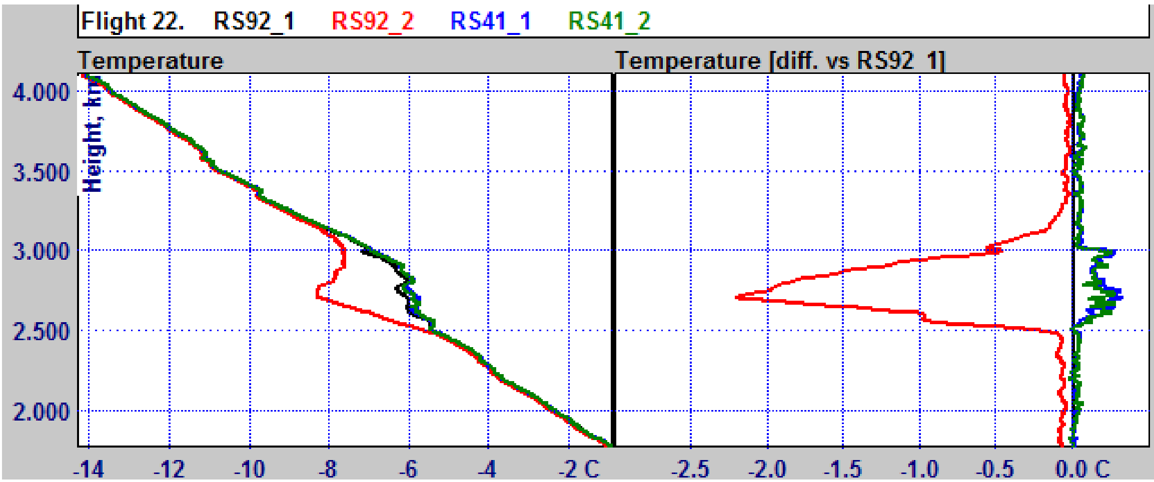

Figure 24 – Detailed section of flight 22 showing the measured temperature differences of the radiosondes relative to the RS92_1 radiosonde in normal conditions and on exit from cloud.

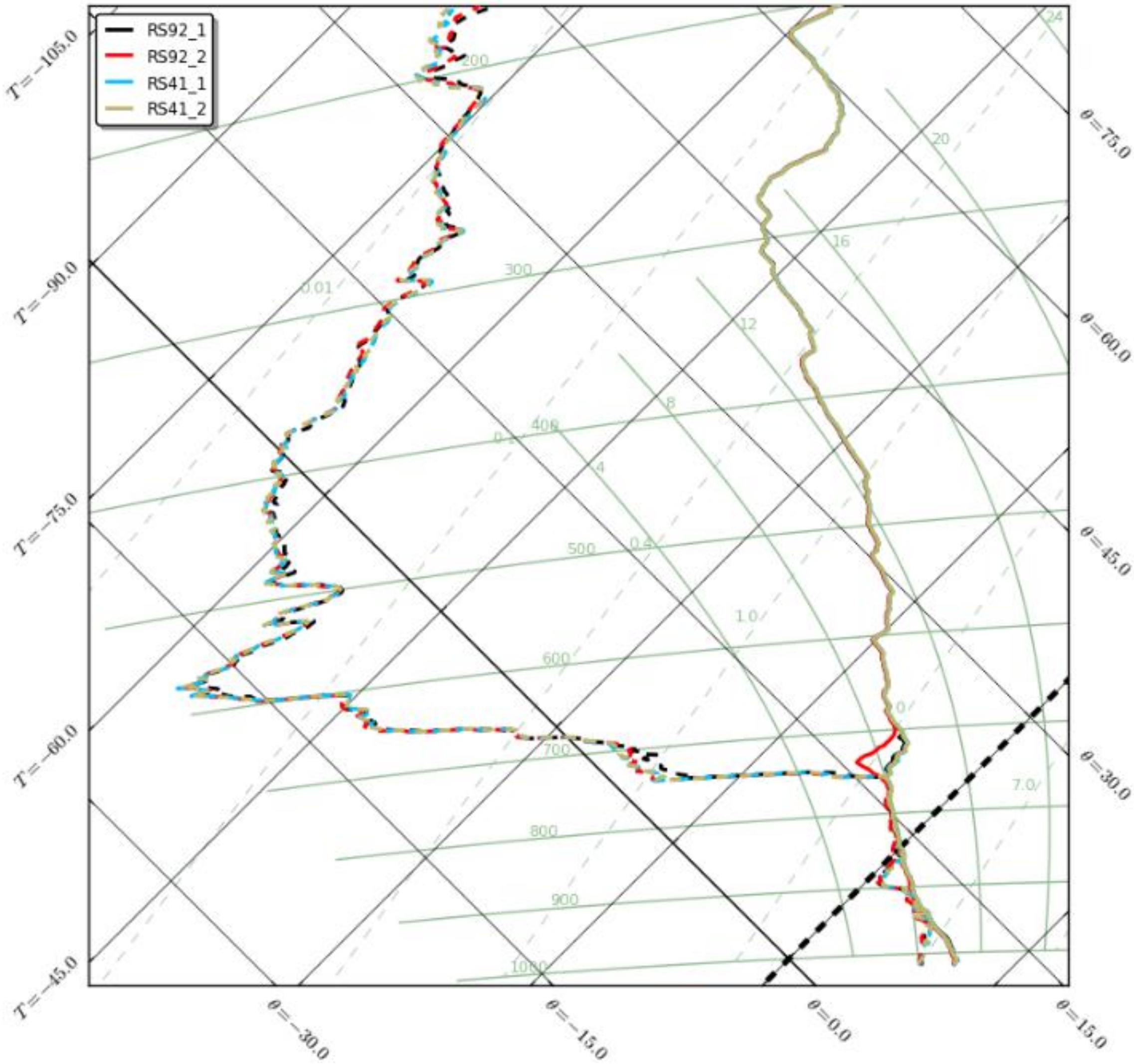

Figure 25 - Example of a cloud exit in flight 22 causing cooling of the RS92_2 temperature sensor relative to the RS41 radiosondes, with the RS92_1 sensor on the same ascent unaffected. Displayed in tephigram format indicating super-adiabatic cooling measured by RS92_2 sensor.

RS92 vs. RS41: Behaviour around clouds – sensor response times

In the example in Figure 26, the RS92 sonde's sensors do not exhibit a wet-bulb effect upon exit from thick cloud, despite the sharp change in humidity and temperature. However, they do appear to have a slightly slower response time to the change in temperature than the RS41 radiosondes. This effect was seen in several ascents, although this is the most notable example. This is probably due to evaporative cooling caused by slight moisture contamination.

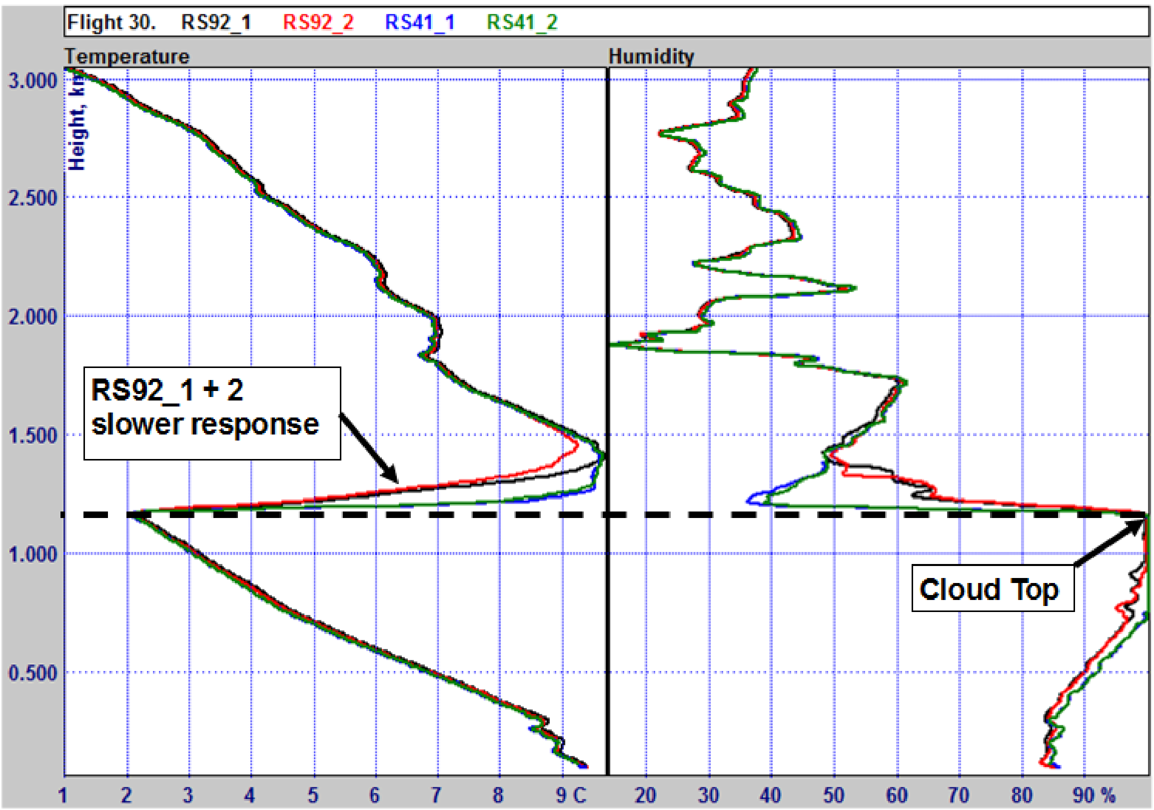

Figure 26 - Example of cloud exit in flight 30 causing a slower response of both of the RS92 temperature sensors relative to both of the RS41 sensors.

The appearance of this effect demonstrates a component of the increase in variability seen in the lowest 4 km in the overall statistics for both types of radiosonde, as seen in Figures 15 and 16. Figures 27 and 28 display the temperature profiles against the differences seen in those profiles relative to those of the other radiosondes. The first shows the RS92_1 against the other three, clearly showing the higher temperatures measured by the RS41 radiosondes, but also the differences between the values measured by the RS92_1 and RS92_2, which are higher than those observed above and below the event.

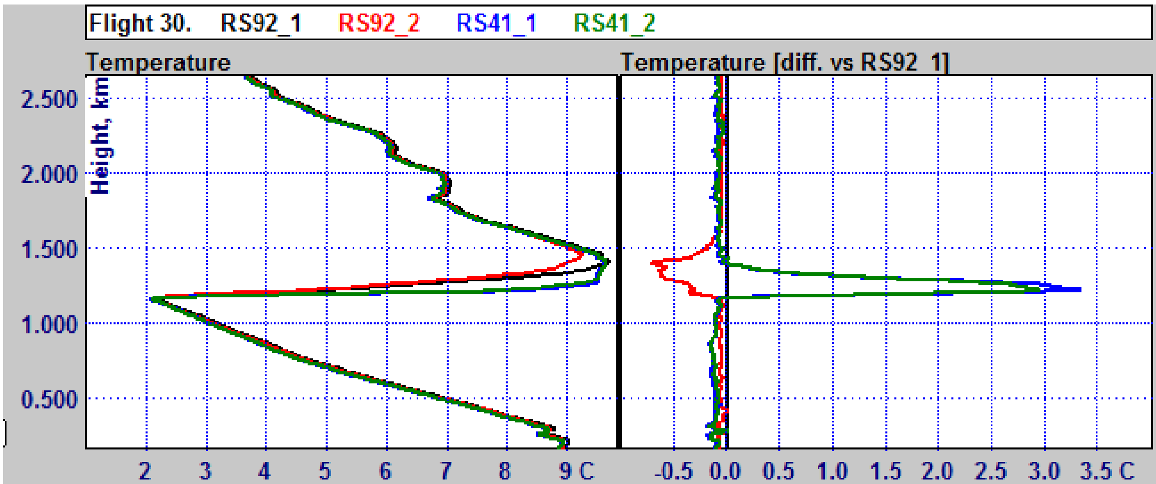

Figure 27 - Detailed section of flight 30 showing the measured temperature differences of the 3 other radiosondes relative to the RS92_1 sonde in normal conditions and on exit from cloud.

The appearance of variability of all 4 sondes caused by the transition from cloud to a low-humidity environment indicates the challenges present in accurately measuring temperature.

Figure 28 shows the same region as Figure 27, but with only the RS41 profiles to demonstrate the equivalent differences seen between the RS41_1 and RS41_2 on the same axes. Although there is an increase in variability for the RS41 radiosondes, the magnitude and duration is lower than that seen with the RS92 radiosondes.

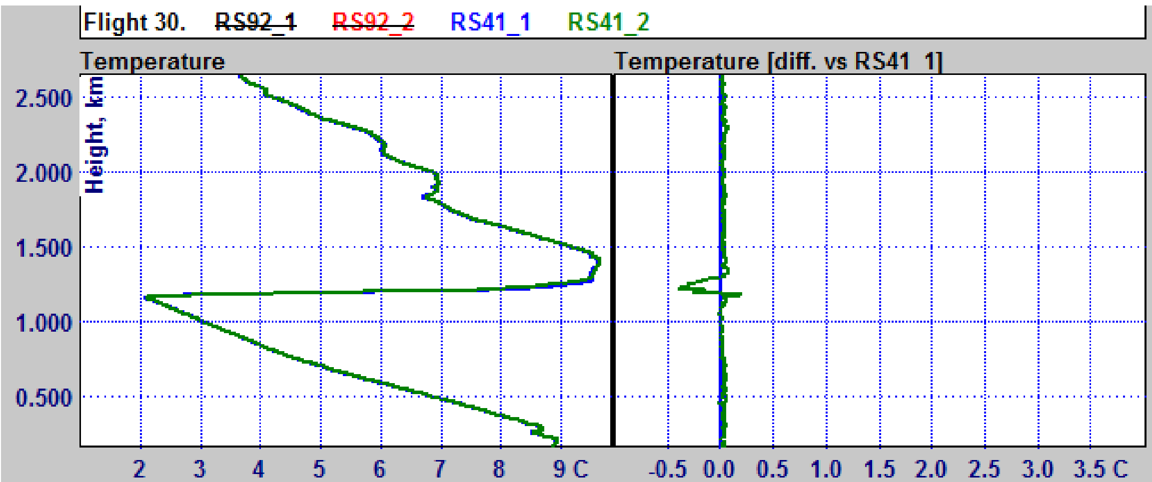

Figure 28 - Detailed section of flight 30 showing the measured temperature differences of the RS41_2 radiosonde relative to the RS41_1 in normal conditions and on exit from cloud.

Temperature Conclusions

Generally, the RS92 and RS41 exhibit very similar performance when observing temperature, with the average difference between the two radiosonde models' measurements typically within ±0.2°C over the course of the trial when measured over either 1 km or 10°C bands to 1 SD.

The consistently reduced standard deviation values between the RS41 radiosondes relative to the RS92 radiosondes, indicates that the RS41 observes temperature with a greater degree of precision than the RS92.

The RS92 temperature correction applied during the ground check is a potential source of systematic bias. As no corrections are applied to the RS41 this potential bias is removed, while the internal checks ensure that faulty radiosonde sensors should still be detected before launch. Overall, this change should improve the accuracy of radiosonde temperature observations while maintaining their reliability.

Despite the difference in radiosonde design, the application of solar radiation corrections to the radiosondes during daytime ascents did not introduce large differences between the RS92 and RS41 temperature measurements observed in this trial.

From a climate perspective, unless flagged in the dataset, wet-bulb events could introduce a negative temperature bias at some levels. On a day-to-day basis, the effect decreases confidence in the integrity of radiosonde data from a forecasting perspective, and the flagging of affected data reduces the useable dataset available for NWP. The minimisation of the impact of wet-bulb events is therefore desirable. In the wet-bulbing situations observed during this trial, the RS41 radiosondes demonstrated a significant improvement in performance relative to the RS92.

Comparison of simultaneous humidity measurements

RS92 vs. RS41 general performance

In general, when measuring relative humidity, the RS92 and RS41 performed very similarly throughout most ascents.

Figure 29 shows a highly variable humidity profile from flight 8, with many shallow features. The left side shows the humidity profiles of all 4 radiosondes plotted on top of each other. The right side shows the humidity differences seen for the other 3 radiosondes relative to the RS92_1 sonde at 5 m resolution, which are generally all within ±5% at any point. It is these differences that are grouped and averaged to generate the overall results and standard deviations seen in the day/night performance and precision sections below.

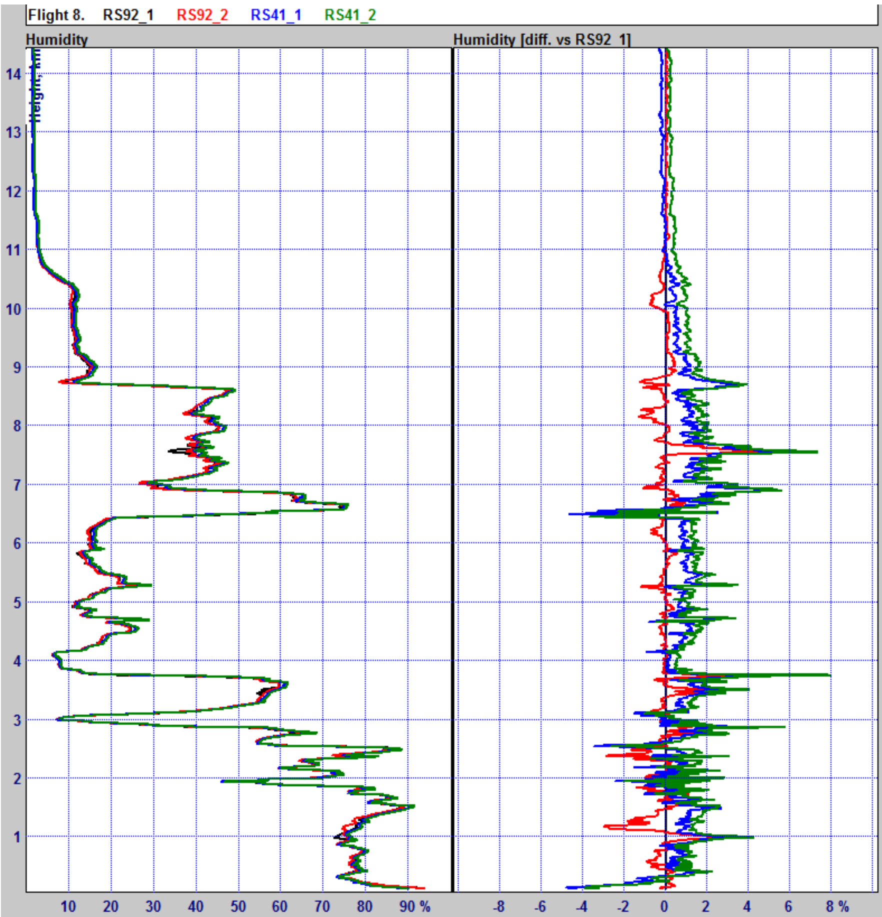

Figure 29 – Flight 8 humidity profile showing the measured humidity profiles (left) and differences of the radiosondes relative to the RS92_1 radiosonde (right).

In the example in Figure 29, the highest areas of variance are shown to be caused by very slight differences in the sensor response times. As these features change so rapidly, the differences are high in magnitude, but short in duration. In Figure 30, the RS41 radiosondes appear to react to a feature slightly slower than the RS92 radiosondes. The delay is approximately 2 seconds. However, this kind of behaviour is seen with both types of radiosonde, and the effect is varies for different ascents.

For example, Figure 31 shows a section of flight 18 which shows the RS92 sondes appearing to react to features slightly slower than the RS41. In general, the RS41 sensors appear to react slightly faster in the lower troposphere up to about 6 km.

Analysis of the raw data files indicated that both effects seen in Figure 30 and Figure 31 are most likely caused by the use of slightly different time lag correction factors applied to the RS92 and RS41 data in the DigiCORA software. The reaction times in the raw data look generally identical.

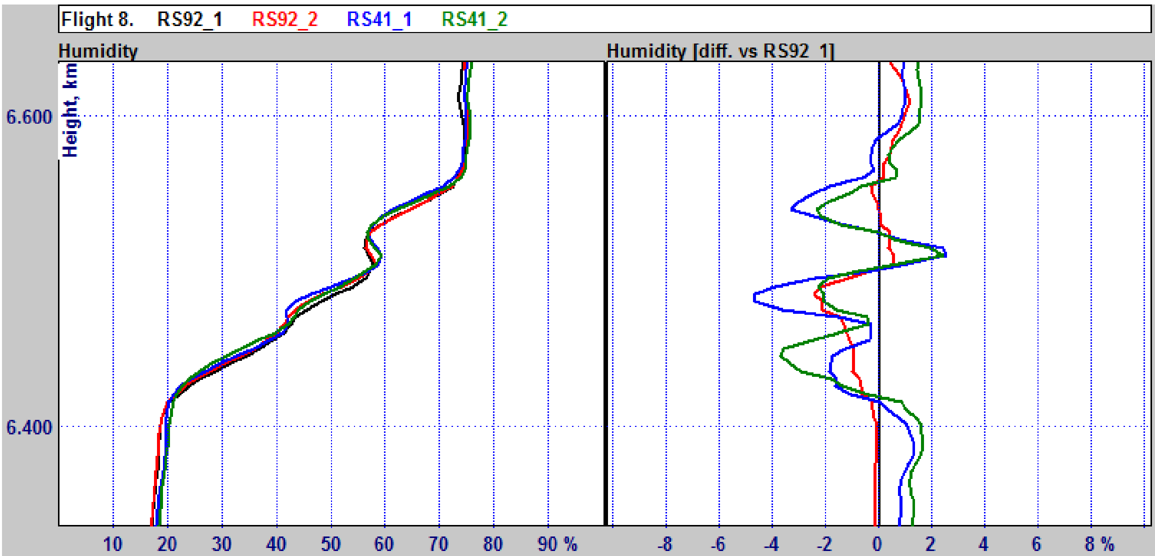

Figure 30 – Expanded section of the flight 8 humidity profile showing the measured humidity profiles (left) and differences of the radiosondes relative to the RS92_1 sonde (right).

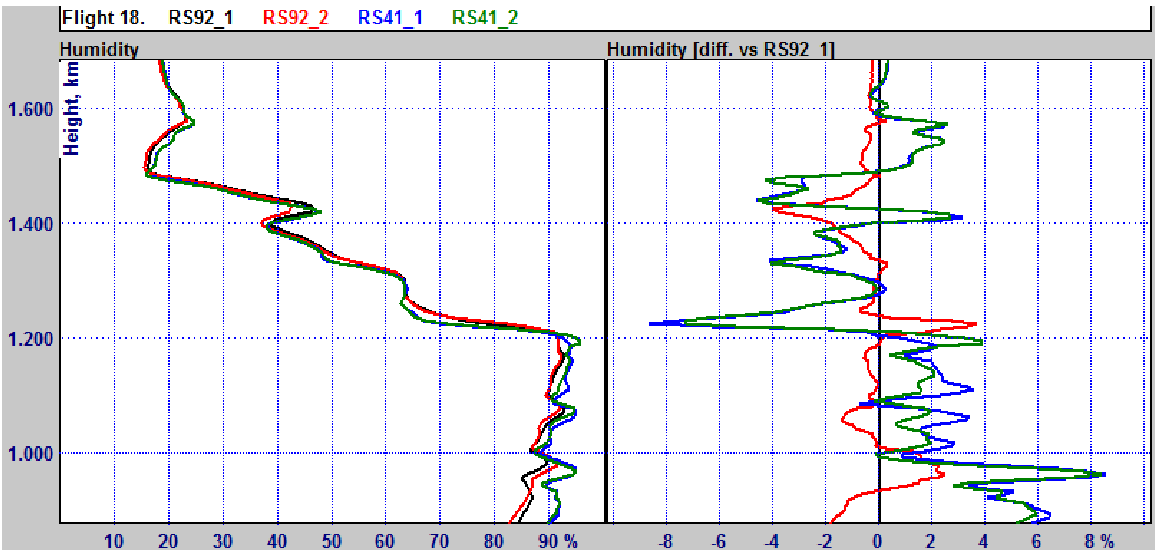

Figure 31 – Expanded section of the flight 18 humidity profile showing the measured humidity profiles (left) and differences of the radiosondes relative to the RS92_1 sonde (right).

RS92 vs. RS41: Day/night performance

Night-time ascents generally show better agreement between the RS92 and RS41 radiosondes. The RS41 radiosondes generally measured slightly higher humidity values (<1.5%) relative to the RS92 radiosondes in the troposphere. There is some variation at around 2 km, apart from around 2 km where cloud tops were typically seen.

Above the tropopause, the RS41 radiosondes measured slightly lower humidity values (typically <1%). The greater difference at the change between these two patterns occurs as the radiosondes approach the tropopause (average altitude 11315m). As such, it is a phenomenon specific to the altitudes in this trial and is not replicated in the humidity analysis against temperature bands in Figure 34 and Figure 35.

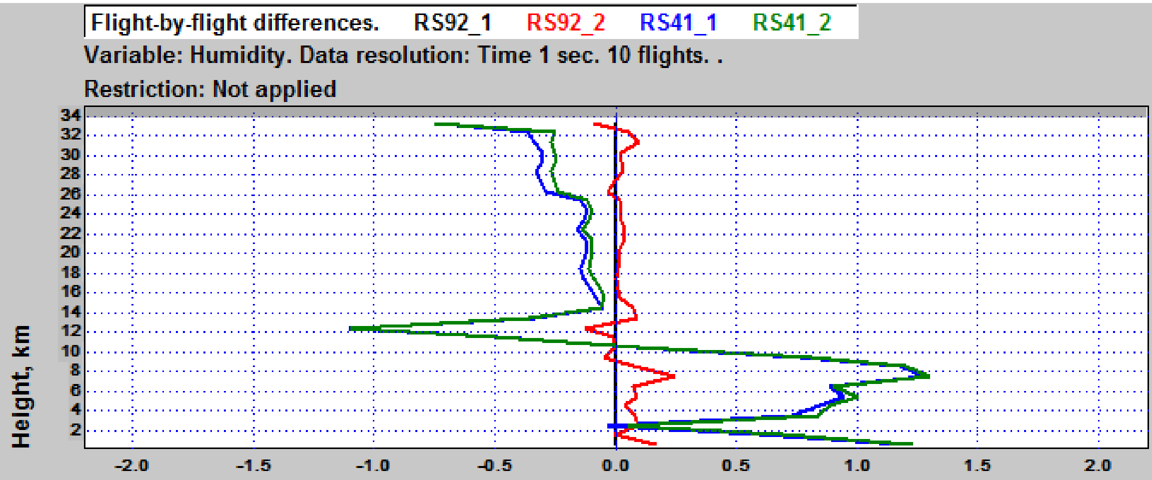

Figure 32 - Night-time humidity comparison between RS92 and RS41 sondes - flight-by-flight direct differences.

During the daytime, the RS41 shows a similar pattern of consistent differences from the RS92 radiosondes as the night-time ascents.

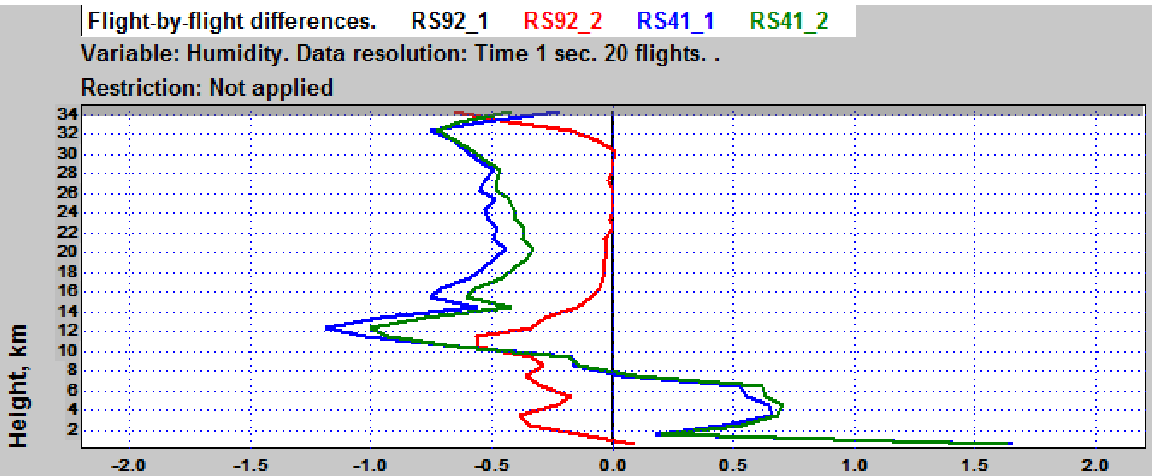

Figure 33 - Daytime humidity comparison between RS92 and RS41 sondes - flight-by-flight direct differences.

As with the temperature analysis, assessing humidity against height is less useful for global comparisons, as the results are largely affected by the height of the tropopause and cloud layers. As these features are highly variable, even within this trial period, the exceptions noted in the sections below are only valid at the levels seen during the trial for the trial period. Therefore an analysis against temperature should give a better impression of how the radiosondes might perform globally from a climatic perspective.

At night-time, the RS41 humidity measurements are slightly higher (< 1.5%) at almost all temperatures except for the lower troposphere and after the tropopause (Figure 34). The causes of both of these exceptions are discussed below.

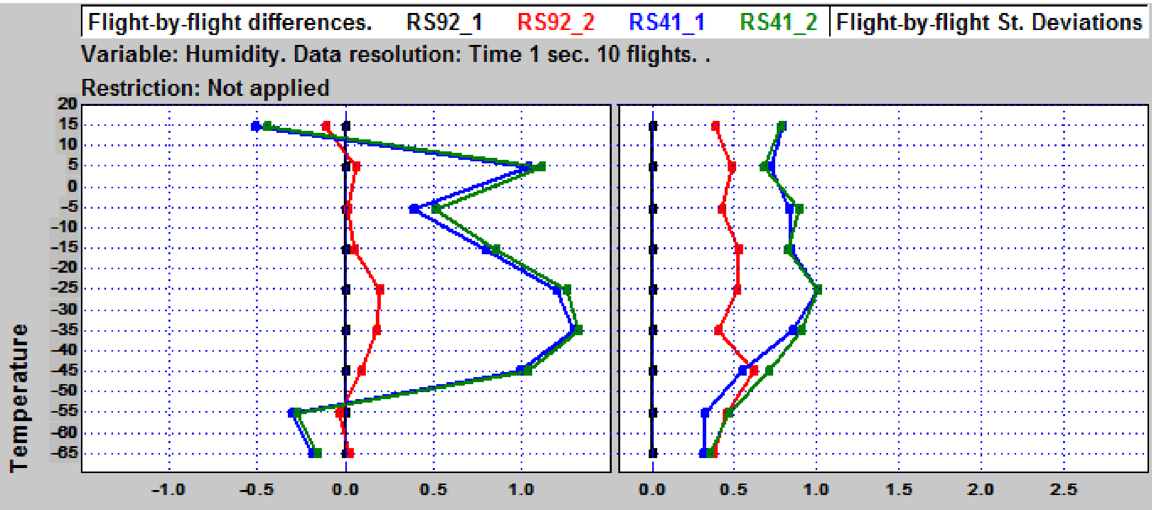

Figure 34 - Night-time humidity comparison average RS92_1 vs. RS92_2 and RS41 flight-by-flight differences (left) and flight-by-flight standard deviations vs. RS92_1 dataset (right).

The RS41 radiosondes observe slightly higher humidity values (<1.0%) than the RS92 radiosondes at temperatures above approximately -45°C during the daytime (Figure 35).

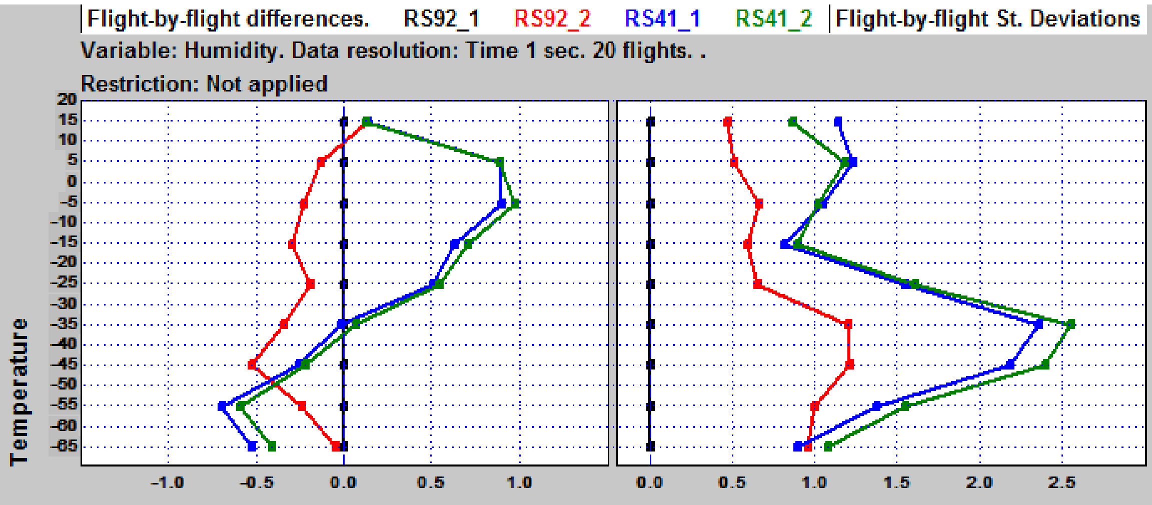

Figure 35 - Daytime humidity comparison average RS92_1 vs. RS92_2 and RS41 flight-by-flight differences (left) and flight-by-flight standard deviations vs. RS92_1 dataset (right).

Daytime performance in humidity bands vs. temperature

Figures 34 and 35 show measured consistent relative humidity differences for the RS41 relative to the RS92 over different temperature ranges. It is necessary, however, to also divide the data into relative humidity ranges, as these consistent differences may be reduced or magnified under certain humidity conditions.

The disadvantage of being more selective in the data being analyzed is the reduction in sample sizes which reduces the reliability of the statistics. When fewer flights are used, the differences between sondes will become increasingly dominated by the characteristics of individual sensors, their calibrations and the effect of atmospheric conditions, as opposed to being truly representative of differences between radiosonde models.

Data from temperature ranges where the sample size was three or less has been highlighted in grey in the following section. The reliability of the statistics can partially be seen in the flight-by-flight differences between the RS92 radiosondes in each plot. When the sample size is small, the mean difference between the RS92s increases, whereas with large sample sizes, the differences between pairs of RS92s tend to average out. The statistics produced by the analysis of data from the daytime were more robust, due to the fact that there were 20 daytime flights compared with 10 at night.

The flight-by-flight differences in measured humidity between radiosondes varied widely when using restricted humidity bands. As such, the x-axis of the plots in Figures 36 - 45 have been set to all be the same, to simplify visual intercomparison between figures.

Day, 0 – 20 % RH

At very low humidities during the day, the RS41 radiosondes show slightly higher humidity values relative to the RS92 radiosondes, with an average flight-by-flight difference in measured relative humidity of around 1% higher than the RS92s between -30°C and -50°C. The RS41 radiosondes show slightly lower humidity values relative to the RS92 radiosondes of around 0.5% between -50°C and -70°C. This ties in well with the consistent difference observed in Figure 35 where no humidity restriction is applied to the daytime data.

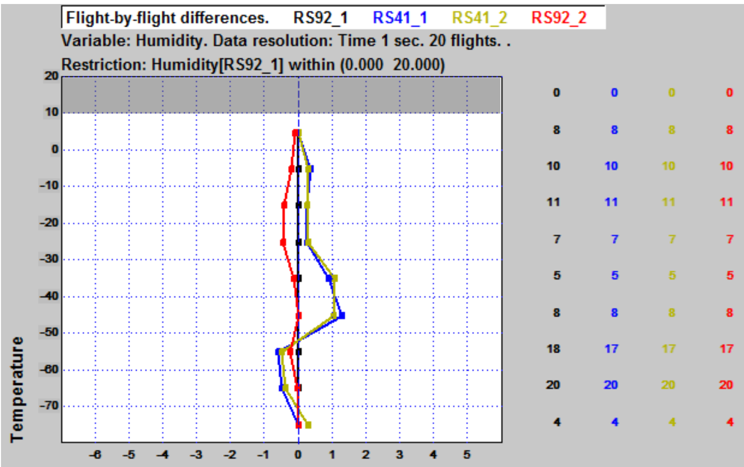

Figure 36 - Daytime flight-by-flight humidity differences between RS92_1 vs. RS92_2 and RS41 radiosondes along with sample size, using only data where 0% < RH(RS92_1) < 20%.

Day, 20 - 40 % RH

At slightly higher humidities during the day, the RS41 radiosondes measured higher humidities relative to the RS92 radiosondes to 1% between -30°C and 0°C, and 2% between -50°C and -30°C. The RS41 radiosondes measured lower humidities relative to the RS92 radiosondes between 0°C and 10°C of 2.5%. The sample size between -70°C to -80°C is too small, and so is marked grey.

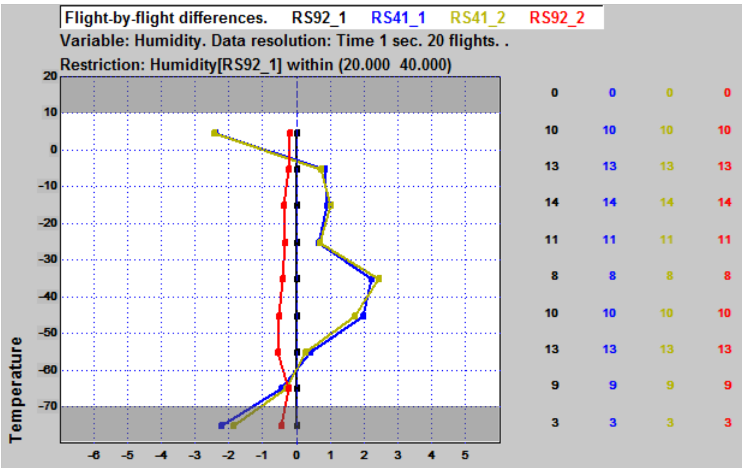

Figure 37 - Daytime flight-by-flight humidity differences between RS92_1 vs. RS92_2 and RS41 radiosondes along with sample size, using only data where 20% < RH(RS92_1) < 40%.

Day, 40 - 60 % RH

The differences between sonde types remain similar to the daytime 20 – 40 % relative humidity restricted data. The consistent difference between -80°C and -70°C has now approximately doubled but is still marked grey. The difference in the -70°C and -60°C temperature range has a larger sample size, indicating that this feature of the data is becoming more reliable.

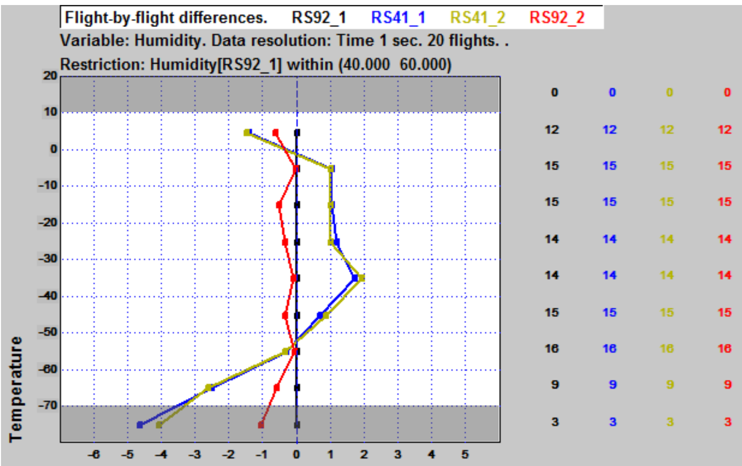

Figure 38 - Daytime flight-by-flight humidity differences between RS92_1 vs. RS92_2 and RS41 radiosondes along with sample size, using only data where 40% < RH(RS92_1) < 60%.

Day, 60 - 80 % RH

At higher humidities, the consistent differences above 0°C and down to -30°C are less pronounced when compared with the previous humidity range. The consistent difference at low temperatures starts below -30°C, and increases to around 6.5 % between -80°C and -70°C. There are only two ascents where such high humidities were detected in this temperature range so it is marked grey. However between -70°C and -60°C there is a greater sample size, and the consistent difference is still present.

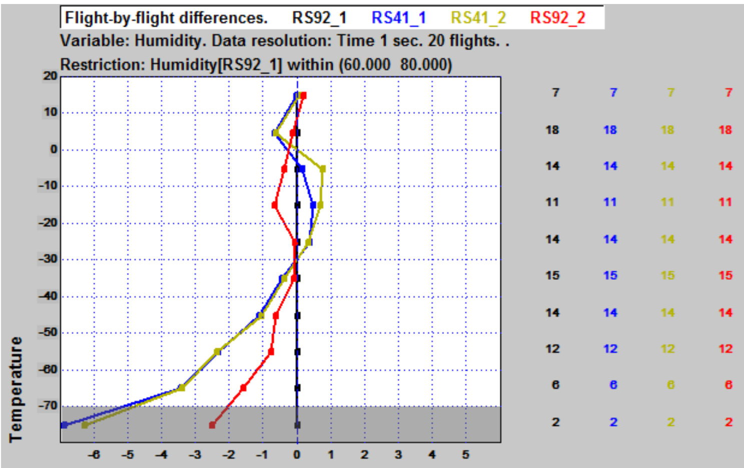

Figure 39 - Daytime flight-by-flight humidity differences between RS92_1 vs. RS92_2 and RS41 radiosondes along with sample size, using only data where 60% < RH(RS92_1) < 80%.

Day, 80 - 100 % RH

During the test, no conditions of relative humidities above 80 % were observed at temperatures below -60°C. Such high humidities relative to water at such cold temperatures would not be expected to be common. In the 80 – 100 % humidity range, the RS41 radiosondes no longer measure lower humidity values on average than the RS92 radiosondes between 0 to 10^{o}C. The RS41 radiosondes measured lower humidities relative to the RS92 radiosondes between -60°C and -20°C, with the greatest effect at lower temperatures, at around 4.5%.

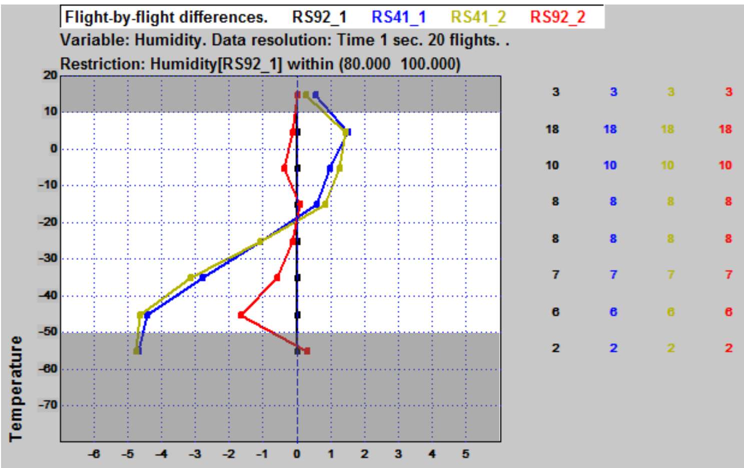

Figure 40 - Daytime flight-by-flight humidity differences between RS92_1 vs. RS92_2 and RS41 radiosondes along with sample size, using only data where 80% < RH(RS92_1) < 100%.

Night-time performance in humidity bands vs. temperature

Night, 0 – 20 % RH

At low humidities during the night, the RS41 radiosondes show consistently lower humidities relative to the RS92 radiosondes between 0°C to -10°C of about 1%. The RS41 radiosondes show consistently higher humidities of about 1% relative to the RS92 radiosondes at lower temperatures, similar to what is observed in some humidity ranges during the daytime. The differences observed in the -80°C to -70°C range are less robust due to the sample consisting of a single flight and are coloured grey.

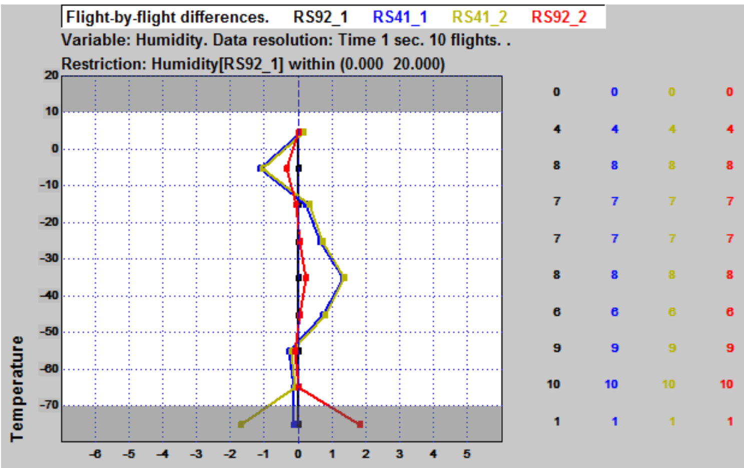

Figure 41 – Night-time flight-by-flight humidity differences between RS92_1 vs. RS92_2 and RS41 radiosondes along with sample size, using only data where 0% < RH(RS92_1) < 20%.

Night, 20 - 40 % RH

The structure of a consistent differences at higher and mid-range temperatures is maintained in the 20 – 40 % RH range. The differences below -60°C are less robust due to small sample sizes and are coloured grey.

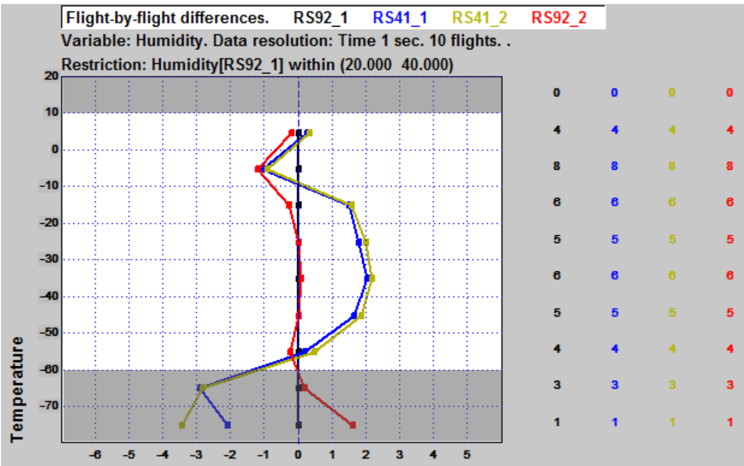

Figure 42 – Night-time flight-by-flight humidity differences between RS92_1 vs. RS92_2 and RS41 radiosondes along with sample size, using only data where 20% < RH(RS92_1) < 40%.

Night, 40 - 60 % RH

The key difference here to the previous range is that the RS41 radiosondes do not show consistently lower humidities relative to the RS92 radiosondes between 0°C to -10°C in the 40 – 60 % RH range. The consistent differences at lower temperatures is still present, and has increased slightly in magnitude in the -40°C to -30°C range to just over 2%. The differences below -60°C are less robust due to small sample sizes and are coloured grey but are consistent with the 20 – 40 % RH range.

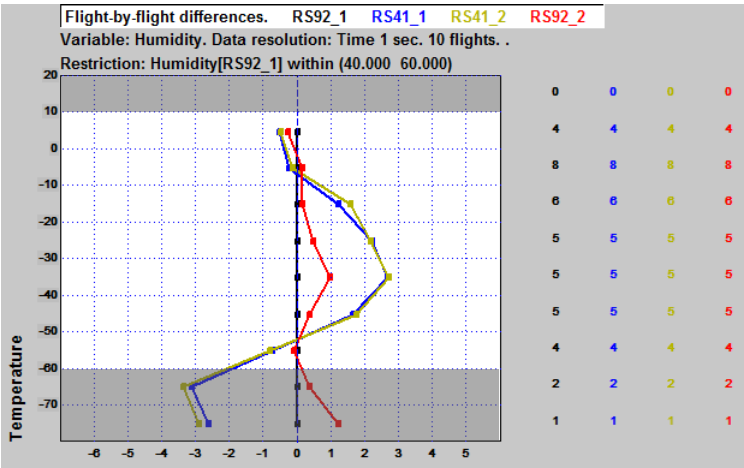

Figure 43 – Night-time flight-by-flight humidity differences between RS92_1 vs. RS92_2 and RS41 radiosondes along with sample size, using only data where 40% < RH(RS92_1) < 60%.

Night, 60 - 80 % RH

Above -10°C, each temperature range alternates between small consistent differences between the two radiosonde types. The RS41 radiosondes show consistently higher humidities in the -20°C to -10°C band of around 1.5 %. The consistently lower RS41 humidities relative to the RS92 radiosondes below -50°C is still present. However, the sample size for all temperature ranges below -20°C was very small and has been marked grey.

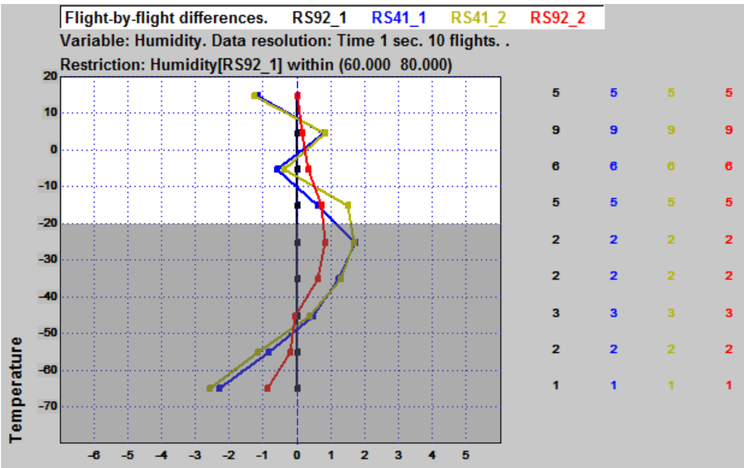

Figure 44 – Night-time flight-by-flight humidity differences between RS92_1 vs. RS92_2 and RS41 radiosondes along with sample size, using only data where 60% < RH(RS92_1) < 80%.

Night, 80 - 100 % RH

Between -10°C and 10°C, the RS41 radiosondes show measured consistently higher humidities than the RS92 radiosondes of around 1.5%. At night, only one flight contained data from temperatures below -10°C where the relative humidity above 80 %, making the statistics less reliable. As in the daytime ascents, high humidities relative to water at low temperatures become rarer.

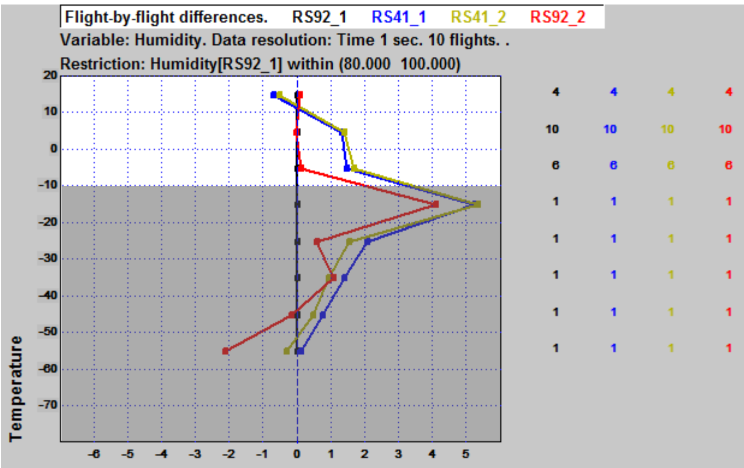

Figure 45 – Night-time flight-by-flight humidity differences between RS92_1 vs. RS92_2 and RS41 radiosondes along with sample size, using only data where 80% < RH(RS92_1) < 100%.

Conclusion from relative humidity vs. temperature range analysis

The analysis of relative humidity in relative humidity ranges provides more insight than could be achieved using only the division of data into daytime and night-time. This is because there are apparent features of the data that move with respect to temperature in different relative humidity ranges and are often caused by meteorological phenomena such as clouds or the very low humidity above the tropopause.

The RS41 radiosondes frequently show consistently higher humidity values relative to the RS92 radiosondes in many of the temperature ranges seen during this trial (approximately -50°C to -10°C) during both the daytime and night-time.

The consistently lower humidity values observed by RS41 relative to the RS92 below -60^{o}C are described in the ‘RS92 vs. RS41: Performance at or above the tropopause’ section.

The consistently higher humidity values observed by RS41 relative to the RS92 in the >80% humidity band during the daytime and night-time is discussed in the ‘RS92 vs. RS41: Behaviour around the lower troposphere and clouds’ section.

The typical average flight by flight agreement of the RS92 and RS41 radiosondes is within ±3% when measured in 10^{o}C temperature bands. This is only exceeded for two temperature and humidity bands within the dataset with sample sizes of over 3 ascents.

RS92 precision

The agreement between the RS92_1 and 2 humidity observations was good at all temperatures observed during the trial although the agreement was better at night-time. The overall average flight-by-flight differences were within 0.5%. The 1 SD agreement between the two systems within ±1.2% humidity, when measured in 10°C bands.

As mentioned above, the RS92 humidity data is has a time lag correction applied. This is applied for both daytime and night-time ascents and is applied more strongly to the later parts of the ascent as the temperature decreases. This does not appear to increase the variability between the two RS92 radiosondes as temperatures decrease at night-time.

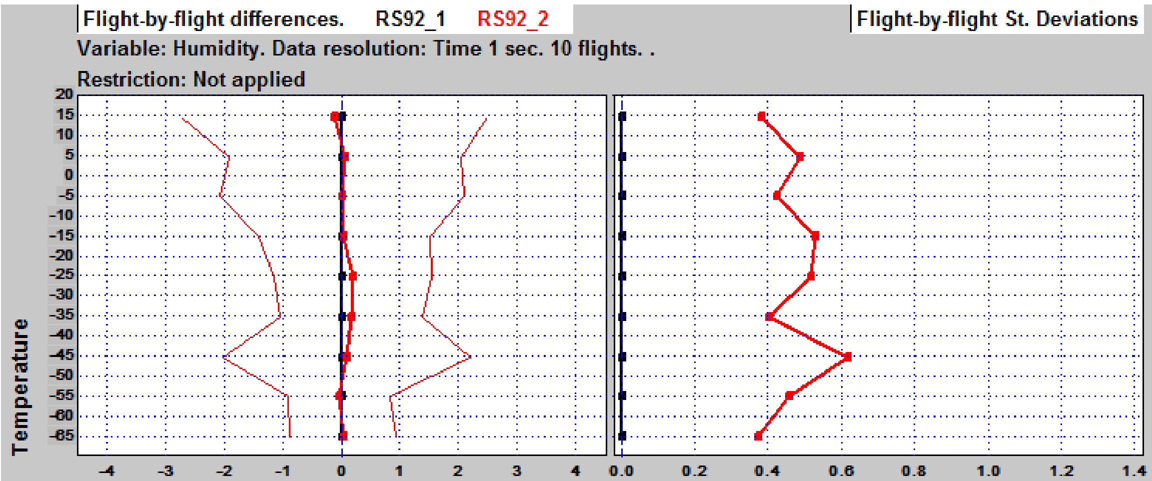

Figure 46 – Night-time humidity - average RS92_1 vs. RS92_2 flight-by-flight direct differences with direct difference 2σ lines (left) and standard deviations (right) across temperature ranges.

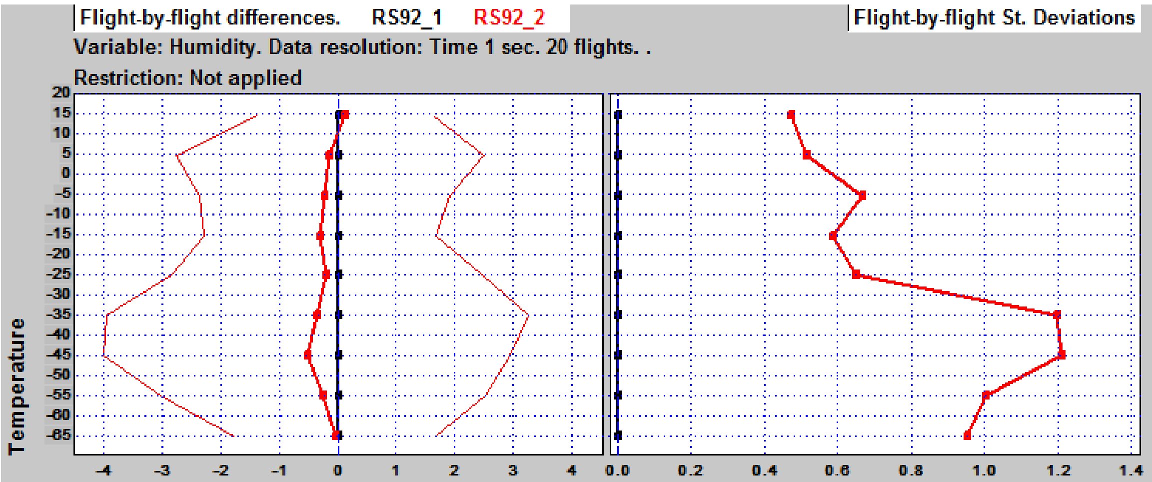

Figure 47 - Daytime humidity - average RS92_1 vs. RS92_2 flight-by-flight direct differences with direct difference 2σ lines (left) and standard deviations (right) across temperature ranges.

The daytime RS92 humidity data has an additional correction applied for solar radiation. When comparing the raw and processed data, this has a variable impact. The correction is larger at higher altitudes and higher humidities, and is based on the solar angle relative to the radiosonde. It is likely to contribute to the higher variability seen during the daytime, especially at lower temperatures.

The *Vaisala RS92-SGP datasheet* indicates that the reproducibility (precision to 1 SD) of RS92 humidity measurements is ±2%. The flight-by-flight standard deviation results in Figure 46 and Figure 47 are within these boundaries at ±0.6% at night and ±1.2% during the day.

Note that the 2σ lines on the figures above are for direct differences rather than flight-by-flight differences, so are only to enable easier visual comparison of the figures. The *Vaisala RS92-SGP datasheet* states total uncertainty in humidity measurements as ±5% for the RS92 to 2σ.

RS41 precision

The agreement between the RS41 systems' humidity observations was very good at all temperatures observed during the trial although the agreement was also slightly better at night-time. The overall average flight-by-flight differences were within ±0.2%. The overall 1 SD agreement between the two systems was within ±0.6% humidity in the 10°C bands used in this trial, which indicates a higher degree of humidity measurement precision than the RS92 radiosondes.

The RS41 humidity data also has a time lag correction applied. This is applied for both daytime and night-time ascents and its application is more noticeable during the later parts of the ascent as the sensor cools. As with the RS92 radiosondes, this does not appear to result in any increased variability between the two RS41 radiosondes.

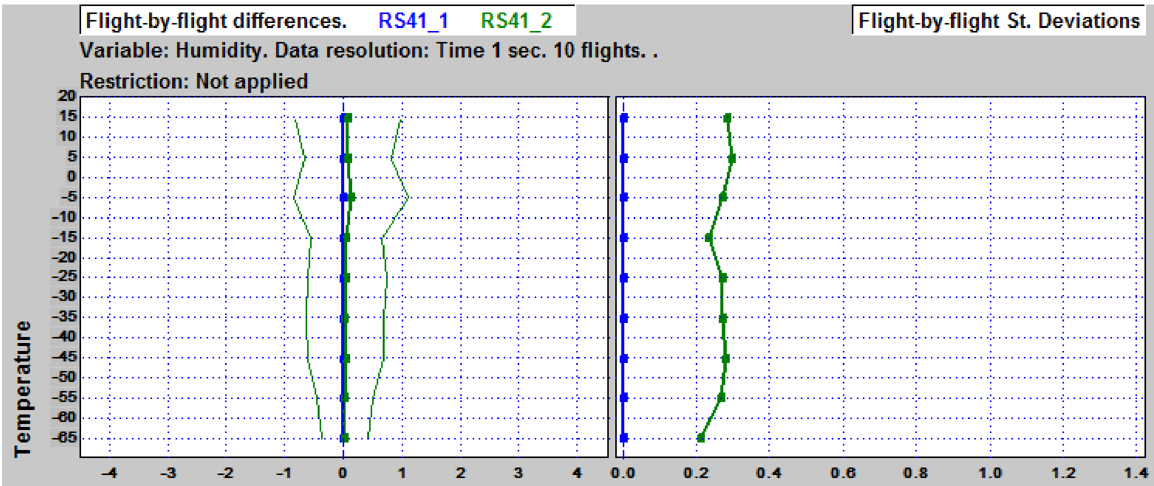

Figure 48 - Night-time humidity - average RS41_1 vs. RS41_2 flight-by-flight direct differences with direct difference 2σ lines (left) and standard deviations (right) across temperature ranges.

The RS41 humidity data accounts for changes in the temperature of the humidity sensor caused by solar radiation, unlike the RS92 where a correction is applied based on calculated solar angle. Solar radiation introduces an additional source of into daytime humidity observations when compared with night-time observations. The RS41 daytime measurements have lower standard deviations than the RS92 daytime measurements, especially at temperatures below -25°C.

The *Vaisala RS41-SG datasheet* indicates that the reproducibility (precision to 1 SD) of RS41 humidity measurements is ±2% (above 3m/s). The flight-by-flight standard deviation results in Figure 48 and Figure 49 are within these boundaries at ±0.3% at night and ±0.6% during the day which is roughly half that of the RS92 SD, indicating significantly improved humidity precision.

Note that the 2σ lines on the figures are for direct differences rather than flight-by-flight differences, so are only to enable easier visual comparison of the figures. The *Vaisala RS41-SG datasheet* states total uncertainty in humidity measurements as ±4% for the RS41 to 2σ.

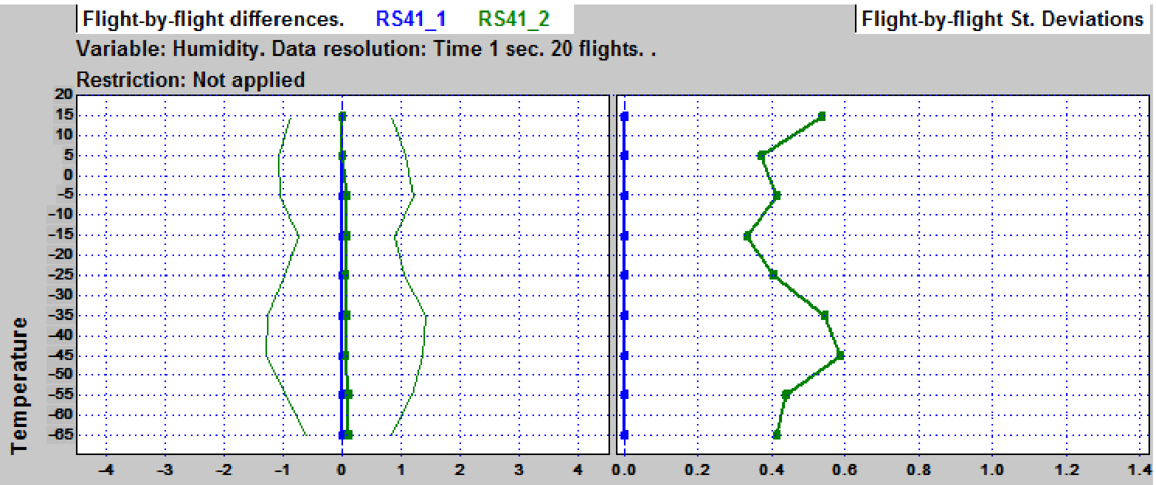

Figure 49 - Daytime humidity - average RS41_1 vs. RS41_2 flight-by-flight direct differences with direct difference 2σ lines (left) and standard deviations (right) across temperature ranges.

RS92 vs. RS41: Behaviour around the lower troposphere and clouds

The RS92 and RS41 performed similarly in the lower troposphere, but as with the temperature observations, radiosonde observations during and upon exit of cloud are often the regions of highest variability between the RS92 and RS41, as was the case in this trial. Figure 50 shows an example of disagreement between the humidity measurements of the RS41 and RS92 when exiting cloud. This may be caused by moisture contamination or a slower response of the RS92 humidity sensor, but the exact cause for the difference is unknown.

The RS41_1 and 2 and RS92_1 and 2 also showed higher humidity variability after exiting cloud in Figure 50, as before and after the cloud exit the humidity measurements were almost identical. This effect is also demonstrated between RS92_1 and 2 in Figure 52.

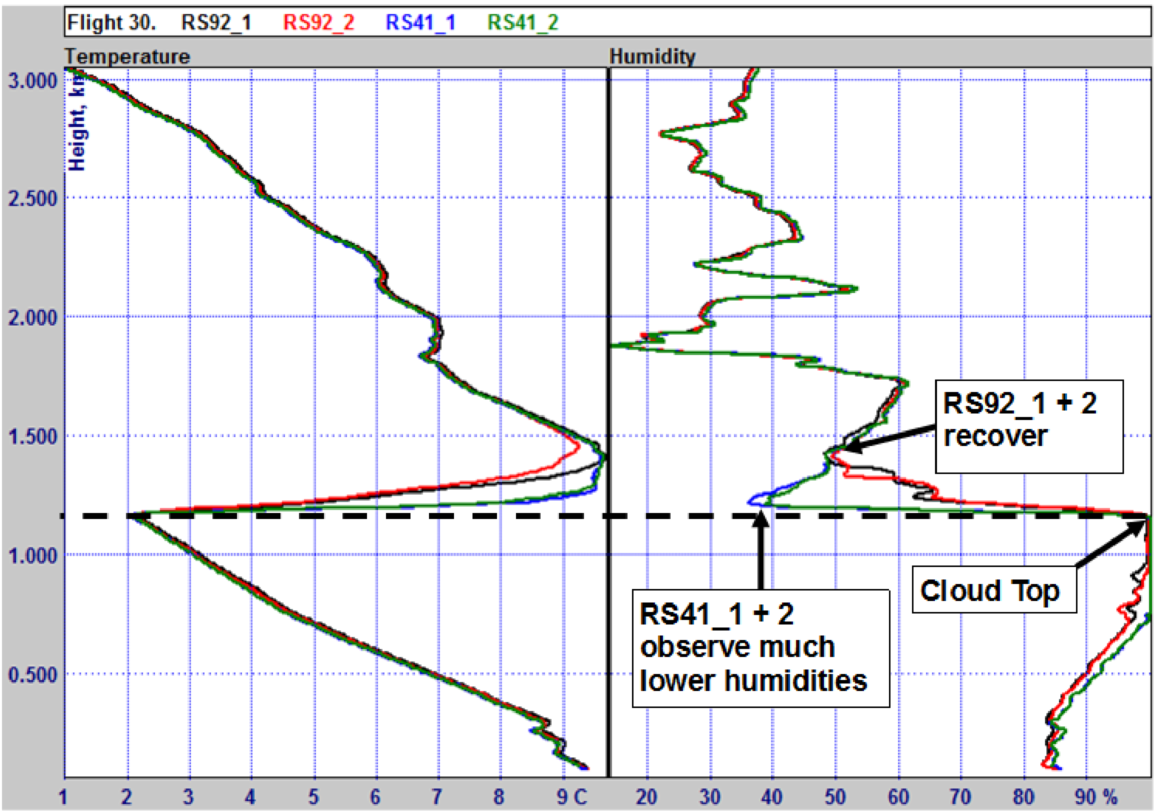

Figure 50 – Detailed section of flight 30 showing differing response times of RS92 and RS41 radiosondes after exiting a cloud layer with sensor moisture contamination.

In the lower troposphere, the RS92 sensors generally showed slightly lower humidity values in high-humidity situations than the RS41, and rarely reached 100% when in clouds. The RS41 sensors appeared to recover slightly faster than the RS92 sensors after exiting relatively thick cloud into a comparatively dry layer, as shown in Figure 50 and Figure 51. The performance behaviour of the RS92_1 and RS92_2 humidity sensors during the same flight was generally consistent, unlike the occurrence of wet-bulb events with the temperature sensors, which sometimes affected one RS92 more than the other.

.

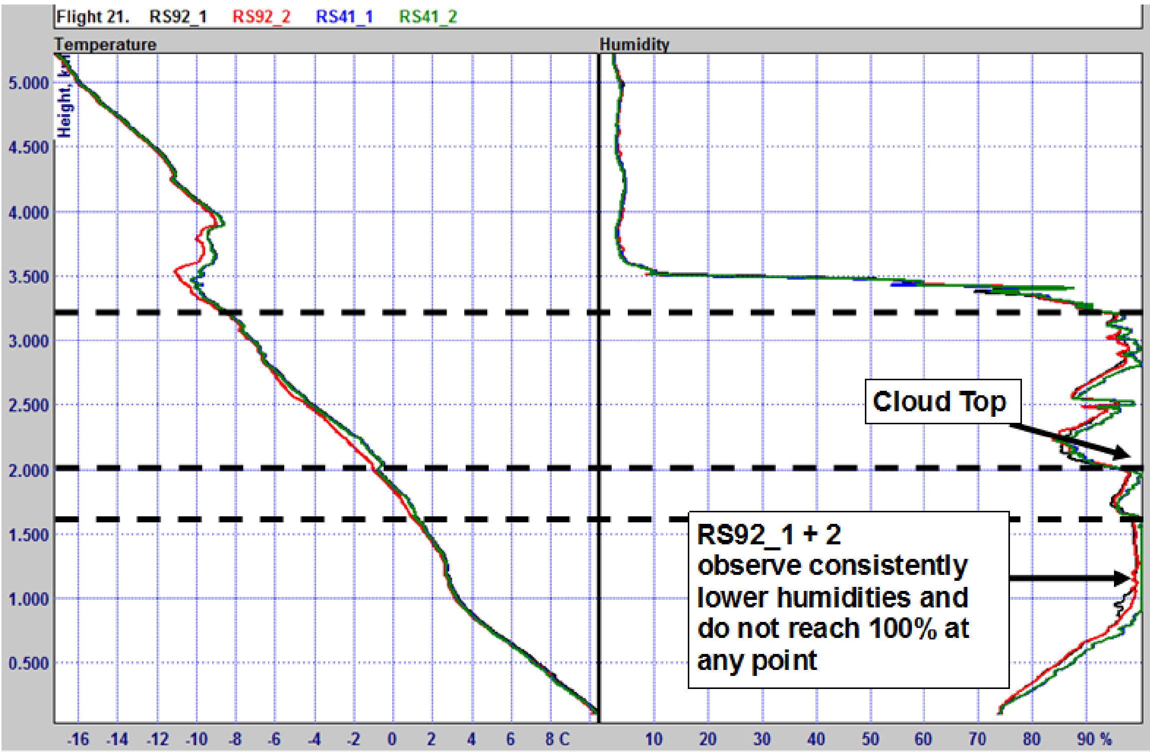

Figure 51 – Detailed section of flight 21 showing different maximum humidities measured by the RS92 and RS41 radiosondes. Temperature profile (left) shows several minor wet-bulb events seen by RS92_2 indicating cloud tops.

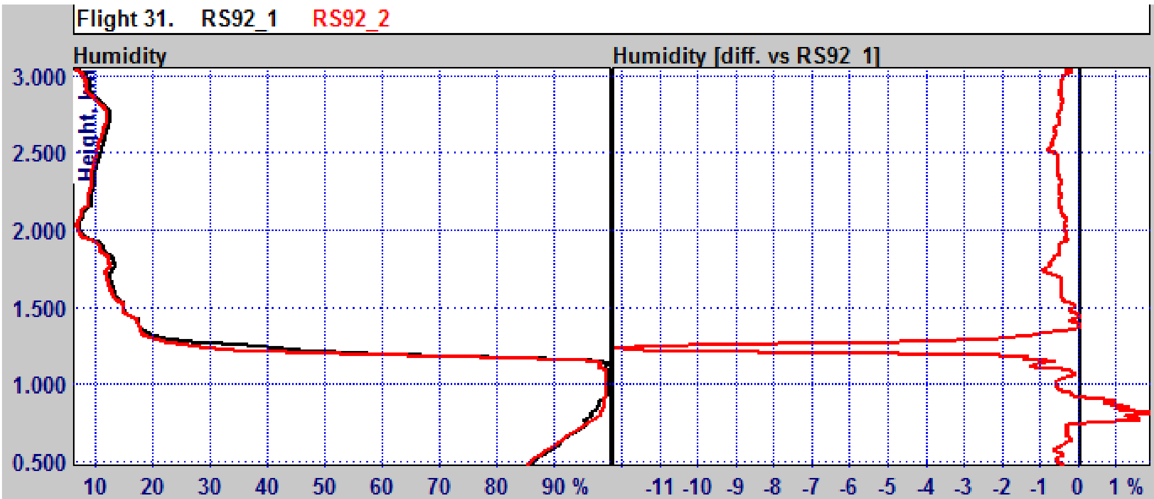

Figure 52 – Detailed section of flight 31 showing an increase in variability between RS92_1 and RS92_2 following an exit from cloud.

The *Vaisala RS92 datasheet* and *Vaisala RS41 datasheet* indicate that the RS41 humidity sensor should respond faster than the RS92 humidity sensors (< 0.3s vs. < 0.5s at 1000hPa and +20°C). It was not possible to confirm this response time during this trial, but it could help to explain the observed differences.

RS92 vs. RS41: Performance in the upper troposphere

The RS92 and RS41 radiosondes produce generally consistent profiles in the lower troposphere, but sometimes show distinct differences in the upper troposphere up to the tropopause. There are two specific phenomena to be discussed: higher RS92 humidity relative to the RS41 during the daytime and higher RS41 humidity relative to the RS92 during the night-time.

Higher RS92 humidity relative to the RS41 during the daytime

There were 7 flights where both RS92 radiosondes showed consistently higher humidities than the RS41 radiosondes for a period in the upper troposphere, which is against the usual trend observed during this trial (see Figure 53 for example). This seemed to happen when the humidities at these levels were high, indicating high-altitude cloud layers. There were also 2 flights where a similar effect was seen at night-time, but closer inspection showed that this was linked to the RS92 response time effect around the tropopause region, discussed in the next section.

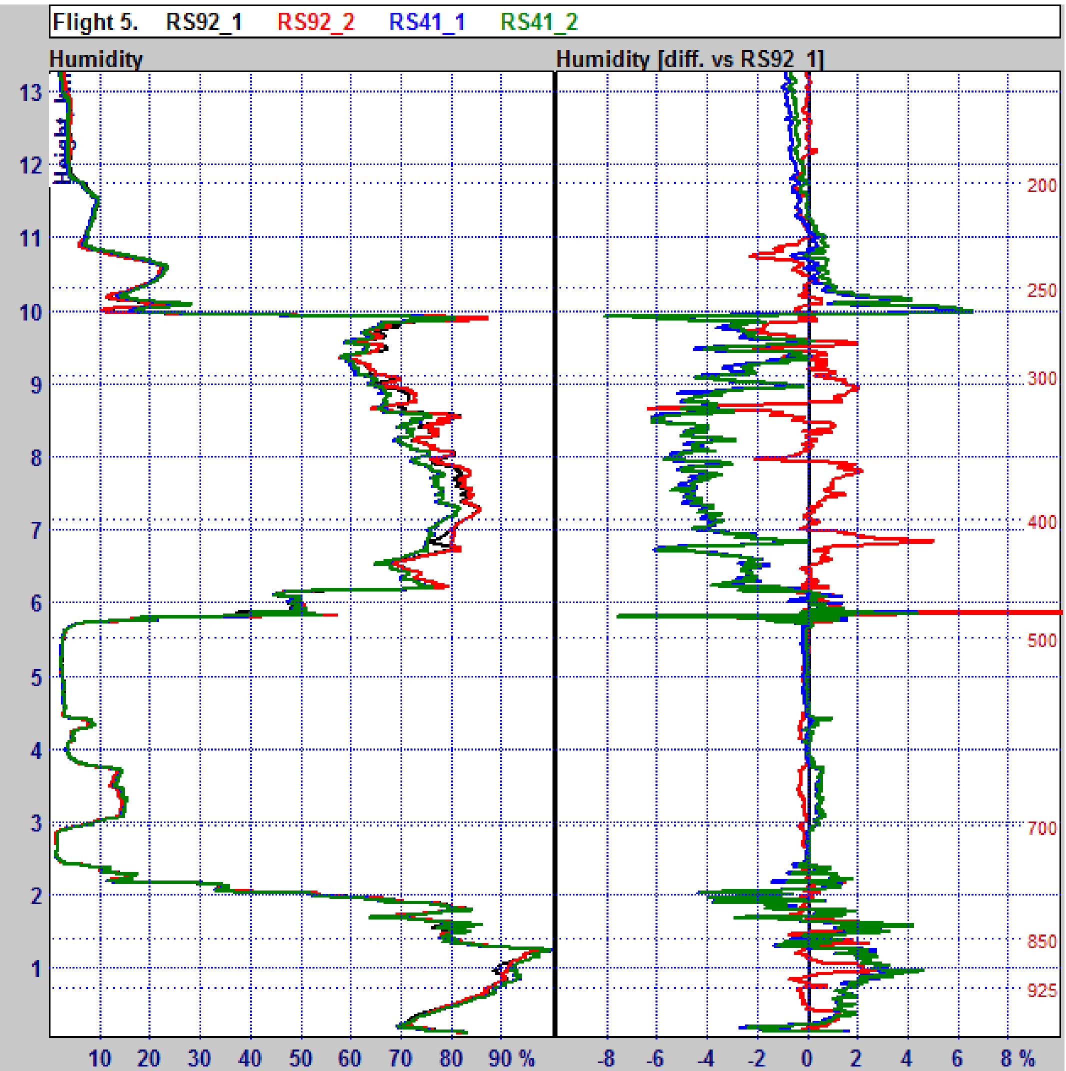

Figure 53 – Example from flight 5 of RS92_1 and 2 showing consistently higher humidities than the RS41_1 and 2 between 6-10 km. Humidity values (left) and differences from RS92_1 (right).

As this effect was inconsistent, even at similar humidities and temperatures on different days, the probable causes are either moisture contamination of the humidity sensor, or the application of the solar radiation correction. As these events occurred within the temperature and pressure levels where the humidity sensor alternate-heating process should have still been working, moisture contamination for the durations observed seems unlikely. This effect appears to demonstrate the effect of the different methods of correcting for solar radiation errors for the two radiosonde models.

During the daytime, humidity sensors are affected by heating from solar radiation, which creates a dry-bias in their measurements relative to night-time ascents. To counteract this, the RS92 humidity measurements are corrected based on a calculated solar angle, with the effect of increasing the reported humidity value above that of the measured humidity. If the radiosonde is receiving a different amount of radiation than would be expected from the calculated solar angle, then the correction being applied would introduce a bias.

As an example, if the radiosonde was inside or in the shadow of a cloud, then the solar radiation being received would be lower than expected by the software, and the radiosonde would therefore be reading a higher humidity than if it was in full sunshine. As a result, when the humidity correction is applied, more humidity is added than necessary, causing a wet-bias.

Analysis of the raw data backs up this theory, as in these particular circumstances, the RS92 humidity measurements are closer to those of the RS41 than usual during the day at those altitudes and temperatures, and appear more similar to their night-time measurements.

In contrast, the RS41 calculates its humidity values based on the actual temperature of the humidity sensor measured by its integrated temperature sensor. This allows for the calculation of humidity while accounting for the actual exposure of the sensor to solar radiation. The removal of this potential source of error should result in more accurate humidity measurements.

Higher RS41 humidity relative to the RS92 during the night-time

As was seen in the detailed night-time humidity performance analysis (Figure 32 and Figure 34), the RS41 measurements show consistently higher humidity relative to the RS92 measurements. This is a slight but consistent difference, typically in the order of 1-2%. It is present in every night-time ascent, although the effect is slightly variable and is dependent on the temperature and humidity at the time of measurement. In general higher humidity values have greater differences, and the effect is larger at low temperatures (Figure 54).

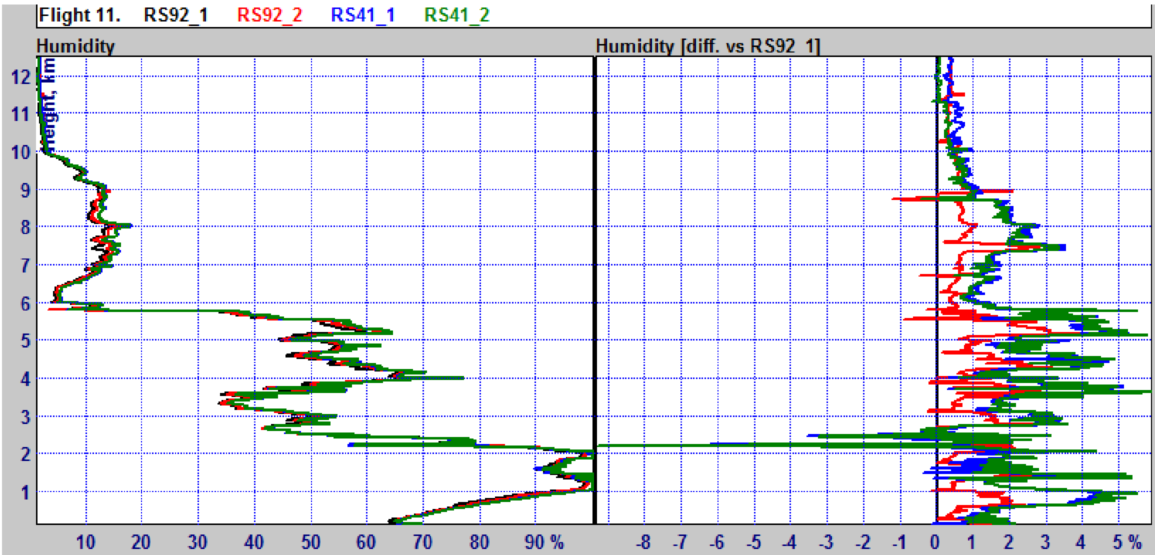

Figure 54 – Detailed section of flight 11 showing a consistent positive bias for humidity measurements of both RS41 radiosondes relative to the RS92 radiosondes.

As this is a night-time effect, only time-lag corrections are being applied, and these would not account for the consistency of this bias throughout the ascent. This is confirmed by analysis of the raw data, which shows the same differences.

Therefore, this indicates a genuine difference in the sensor measurements between the two radiosonde models, with the RS41 measuring consistently a higher humidity of < 1.5% than RS92_1 at almost all temperatures, except for the lower troposphere and after the tropopause (Figure 34). The difference between the RS92_1 and 2 radiosondes for the same period was < 0.3%, which indicates that the effect is consistent between the RS92 and RS41 generally.

The difference occurs for both RS41 radiosondes relative to both RS92 radiosondes and so appears genuine during this trial including the variability of the RS92 and RS41 radiosondes.

RS92 vs. RS41: Performance at or above the tropopause

A known problem with radiosonde humidity sensors in general is moisture contamination of the sensors in the upper troposphere leading to unrealistically high humidity readings. These can sometimes persist until the end of the ascent. Two key problems with measuring humidity at high altitudes are the slow response time of sensors at low temperatures and pressures, and the slow sublimation rate of ice at low pressures. Both of these can lead to higher humidity readings than are measured by more accurate scientific instruments as demonstrated in the *2010 WMO intercomparison*.

The RS92 has both hardware and software features to try and minimise the effect of these problems, and these demonstrated good performance when compared with the cryogenic frost-point hygrometer (CFH) radiosonde in the *2010 WMO intercomparison*. The RS41 uses different hardware features, but similar software features.

Moisture contamination

Water and ice can contaminate the surface of a sensor when the radiosonde passes through a cloud or area of high humidity. The rate at which this moisture contamination will naturally evaporate or sublimate from a surface is determined by several factors, including atmospheric temperature, pressure and the water vapour content of the air. At lower temperatures and pressures, this rate is slower, meaning that the moisture contamination can persist for longer after it was deposited on the surface of the sensor.

The alternate heating process of the RS92 humidity sensors is designed to reduce the impact of moisture contamination, but this is switched off to conserve power once certain temperature or pressure criteria are met. This could lead to persistent moisture contamination in the upper troposphere and lower stratosphere, although 59 of the 60 RS92 ascents showed no notable moisture contamination.

For the RS92 radiosondes, RS92_1 in flight 6 was contaminated, as shown in Figure 57. There were several instances of consistent humidity differences between the radiosondes after the tropopause of 1-2%, or of noisy humidity measurements after the tropopause (Figure 55). Most flights showed small but consistent stratospheric differences between RS92_1 and RS92_2.

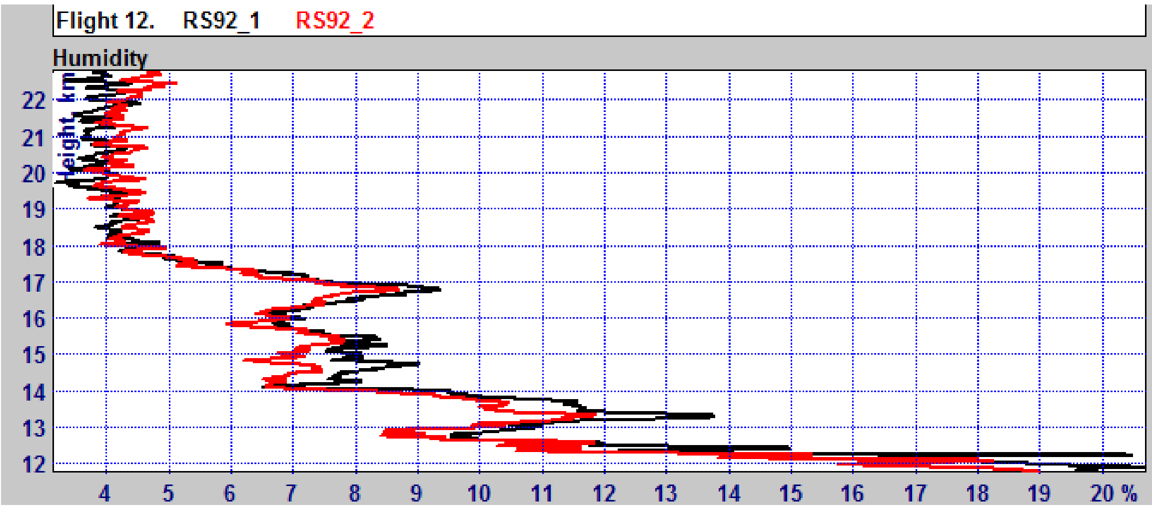

Figure 55 – Detailed section of flight 12 showing noisy stratospheric humidity data from both RS92 radiosondes above 18 km.

For the RS41 radiosondes, there were no notable instances of moisture contamination. There were a similar number of small, consistent differences between RS41_1 and RS41_2 radiosondes in the stratosphere, as were seen with the RS92 radiosondes. There were no instances of the noisy stratospheric humidity data seen with the RS92.

Table 2 in annex 2 shows the instances where the consistent differences were seen between RS92_1 and, 2 and RS41_1 and 2, showing 19 instances for each radiosonde type.

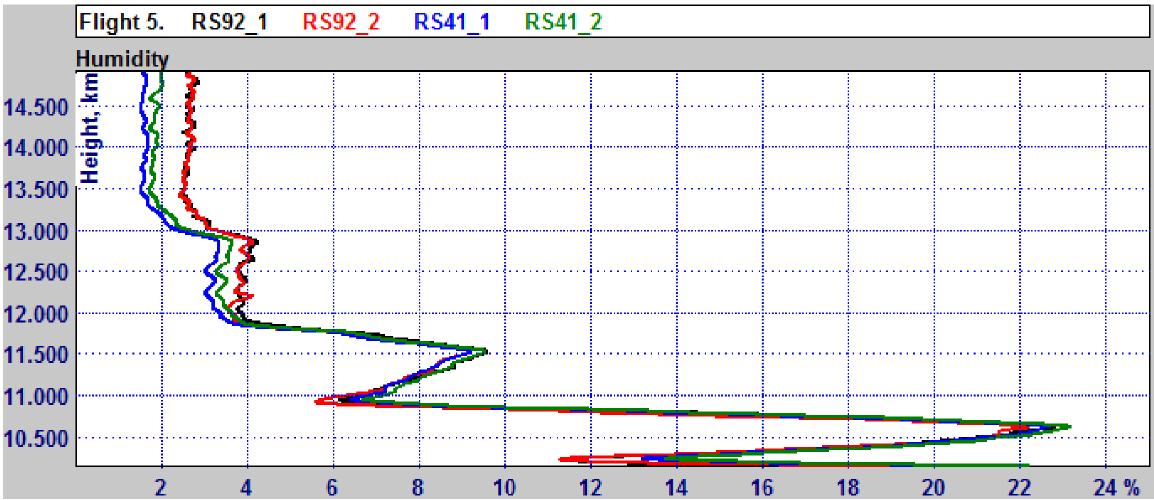

Figure 56 – Detailed section of flight 9 showing consistent differences between the RS41 radiosondes in the stratosphere, and generally higher humidity values measured by the RS92 radiosondes.

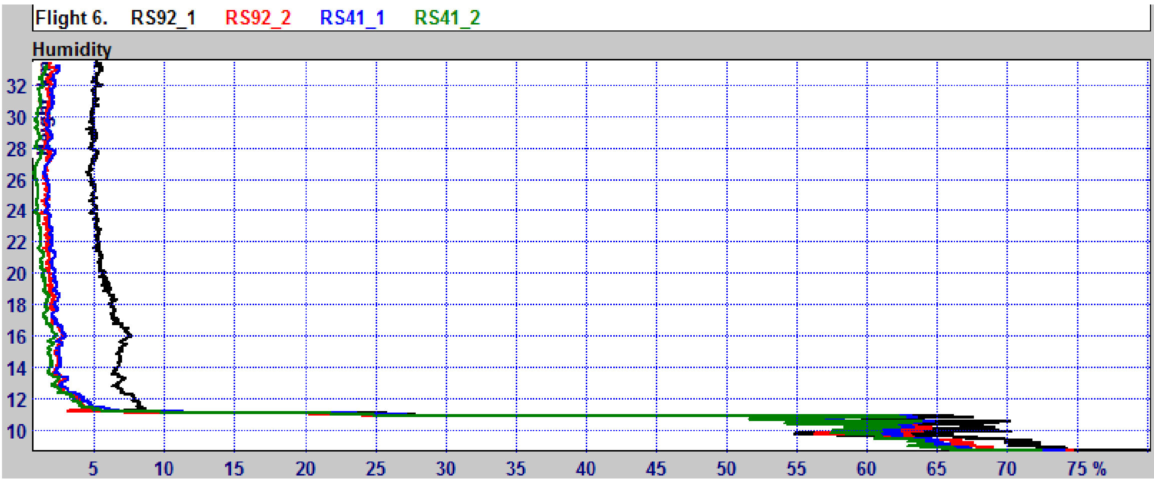

Figure 57 – Detailed section of flight 6 showing RS92_1 with humidity sensor moisture contamination in the stratosphere.

The slight consistent differences measured between the RS92 and RS41 radiosondes in the upper troposphere and lower stratosphere may not be due to moisture contamination, but could be due to genuine slight differences in the humidity sensor performance for each radiosonde at low pressures and temperatures.

The results of this trial show both the RS92 and RS41 hardware features are effective in reducing the risk of humidity sensor contamination by moisture. As the RS41 humidity heating element does not need to be switched off, the RS41 should be more resistant to these events than the RS92, resulting in more accurate humidity measurements.

In general, the RS41 measured slightly lower humidity values above the tropopause than the RS92, leading to the consistent differences seen in Figures 32 and 33.

Differences in sensor response times

The response times to changes in humidity measured by the sensors used by the RS92 and RS41 radiosondes are known to slow down at low pressures and temperatures. This is typical of radiosonde humidity measurements in general. The *Vaisala RS92 datasheet* and *Vaisala RS41 datasheet* state the response times as:

- < 0.5s for RS92 and < 0.3s for RS41 at 6m/s, 1000 hPa and +20^{o}C
- < 20s for RS92 and < 10s for RS41 at 6m/s, 1000 hPa and -40^{o}C

To counter this, a time lag correction factor is applied to both sets of data. A discussion on how this is implemented and its effects are outside of the scope of this report, but have been documented previously by Vaisala and during the *2010 WMO intercomparison*. The effect of the time lag correction is variable throughout the ascent, but during this trial it became most noticeable in the upper troposphere.

Figure 58 – Detailed section of flight 27 showing unusually high RS92 humidity values which are less sharply defined than usual.

Table 2 in the annex shows the 16 occasions when the humidity sensors of the RS92 radiosondes exhibited slower response times than usual, showing less sharply defined humidity values, and 1 occasion where this was seen with the RS41. This effect is hard to categorise and may be down to the corrections applied by the software, but it represents a genuine difference in the humidity data between the RS92 and RS41 models. This effect is responsible for the sudden shift in consistent differences and increase in variability seen between the RS92 and RS41 radiosondes in Figures 32 and 33.

Humidity conclusions

The comparison of humidity between the RS41 and RS92 is complex due to the varying impacts of atmospheric conditions, sensor hardware and software corrections. However, it has been possible to identify key differences between the radiosonde systems.

Generally, the RS41 observes slightly higher humidity values than the RS92 below the tropopause and in the lower troposphere, as highlighted by the consistent daytime and night-time differences throughout the humidity and temperature bands. This consistent difference is typically < 1.5%.

During the day, the RS92 sometimes measures consistently higher humidity when in upper level areas of high humidity. This appears to be because the solar radiation corrections applied are only based on calculated solar angle. The humidity sensor of the RS41 which contains an integrated temperature sensor should eliminate this potential source of error, providing more accurate humidity measurements than the RS92 in these situations.

There are slight timing differences in the positions of some features between the two radiosonde types, but these are caused by software corrections rather than genuine differences in sensor performance and were generally of negligible impact.

In the lower troposphere, the RS41 sometimes exhibited faster response times to sudden changes in humidity when exiting clouds, and also slightly greater humidity values when measuring inside of clouds. The RS41 should therefore provide more accurate humidity measurements than the RS92 in these situations. Both radiosonde models exhibited increases in humidity variability when exiting cloud in some situations, indicating that the sensors can be affected by moisture contamination.

When approaching the tropopause following a region of relatively high humidity, the RS92 was sometimes exhibited slower humidity sensor response times than the RS41, resulting in differences between the two radiosonde types. While the software time lag corrections usually ensure very similar performance of the RS41 and RS92 in this region, there is a genuine difference in performance in these specific conditions.

Above the tropopause, the RS41 observes lower humidity values than the RS92 causing a small but consistent dry bias. It is not clear whether this is due to slight moisture contamination of the RS92 sensors or due to genuine differences in the performance of the sensors. The RS92 humidity sensor was seen to be contaminated on one occasion, indicating that this is not a major problem, but could contribute to the overall dry-bias exhibited by the RS41 relative to the RS92 if it does not experience moisture contamination in a similar way. The continuation of the heating capability of the RS41 humidity sensor for the duration of the flight should reduce the risk of contaminated stratospheric humidity values, and should therefore provide more accurate humidity measurements than the RS92 in these situations.

The RS41 demonstrated greater humidity measurement precision than the RS92 at all temperature ranges during the night-time to 1 SD, and all but the 10-20°C band during the daytime to 1 SD.

Overall, the RS41 demonstrates several small improvements to humidity measurement performance over the RS92, which should result in more accurate humidity observations, measured to a higher degree of precision. The consistent differences discussed above are within ±1.5% when measured in 10°C temperature bands. They have climatic significance and should be accounted for. Note that the altitudes and temperature ranges of some features will be variable due to their dependence on meteorological phenomena which vary globally.

Comparison of simultaneous wind measurements

RS92 vs. RS41

Due to the capabilities of modern GPS location technology, the averaged flight-by-flight differences between the wind speed components measured by each sonde and the RS92_1, shown in Figures 59 and 60 were approximately 1 or 2 cm/s. The standard deviations of these differences were generally less than 10 cm.

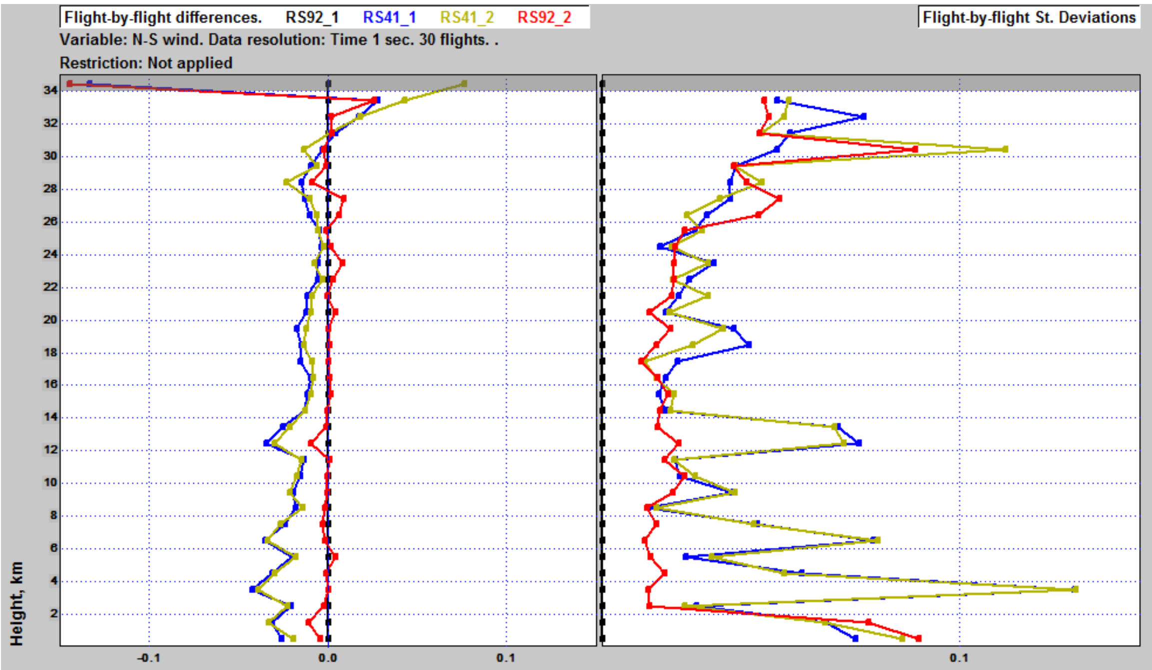

Figure 59 – N-S wind component comparison average RS92_1 vs. RS92_2 and RS41 flight-by-flight differences (left) and flight-by-flight standard deviations vs. RS92_1 dataset (right).

The average differences in the RS41 radiosondes compared with the RS92 radiosondes are an E-W consistent difference of around +1 cm/s and a N-S consistent difference of around -1 to -3 cm/s. This effect is thought to be caused by some effect of filtering. The wind components are not calculated from the GPS location of the radiosondes, but instead from the GPS signals so these differences would not result in a difference in the final location of the radiosondes.

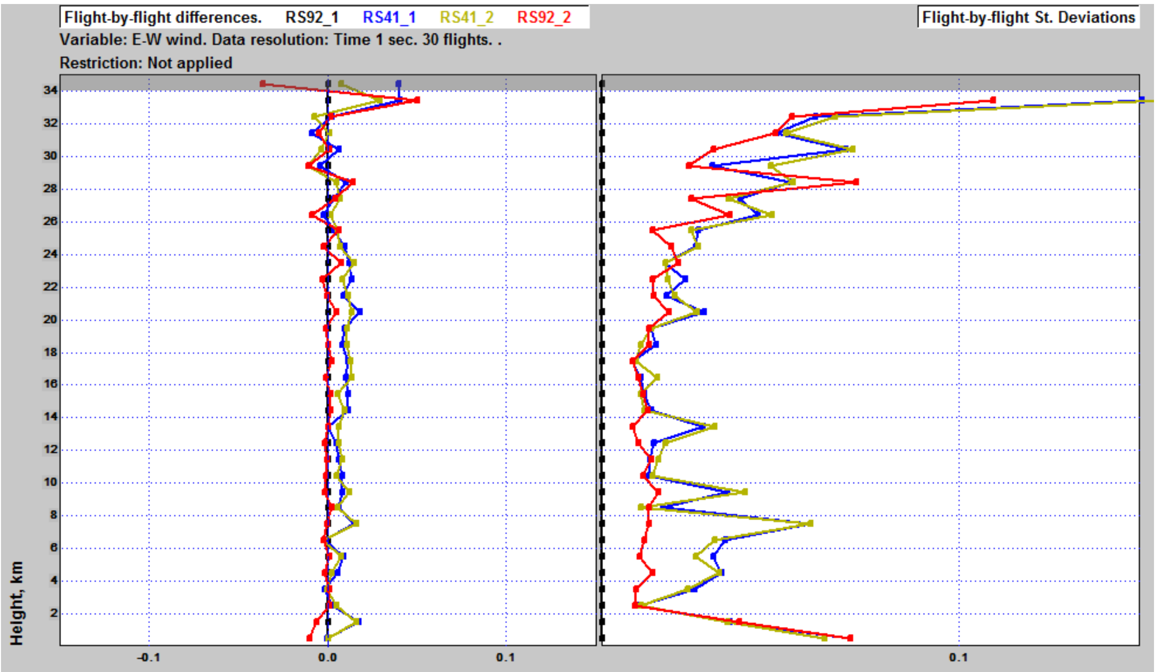

Figure 60 – E-W wind component comparison average RS92_1 vs. RS92_2 and RS41 flight-by-flight differences (left) and flight-by-flight standard deviations vs. RS92_1 dataset (right).

Precision

Figures 61 to 64 show the flight-by-flight differences between the wind speeds measured by the RS41 radiosondes against each other and RS92 radiosondes against each other. Differences for both sonde types are generally around 1 cm/s, as were standard deviations in the flight-by-flight differences.

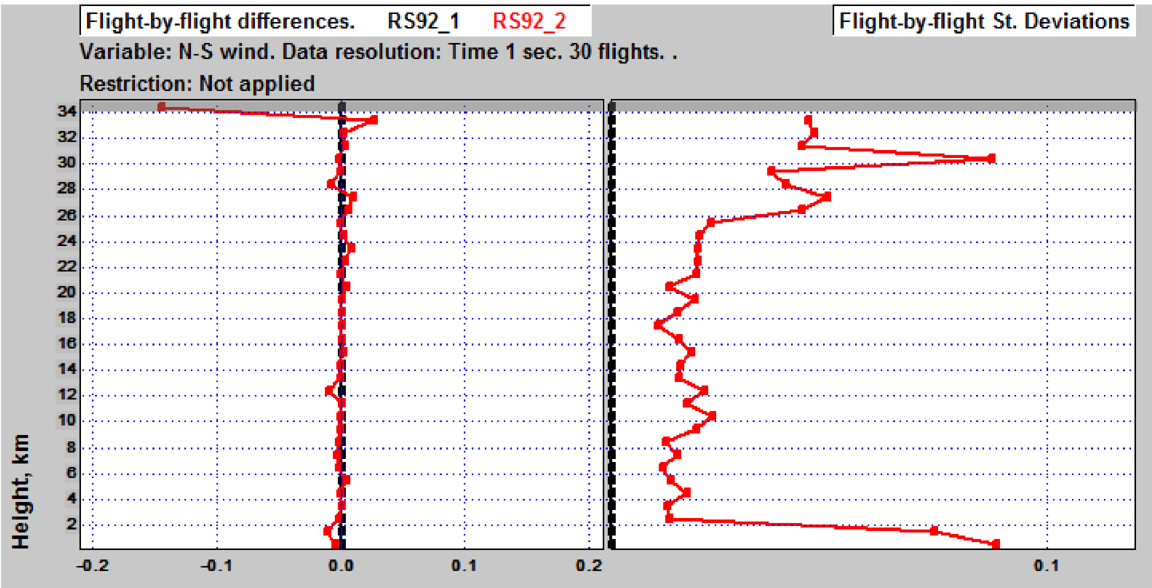

Figure 61 - average RS92_1 vs. RS92_2 flight-by-flight direct differences in N-S winds (left) and standard deviations (right).

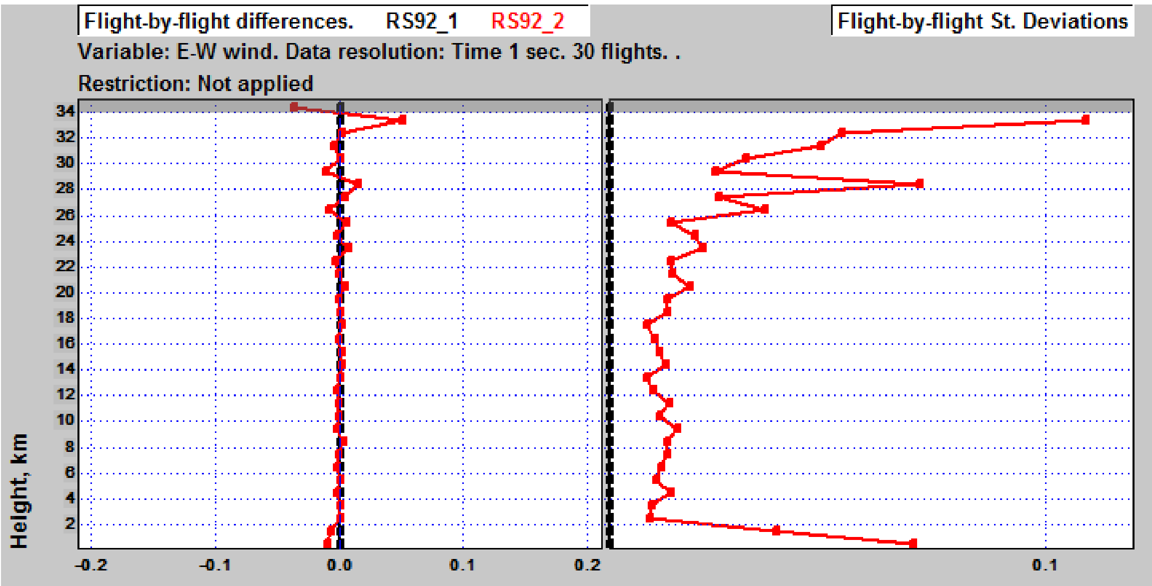

Figure 62 - average RS92_1 vs. RS92_2 flight-by-flight direct differences in E-W winds (left) and standard deviations (right).

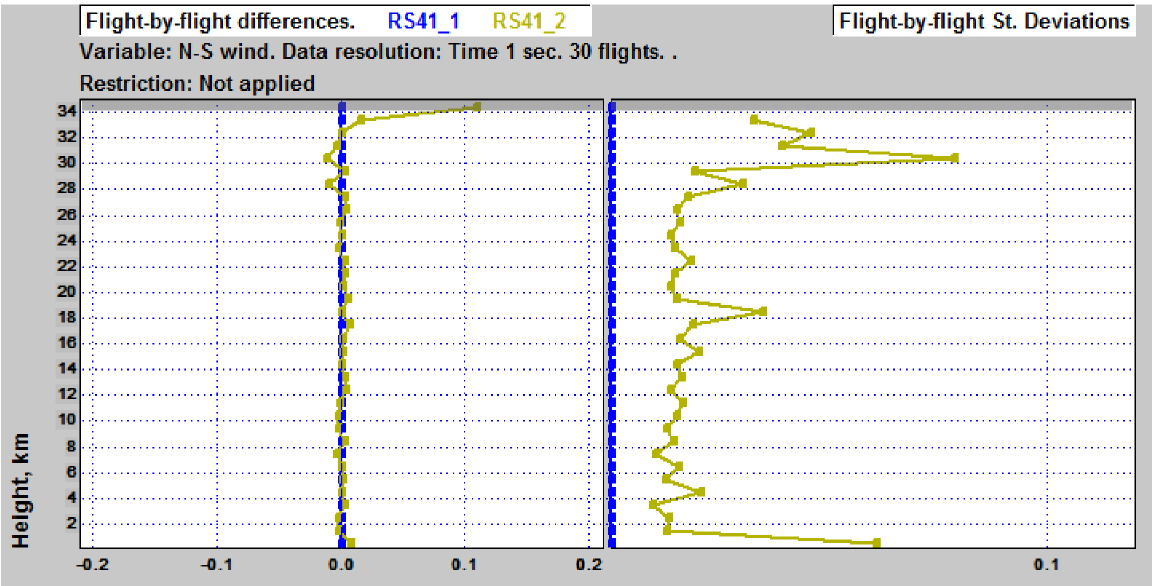

Figure 63 - average RS41_1 vs. RS41_2 flight-by-flight direct differences in N-S winds (left) and standard deviations (right).

The standard deviation of differences between RS92 and RS41 radiosondes is very similar (around 1 cm/s) up to around 26 km, and then the difference between RS92 radiosondes becomes more variable. This may be due to the same effect that leads to the increase in the standard deviation of the height flight-by-flight difference standard deviations of the RS92, which are generally greater than those of the RS41.

Note that the direct difference 2σ lines are not present in these precision plots due to the way that WSTAT handles changes in direction that cross the 0^{o}-360^{o} boundary. This lead to erroneously large standard deviation values when using direct differences rather than flight-by-flight differences.

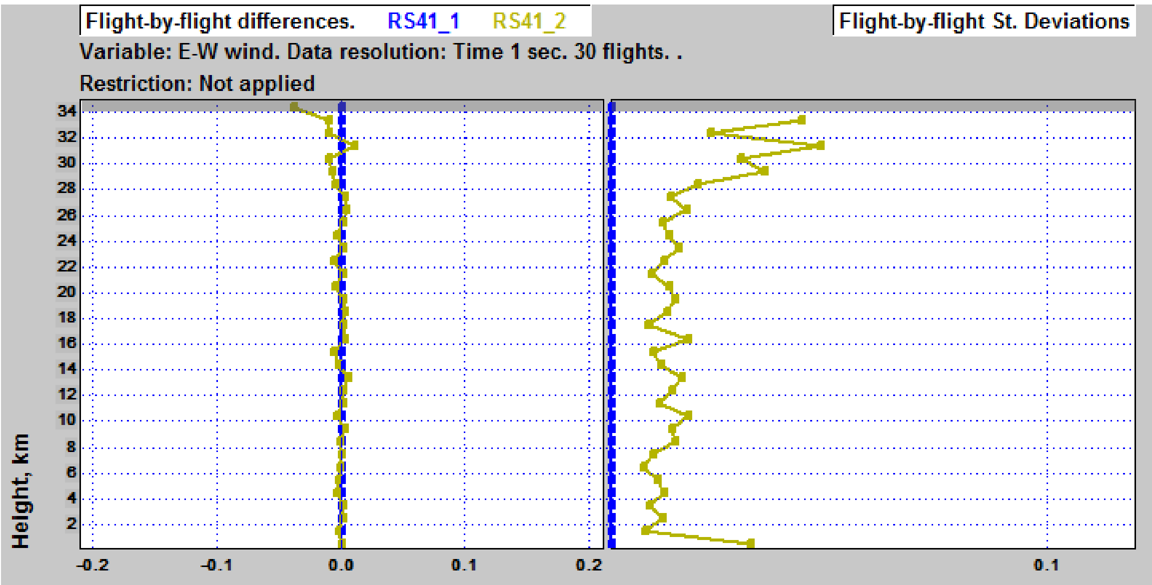

Figure 64 - average RS41_1 vs. RS41_2 flight-by-flight direct differences in E-W winds (left) and standard deviations (right).

Conclusions

The accuracy of RS92 and RS41 wind component measurements are based on the same GPS signals and similar processing, so the differences are minimal. However, the RS41 does indicate a slight improvement in precision in both wind components. This difference is unlikely to have an operational or climatic impact.

Comparison of simultaneous height measurements

RS92 vs. RS41

Figure 65 shows the averaged flight-by-flight differences between the height measurements of the radiosondes relative to the RS92_1. It is apparent that the RS41 radiosondes show a small positive consistent difference in height of less than < 1.0m at most heights, perhaps more exaggerated in higher altitudes. This possible bias is relatively small compared with the systematic biases observed between sondes from different manufacturers in the *WMO Intercomparison of high quality radiosonde systems, Yangjiang, China, 2010*.

Standard deviations of the average flight-by-flight simultaneous differences between the RS41_1 and 2 and RS92_1 are < ±2.5 m at most altitudes.

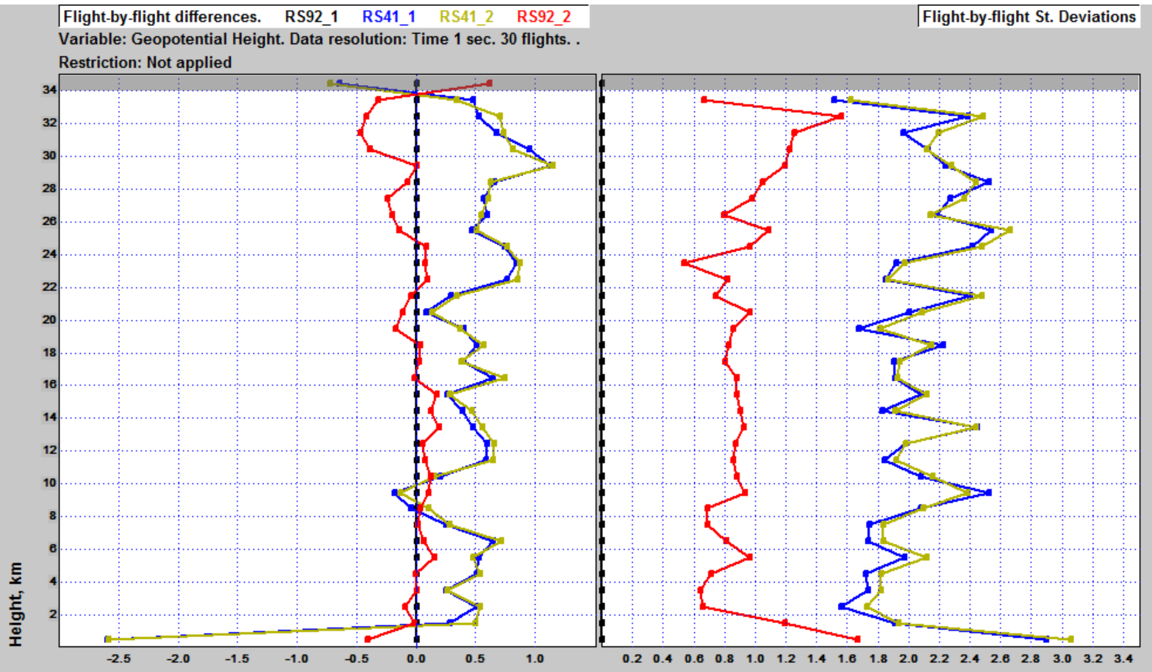

Figure 65 - Height comparison average RS92_1 vs. RS92_2 and RS41 flight-by-flight differences (left) and flight-by-flight standard deviations vs. RS92_1 dataset (right).

Precision

It can be seen from Figure 65 that the differences between the RS41 radiosondes were quite small, as the differences of each RS41 from the RS92_1 were consistently very similar. Figure 67 shows that the average flight-by-flight difference between the RS41 radiosondes was approximately 10 cm. This difference is typically less than the difference between the RS92 radiosondes (Figure 66), particularly at higher altitudes.

For the RS92 radiosondes, the standard deviation of differences was approximately ±0.6 – 1.4 m, compared with values of approximately ±0.4 – 0.8 m for the RS41 radiosondes. The consistency of the RS92 apparently decreases with increasing altitude. The smaller differences and standard deviations between the RS41 compared with the RS92 indicate that the RS41 height data is more precise.

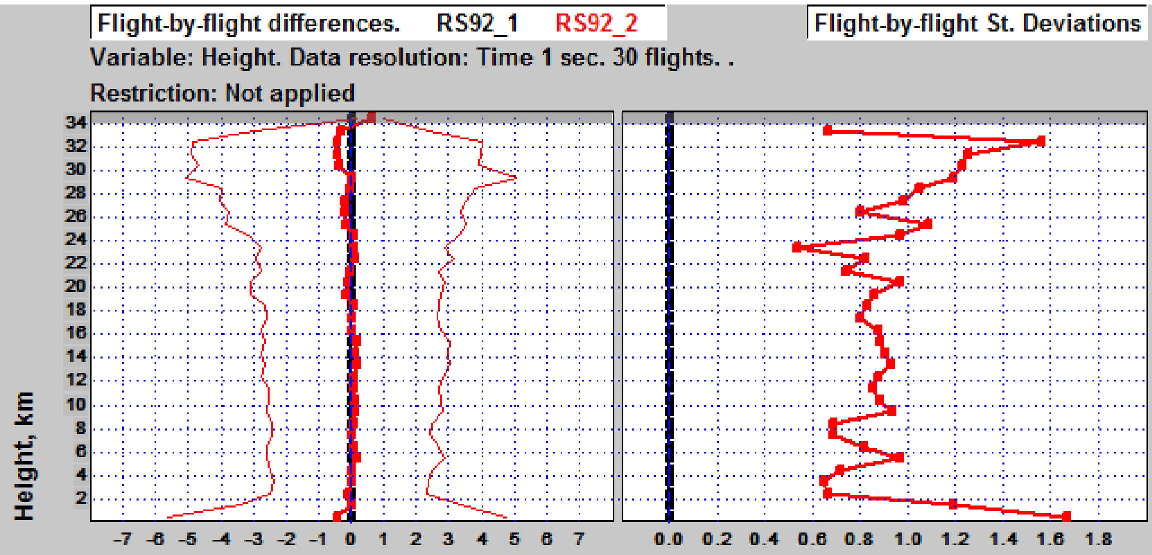

Figure 66 - Height comparison average RS92_1 vs. RS92_2 flight-by-flight differences (left) including 2σ direct difference bands and flight-by-flight standard deviations (right).

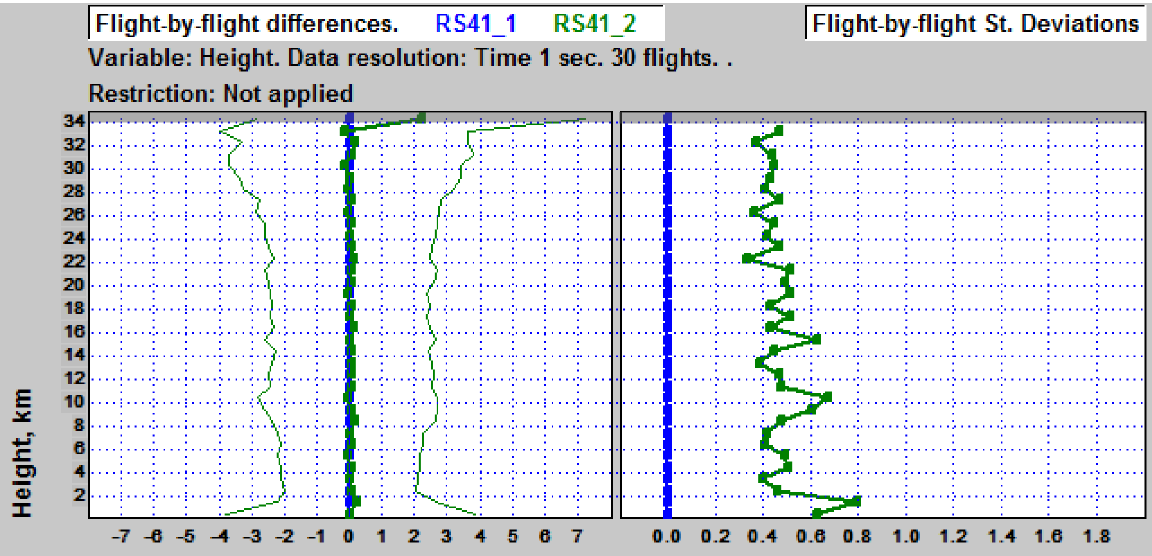

Figure 67 - Height comparison average RS41_1 vs. RS41_2 flight-by-flight differences (left) including 2σ direct difference bands and flight-by-flight standard deviations (right).

Conclusion

Developments in the approach to measuring the height of a radiosonde using GPS appear to have lead to an improvement in the precision of the RS41 measurements relative to the RS92.

- The standard deviations of RS92_1 vs. RS92_2 altitude differences were < ±1.8m throughout the trial when measured in 1 km bands.
- The standard deviations of RS41_1 vs. RS41_2 altitude differences were < ±0.8m throughout the trial when measured in 1 km bands.

Comparison of GPS derived height with pressure sensor derived height

As many users still use the integrated pressure sensor pressure of the RS92 to derive height rather than using GPS, height derived from GPS for both RS92 sondes and RS41 radiosondes was compared against RS92 data with heights derived from its pressure sensor. The same RS92 radiosonde was used for both sets of RS92 results, but the data was simply reprocessed using Vaisala's DigiCORA software to use either the pressure sensor or GPS sensor to derive height.

In the following analysis, RS92_1, RS92_2, RS41_1 and RS41_2 are all using GPS derived height as in the remainder of this report. RS92_1P and RS92_2P use heights derived from their pressure sensors.

The datasets for day and night were not separated, as there is not a notable difference between day and night for either measurement method. As pressure derived heights are rather variable, those flights which burst early at around 26 km were omitted (flights 9, 15, 23 and 28) as they created a 'kink' in the dataset at around 26 km which was not representative of the overall performance of the systems. Additionally, the sample sizes above 31 km drop off due to the burst heights of the balloons in the trial, so the results above this are less reliable than those between 0 - 31 km.

RS92 with pressure derived height vs. RS92 with GPS derived height

Figure 68 shows the flight-by-flight differences in height measured by the RS92_1, RS92_2 and RS92_2P against the RS92_1P as a reference. This demonstrates the results that another user might see if they were to switch between using pressure sensor derived heights and GPS derived heights for the same radiosonde.

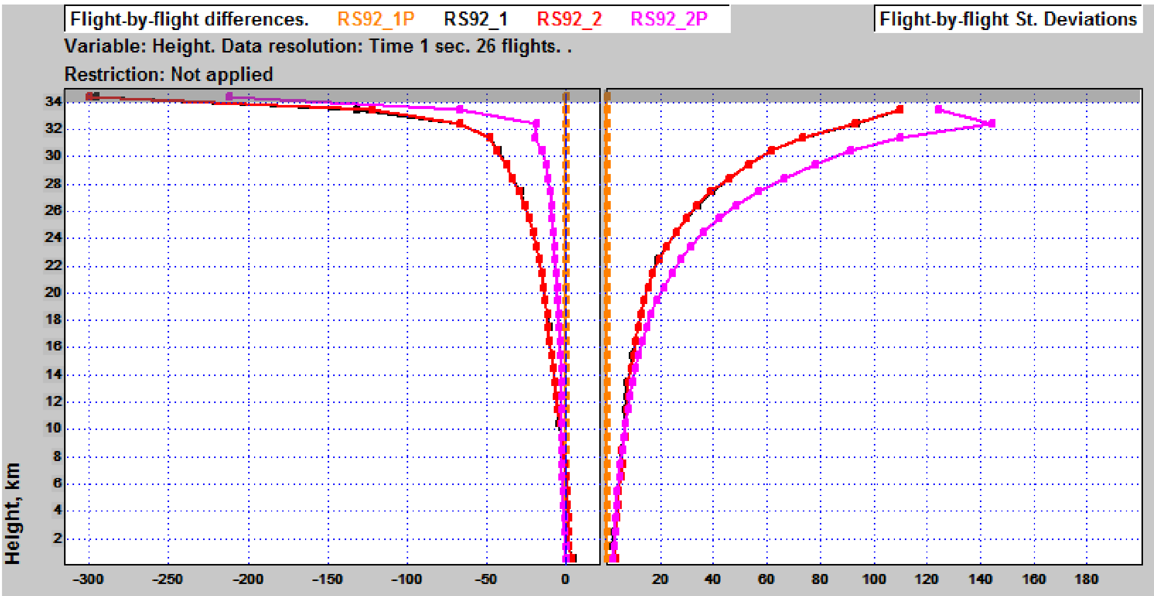

Figure 68 – Height comparison average RS92_1P vs. RS92_2P, RS91_1 and RS92_2 flight-by-flight differences (left) and flight-by-flight standard deviations (right).

There are 2 key outcomes from Figure 68:

1. GPS derived heights differed significantly from pressure derived heights as height increased, displaying a negative height bias in this trial.
    - The average flight-by-flight differences of pressure derived heights were < 10m up to 14 km, increasing to approximately 25m at 33 km when measured in 1 km bands.
    - GPS derived average flight-by-flight height differences were consistently <0.5m throughout the trial

2. Pressure derived heights are less precise than GPS derived heights.
    - The standard deviations of RS92_1P vs. RS92_2P pressure derived altitude differences were ±10m at 14 km increasing to ±90m at 30 km when measured in 1 km bands.
    - The standard deviations of RS92_1 vs. RS92_2 GPS derived altitude differences were ±1.8m throughout the trial when measured in 1 km bands.
    - Compare Figure 65 and Figure 68. Figure 69 shows an example of the improved measurement precision when using GPS derived height.

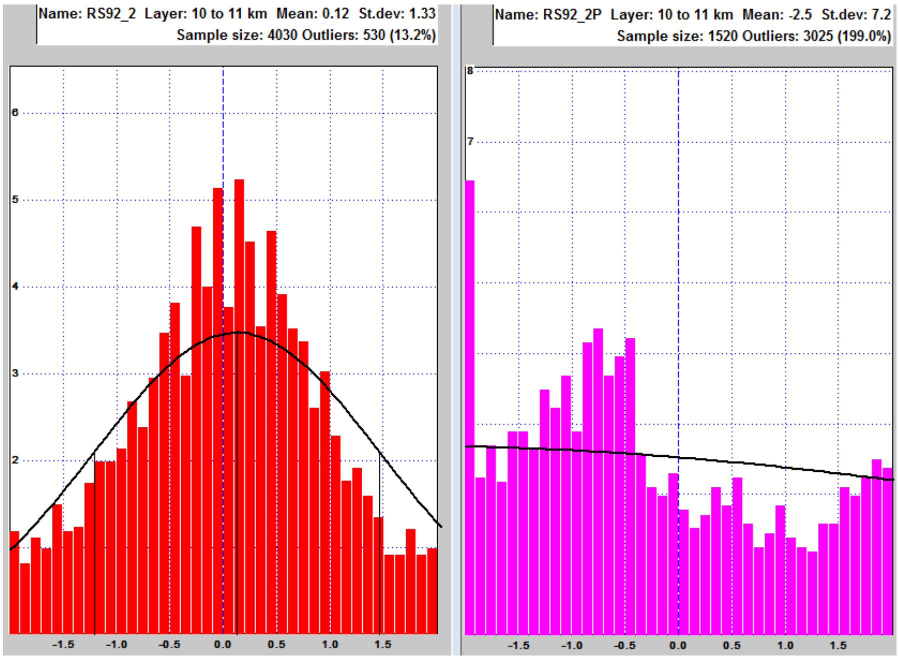

Figure 69 – Histograms of height showing precision of RS92_1 vs. RS92_2 flight-by-flight differences of GPS derived height (left) and RS92_1P vs. RS92_2P flight-by-flight differences of pressure derived height (right) for the 10-11 km level.

The steady increase in difference and standard deviations as height increases is probably due to the increasing effect of uncertainty in the pressure sensor measurements as pressure decreases. The stated uncertainties of the RS92 pressure sensor according to *Vaisala RS92-SGP datasheet* are:

1080 - 100hPa = 1hPa

100 – 3hPa = 0.6hPa

For example, 1 hPa uncertainty at 1000 hPa is equivalent to 0.1% of the total value, but 0.6 hPa at 3 hPa is equivalent to 20% of the total value. As pressure decreases exponentially, this effect becomes very significant as height increases, as is demonstrated in Figure 70. Note that the sudden change at approximately 17000m in Figure 70 is an artefact of the calculation caused by the change in stated pressure uncertainty from 1.0 to 0.6hPa at 100hPa.

The stated vertical uncertainty for the RS92 GPS sensor according to the *Vaisala RS92-SGP datasheet* is 20 m at all heights. This has the opposite effect as that of the pressure sensor uncertainty. For example at 100 m, the uncertainty is equivalent to 20% of the value and by 1000 m it drops to 2%. At 34000 m, it is only equivalent to 0.06% of the value.

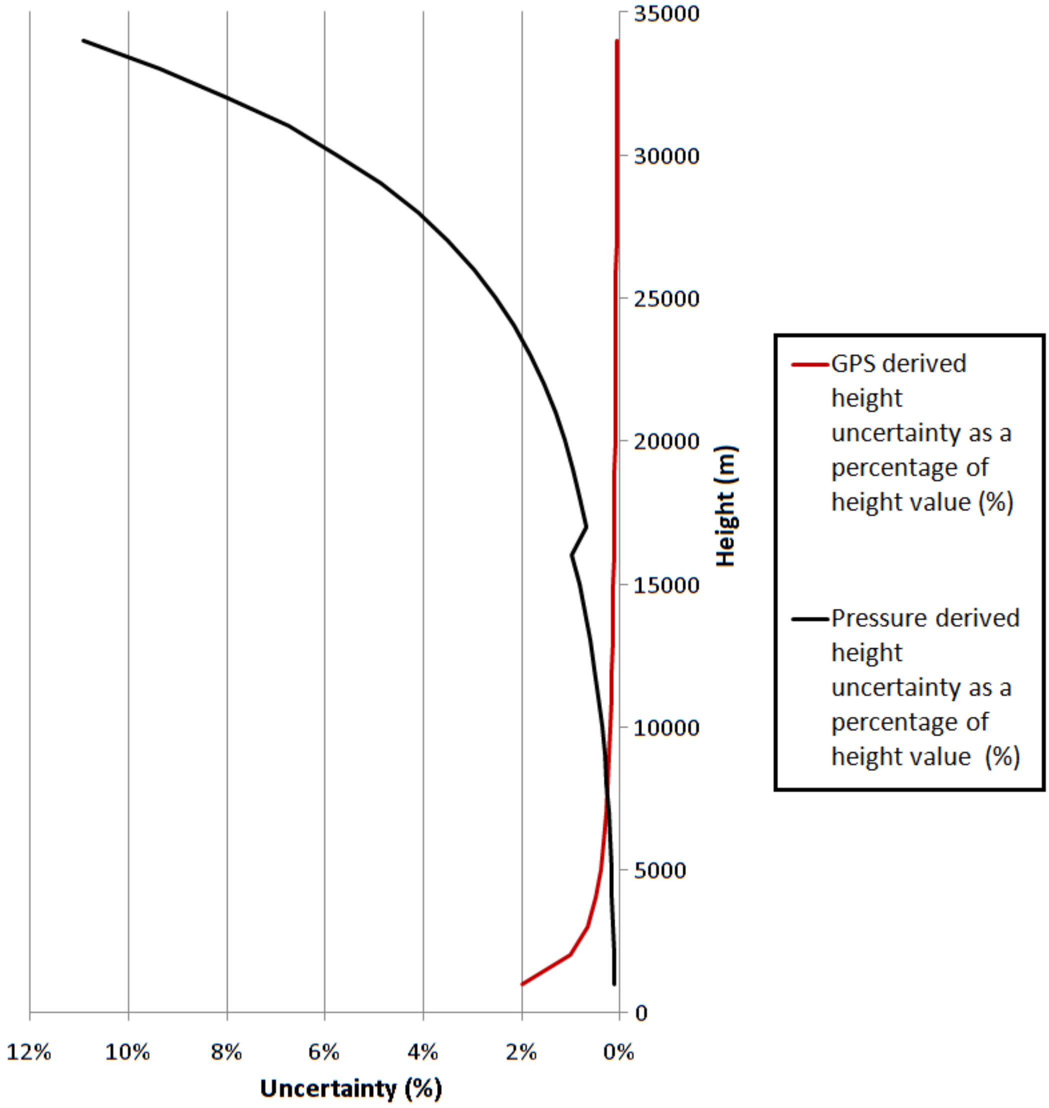

Figure 70 – Graph showing relative RS92 height uncertainty when derived from GPS or pressure with respect to height. Example calculated from flight 31 GPS height and pressure data at 1 km intervals, and Vaisala stated uncertainty values.

For comparison, the differences seen with GPS derived height are much smaller, with a much greater level of consistency and precision measured across the ascent. The following figures demonstrate the comparative differences including 2σ direct difference bands for each 1 km height group. The axes are the same in Figure 71 and Figure 72 to allow visual comparison of the flight-by-flight differences and standard deviations for the pressure derived and GPS datasets. The RS92 GPS derived height differences with narrower axes can be seen in Figure 85 the previous section.

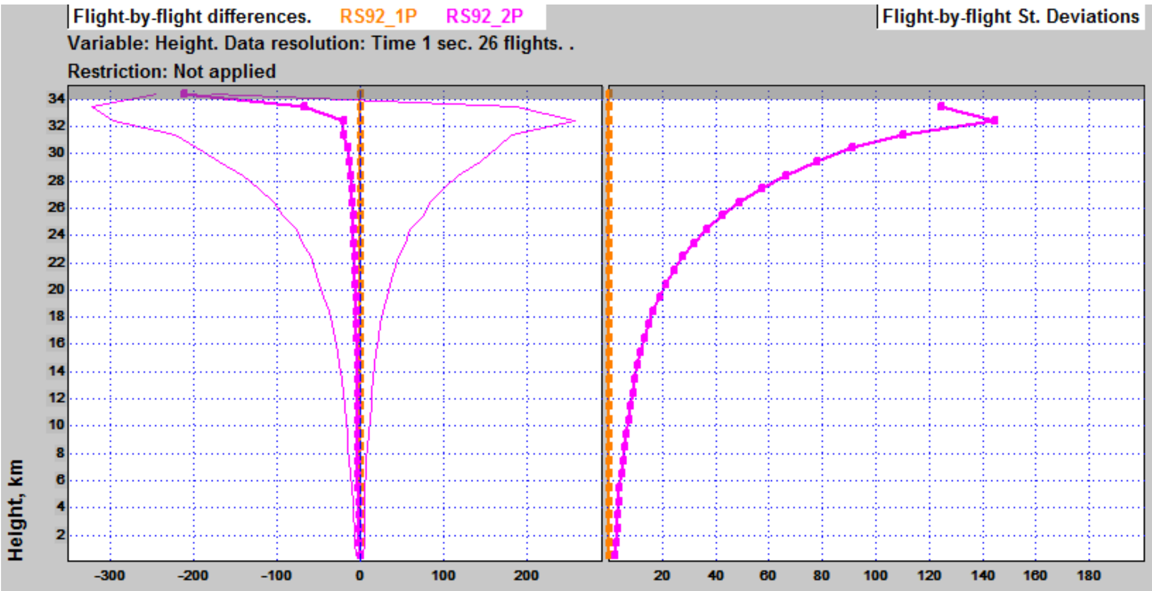

Figure 71 - Height comparison average RS92_1P vs. RS92_2P flight-by-flight differences (left) including 2σ direct difference bands and flight-by-flight standard deviations (right).

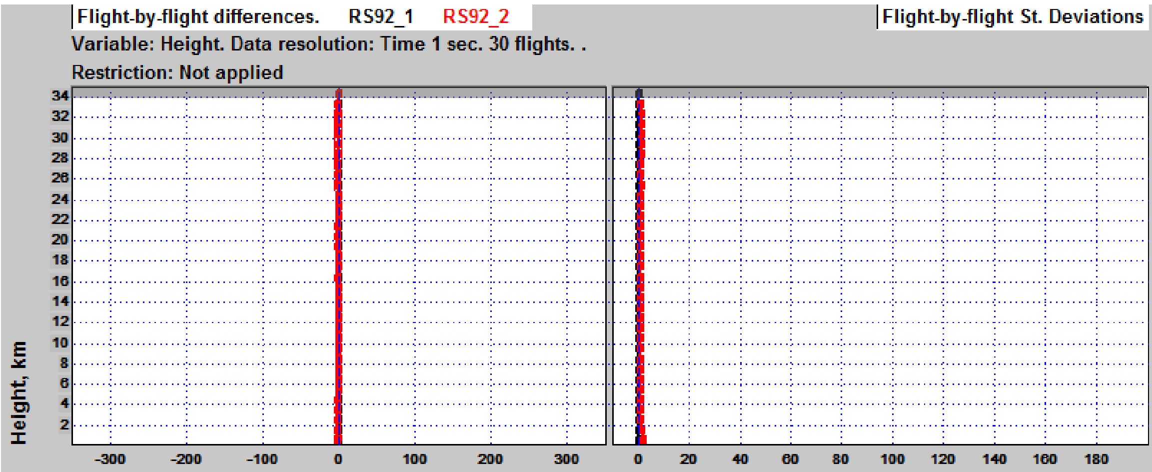

Figure 72 - Height comparison average RS92_1 vs. RS92_2 flight-by-flight differences (left) including 2σ direct difference bands and flight-by-flight standard deviations (right). Plotted on the same axes as Figure 71.

RS92 with pressure derived height vs. RS41 with GPS derived height

As discussed in the section focusing on GPS derived height comparisons between the RS92 and RS41 models, the radiosondes demonstrated very similar results. It is no surprise therefore that the RS41 performs in a very similar way to the RS92 when comparing its GPS derived heights to the pressure derived heights of the RS92. Please see Figure 85 in the previous section for relevant differences and standard deviations.

In Figure 73, the RS92_1, RS92_2 and RS41_1 GPS derived heights are generally hidden under the green RS41_2 line, as they are indistinguishable when plotted on the axes necessary to show the pressure results.

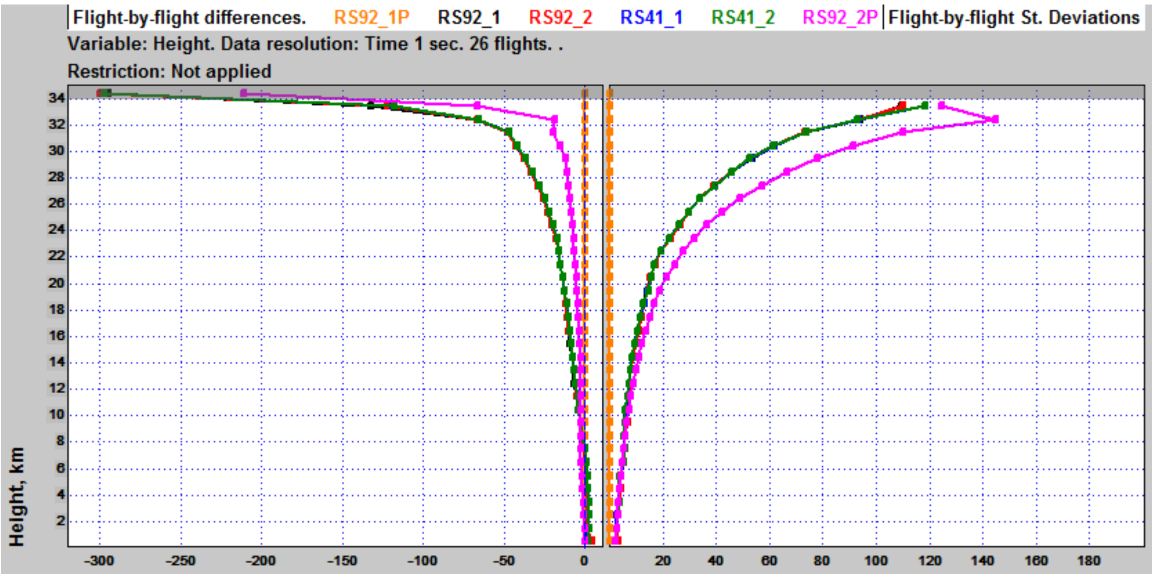

Figure 73 - Height comparison average RS92_1P vs. RS92_2P, RS91_1, RS92_2, RS41_1 and RS41_2 flight-by-flight differences (left) and flight-by-flight standard deviations (right).

Impacts of using pressure derived height

The direct result of the increased uncertainty in pressure sensor derived heights is the impact on the position of features in radiosonde ascents. Figure 74 is an example from flight 14 showing particularly large differences in the altitudes of temperature and velocity measurements, as reported by radiosondes RS92_1P and RS92_2P.

As the radiosondes were mounted to the same rig, their actual difference in height could only be a few centimetres. The pressure derived height differences can be over 100 m towards the top of the ascent, and it is possible to see the differences increase with height during this trial. In the example of flight 14 below, the RS92_1P agreed well with the GPS derived heights, but RS92_2 did not.

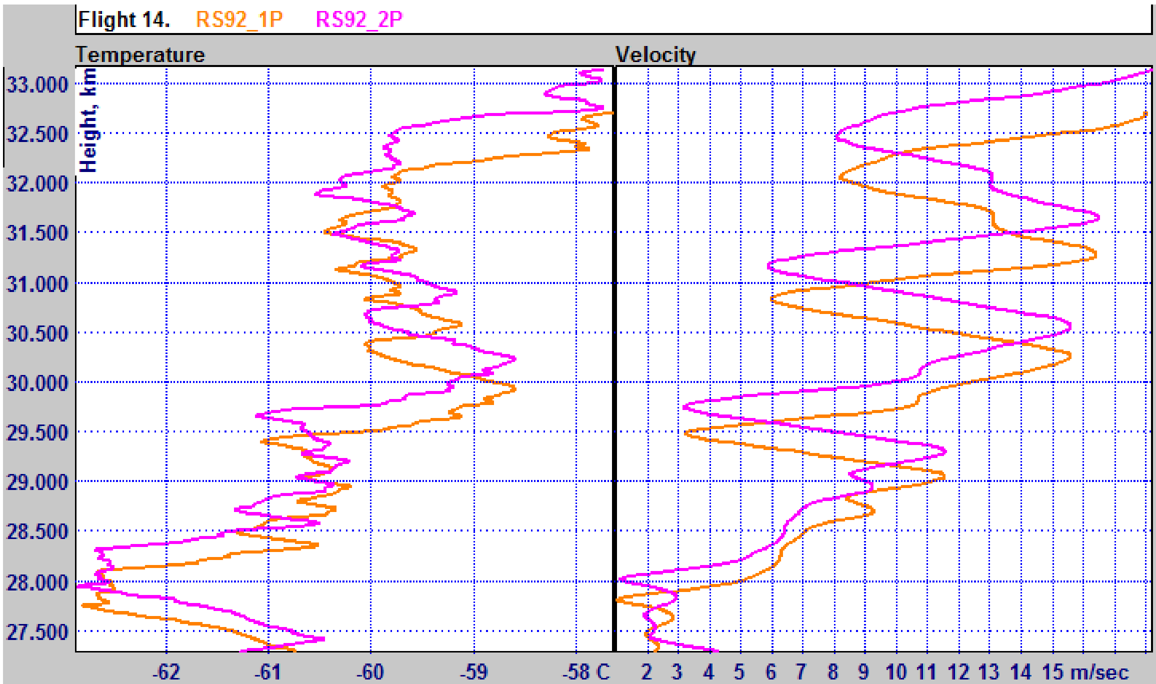

Figure 74 – Detailed section of flight 14 showing the difference in data heights from RS92_1P and RS92_2P when derived from their respective pressure sensors.

In contrast, the GPS derived heights follow each other almost exactly in the same region in Figure 75.

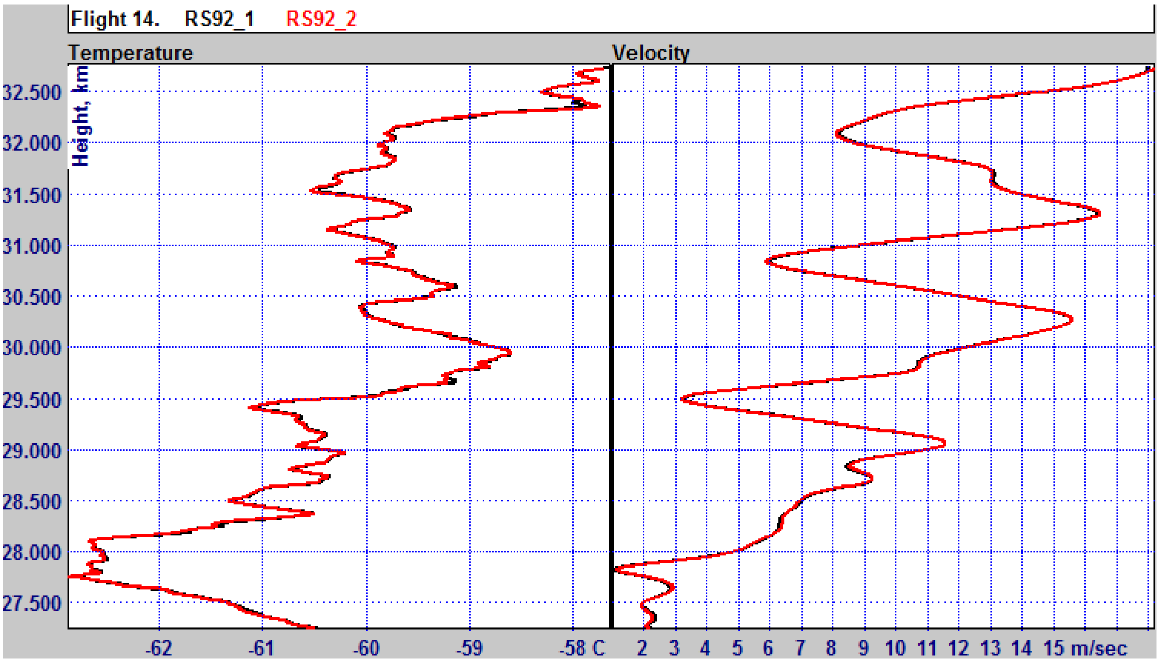

Figure 75 - Detailed section of flight 14 showing the difference in data heights from RS92_1 and RS92_2 when derived from their respective GPS measurements.

Pressure and GPS derived height conclusions

Using pressure to derive height is not as accurate as using GPS to derive height. This was discussed previously in the *WMO intercomparison of high quality radiosondes, Mauritius, 2005*. This is probably because of the increasing effect of relative uncertainties in the sensors and the potential for systematic biases to be introduced during the ground-check of the radiosonde.

Pressure derived heights are also less precise, as there is much greater variability in the measurements and this effect increases with height. The indicated values of >100m difference above approximately 31 km between two sondes on the same rig, is demonstrated in Figure 68. The effects that this can have on the radiosonde data altitudes and therefore accuracy are significant. The differences demonstrated are significant, as they indicate that GPS derived heights during this trial were generally lower in altitude than pressure derived heights. They also indicate that this difference increases as altitude increases. This could have climatic effects and should be accounted for.

In general, using GPS derived heights for the RS92 or RS41 will produce very similar results, so the impact of changing from either pressure derived RS92 to GPS derived RS92 or RS41 should be approximately identical. Similarly, changing from GPS derived RS92 to GPS derived RS41 should have no climatic impact on the assigned heights of data points.

Overall, changing from pressure derived heights to GPS derived heights would be beneficial to both data accuracy and precision for all parameters measured by the radiosonde.

In the standard radiosonde TEMP and BUFR encoded messages, pressure is used as the vertical coordinate. If this is taken from an integrated pressure sensor as in the RS92-SGP, then the user would need to switch to using GPS derived heights to gain the benefits discussed above, as pressure would then also be calculated based on GPS derived height.

The impact of switching to GPS derived pressures is outside the scope of this trial. As the variability increases so much with height, it is not possible to state that the negative bias observed during this trial would occur at other sites or over a longer period of observation. Further work would be necessary to investigate the impact of this change on a climatic basis.

Additionally, if GPS derived heights are used, changing from pressure to GPS derived height as the vertical component in radiosonde BUFR messages should also deliver a slight improvement to data accuracy. This is due to the reduced impact of the rounding error when converting from GPS height to pressure, in a similar way to the uncertainty demonstration in Figure 70. Please see Figure 78 in annex 1 for a demonstration of this effect.

Overall conclusions

Radiosonde systems

The RS92 and RS41 radiosondes were both very reliable throughout the trial period in Camborne. The quantity of missing data was very low and the typical duration of missing data was no longer than 2 seconds at any point throughout the ascent from both radiosonde models. There were no instances of in-flight telemetry failures or sensor failures. All 4 sets of hardware and software were very reliable with no problems occurring.

Overall temperature and humidity

The RS41 demonstrates several differences and improvements in the observation of temperature and humidity relative to the RS92. It is not possible to determine which radiosonde provided more accurate measurements due to the lack of a reference system, but the reduction in the impact of known temperature and humidity phenomena should improve the data quality of the RS41 relative to the RS92, and may improve accuracy as a result.

The RS41 is not at risk of a systematic bias being introduced by the application of incorrect ground check calibrations to the humidity or temperature measurements, which is possible with the RS92 using the GC25 ground check. This should improve the overall accuracy of temperature and humidity measurements operationally. The RS41 temperature and humidity sensors are still tested for faults before launch in the RI41 ground check. Additionally, the RS41 humidity sensor is reconditioned using its integrated heating element. This also generates a 0% humidity reference point which the sensor is correct to before launch. The consistency of RS41 measurements without the application of ground check corrections against independent references gives confidence in the factory or internal calibrations during this trial.

Temperature

The temperature observations of the RS41 are more precise and less susceptible to the problems caused by moisture contamination when exiting cloud than the RS92. No consistent temperature differences were observed between the RS41 and RS92 when measured over 10^{o}C bands.

- During this trial the average flight-by-flight differences of RS41_1 and RS41_2 temperatures relative to RS92_1 were within ±0.1^{o}C at night and ±0.2^{o}C during the day to 1 standard deviation when measured in 10^{o}C bands.

The precision of the RS92 and RS41 temperature sensors can be estimated based on the standard deviations of average flight-by-flight differences between the radiosonde pairs of each type:

- The standard deviation of RS92_1 vs. RS92_2 temperatures were within ±0.3°C at night and ±0.2°C during the day to 1 standard deviation when measured in 1 km bands.
  - Note: the RS92 night-time standard deviations are smaller (within ±0.1°C) than the daytime standard deviations except in the lower troposphere where moisture contamination caused a localised increase in standard deviations to over ±0.2°C.
- The standard deviation of RS41_1 vs. RS41_2 temperatures were within ±0.1°C at night and ±0.2°C during the day to 1 standard deviation when measured in 1 km bands.

Moisture contamination events still cause a slight degradation of RS41 precision (increase in standard deviations from approximately ±0.01°C to ±0.05°C at night), but the impact is much smaller in magnitude that on RS92 precision (from approximately ±0.05°C to ±0.22°C at night). In the wet-bulbing situations observed during this trial, the RS41 radiosondes demonstrated a significant improvement in performance relative to the RS92.

Changing from the RS92 to the RS41 operationally may improve the measurement accuracy of temperature and will provide more precise temperature measurements, reducing total temperature measurement uncertainty.

Humidity

The humidity measurements of the RS41 are more precise and should be less prone to moisture contamination than the RS92, especially in the upper troposphere and stratosphere. The RS92 applies solar radiation corrections to humidity based on calculated solar angle, which is a potential source of error. The RS41 calculates humidity based on the temperature measured by the separate temperature sensor integrated into its humidity sensor. This removes the need for the application of a solar radiation correction, which eliminates that potential source of error.

Some slight consistent differences were observed between the RS41 and RS92 of approximately 1-2%. The key differences were the greater humidity measured by the RS92 after the tropopause relative to the RS41 and the greater humidity measured by the RS41 below the tropopause. The impact of these differences would be small operationally, but may be measureable in the climate record of a station.

During this trial:

- The average flight-by-flight differences for of RS41_1 and RS41_2 humidities relative to RS92_1 were within ±1.0% at night and ±2.6% during the day to 1 standard deviation when measured in 10°C bands.

The precision of the RS92 and RS41 humidity sensors can be estimated based on the standard deviations of average flight-by-flight differences between the radiosonde pairs of each type.

- The standard deviation of RS92_1 vs. RS92_2 humidities were within ±0.7% at night and ±1.3% during the day when measured in 10^{o}C bands.
- The standard deviation of RS41_1 vs. RS41_2 humidities were within ±0.3% at night and ±0.6% during the day to 1 standard deviation when measured in 10^{o}C bands.

GPS derived wind and altitude

The GPS derived wind components calculated by the RS41 were consistent with the performance of the RS92 and showed very similar precision.

During this trial:

- The average flight-by-flight differences of RS41_1 and RS41_2 wind components relative to RS92_1 were within ±0.2m/s at all heights to 1 standard deviation throughout the trial when measured in 1 km bands.

The precision of the RS92 and RS41 wind components can be estimated based on the standard deviations of average flight-by-flight differences between the radiosonde pairs of each type.

- The standard deviations of RS92_1 vs. RS92_2 wind components were within ±0.2m/s throughout the trial when measured in 1 km bands.
- The standard deviations of RS41_1 vs. RS41_2 wind components were within ±0.1m/s throughout the trial when measured in 1 km bands.

The GPS derived altitudes observed by the RS41 were consistent with the performance of the RS92, but demonstrated greater precision.

- The standard deviations of RS92_1 vs. RS92_2 altitude differences were < ±1.8m throughout the trial when measured in 1 km bands.
- The standard deviations of RS41_1 vs. RS41_2 altitude differences were < ±0.8m throughout the trial when measured in 1 km bands.

Changing from the RS92 to the RS41 operationally should not result in any operational difference for GPS wind or altitude.

Pressure derived altitude vs. GPS derived altitude

Relative to pressure derived altitude observed by the RS92, GPS derived altitude from both the RS92 and RS41 demonstrate significantly improved precision and potentially greater accuracy.

The precision of pressure derived altitude decreased very significantly with height during this trial. The precision of the RS92_1P and RS92_2P altitudes can be estimated based on the standard deviations of average flight-by-flight differences between the radiosonde pairs of each type.

Note: RS92_1P and RS92_2P were the same radiosondes as RS92_1 and RS92_2, but the data was rerun using DigiCORA software to use pressure rather than GPS derived altitudes.

During this trial:

- The average flight-by-flight altitude differences of RS92_1P and RS92_2P were within 10m up to 14 km, increasing to 25m up to 33 km when measured in 1 km bands.
- The standard deviations of RS92_1P vs. RS92_2P altitude differences were ±10m at 14 km increasing to ±90m at 30 km when measured in 1 km bands.
- The average flight-by-flight differences between RS92_1P and the RS92 and RS41 radiosondes using GPS derived altitudes were within 10m up to 14 km, increasing to 50m up to 33 km when measured in 1 km bands.

Using GPS rather than pressure derived altitudes should improve the precision and possibly the accuracy of temperature, humidity and wind measurements. This is due to the increased uncertainty in pressure derived altitude relative to GPS derived altitude.

If GPS derived altitude is selected in the Vaisala software, then pressure is calculated from GPS derived altitude, rather than measured by the pressure sensor. Extra care must be taken to ensure that the ground data is correct when using GPS altitude derived pressure.

Overall

During this trial, the RS92 and RS41 both offered very similar levels of performance across all parameters, with the RS41 demonstrating improved measurement precision for temperature, humidity and height. The RS41 demonstrated performance improvements for temperature and humidity which should improve measurement accuracy.

The most significant performance improvement seen during this trial was the reduction in the impact of 'wet-bulb' moisture contamination on the temperature measurements of the RS41 relative to the RS92.

References

Nash, J., R. Smout, T. Oakley, B. Pathack and S. Kurnosenko (2006), WMO Intercomparison of High Quality Radiosonde Systems, Vacoas, Mauritius, 2-25 February 2005, Final Report. *World Meteorological Organization*

Nash, J., T. Oakley, H. Vömel, and W. Li (2011), WMO Intercomparison of High Quality Radiosonde Systems, Yangjiang, China, 12 July–3 August 2010. *World Meteorological Organization, Instruments and Observing methods, report No. 107*

Vaisala (2013), Vaisala Radiosonde RS41-SG datasheet in English, B211321EN-A, *Vaisala*, available on (2014/01/31) http://www.vaisala.com/Vaisala%20Documents/Brochures%20and%20Datasheets/RS41_Datasheet.pdf

Vaisala (2013), Vaisala Radiosonde RS92-SGP datasheet in English, B210358EN-F, *Vaisala*, available on (2014/01/31) http://www.vaisala.com/Vaisala%20Documents/Brochures%20and%20Datasheets/RS92SGP-Datasheet-B210358EN-F-LOW.pdf

World Meteorological Organisation (2012), Guide to Meteorological Instruments and Methods of Observation, WMO-No. 8, 2008 edition updated in 2010. *World Meteorological Organization, WMO-No. 8*

Annex 1 – Additional Information

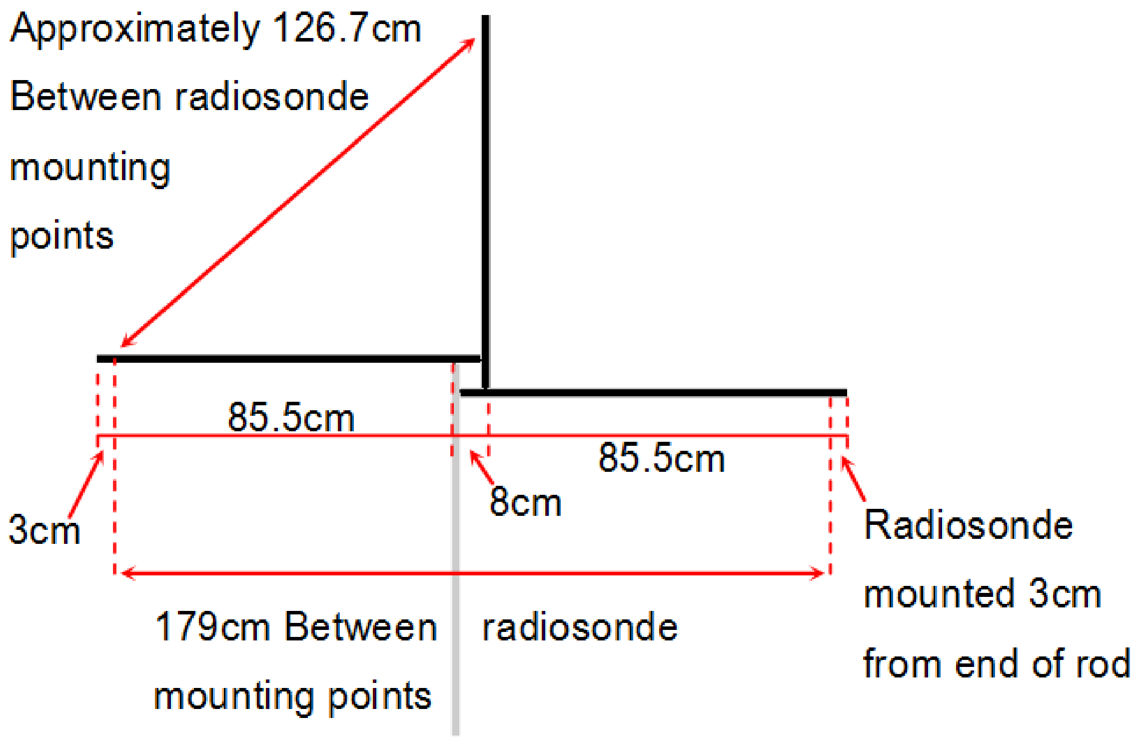

Figure 76 - Details of rig design with measurements.

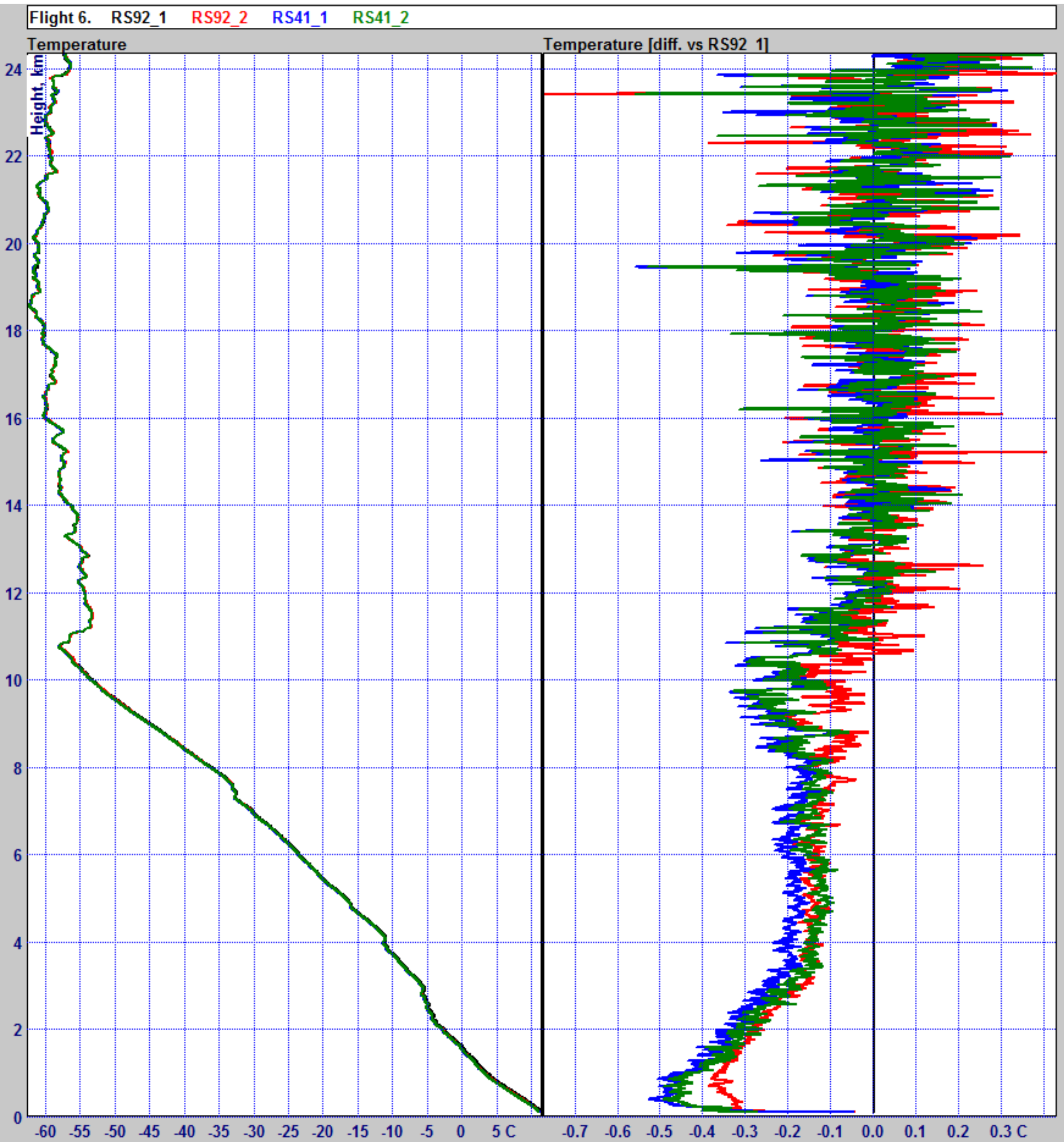

Figure 77 - Flight 6 temperature profile showing the measured temperature profiles (left) and the differences of the radiosonde temperature profiles relative to the RS92_1 sonde (right).

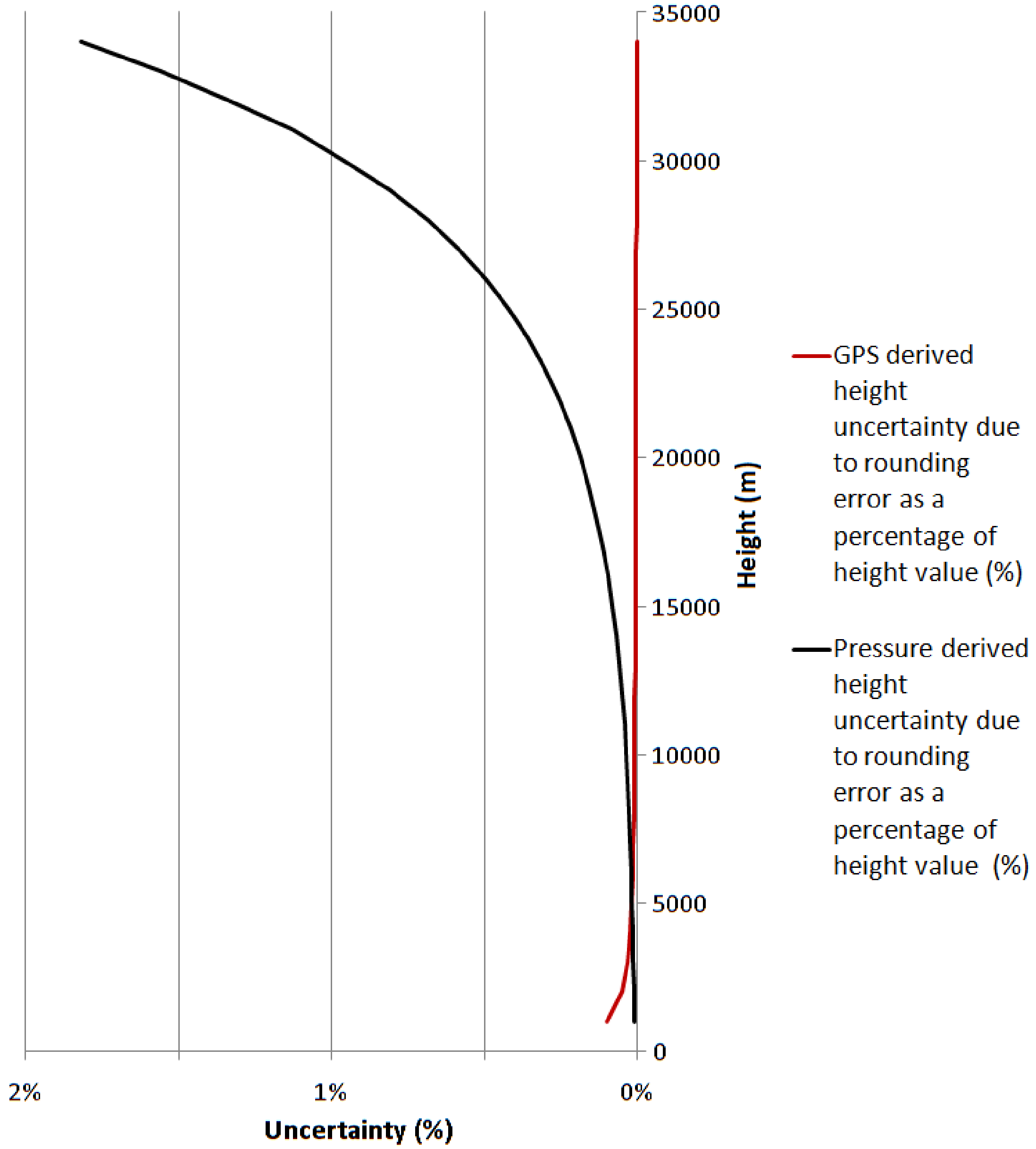

Figure 78 - Graph showing impact of rounding errors when reporting RS92 altitude when derived from GPS or pressure with respect to height. Rounding errors taken from BUFR encoding of 1m and 0.1 hPa respectively. Example calculated from flight 31 GPS height and pressure data at 1 km intervals.

Annex 2 – Metadata table of phenomena

Flight number	Series	Date	Temperature Wet bulb effect observed relative to other sensors in trial				Temperature Slower temperature response observed relative to other sensors in trial				Relative Humidity Upper tropospheric wet bias relative to RS41s		Relative Humidity Consistent stratospheric humidity difference >0.1%		Relative Humidity Slower humidity response observed relative to other sensors in trial			
			RS92_1	RS92_2	RS41_1	RS41_2	RS92_1	RS92_2	RS41_1	RS41_2	RS92_1	RS92_2	RS92 1 vs. 2	RS41 1 vs. 2	RS92_1	RS92_2	RS41_1	RS41_2
5	Day	07/11/2013	N	N	N	N	N	N	N	N	Y	Y	N	Y	N	N	N	N
6	Day	07/11/2013	N	N	N	N	N	N	N	N	Y	Y	Y	Y	Y	N	Y	N
7	Night	07/11/2013	N	N	N	N	N	N	N	N	N	N	N	N	N	N	N	N
8	Night	07/11/2013	N	N	N	N	N	N	N	N	N	N	N	Y	N	N	N	N
9	Day	08/11/2013	N	N	N	N	N	N	N	N	N	N	Y	Y	N	N	N	N
10	Day	08/11/2013	N	N	N	N	N	N	N	N	N	N	Y	N	N	N	N	N
11	Night	08/11/2013	N	N	N	N	N	Y	N	N	N	N	Y	Y	Y	N	N	N
12	Day	11/11/2013	N	N	N	N	Y	N	N	N	N	N	N	Y	N	N	N	N
13	Day	11/11/2013	N	N	N	N	N	Y	N	N	N	N	N	Y	N	N	N	N
14	Night	11/11/2013	Y	N	N	N	Y	Y	N	N	N	N	Y	Y	N	N	N	N
15	Night	11/11/2013	N	Y	N	N	Y	Y	Y	N	N	N	Y	Y	N	N	N	N
16	Day	12/11/2013	N	Y	N	N	N	Y	N	N	N	N	Y	N	N	N	N	N
17	Day	12/11/2013	N	N	N	N	N	N	N	N	N	N	Y	Y	N	N	N	N
18	Night	12/11/2013	N	N	N	N	N	N	N	N	N	N	Y	Y	N	N	N	N
19	Day	13/11/2013	N	N	N	N	N	N	N	N	Y	Y	N	N	Y	Y	N	N
20	Day	13/11/2013	Y	Y	N	Y	Y	Y	N	Y	N	N	Y	N	N	N	N	N
21	Night	13/11/2013	N	Y	N	N	N	Y	N	N	N	N	Y	N	Y	Y	N	N
22	Night	13/11/2013	N	Y	N	N	N	Y	N	N	N	N	N	N	Y	Y	N	N
23	Day	14/11/2013	N	N	N	N	N	N	N	N	N	N	Y	Y	N	N	N	N
25	Night	14/11/2013	N	N	N	N	Y	Y	Y	N	Y	Y	Y	Y	Y	Y	N	N
26	Day	15/11/2013	N	N	N	N	Y	Y	Y	N	Y	Y	Y	Y	Y	Y	N	N
27	Day	15/11/2013	N	N	N	N	Y	Y	N	Y	Y	Y	Y	Y	Y	Y	N	N
28	Night	15/11/2013	N	N	N	N	Y	Y	N	N	Y	Y	Y	Y	Y	Y	N	N
29	Day	16/11/2013	N	N	N	N	Y	Y	N	N	Y	Y	N	N	N	N	N	N
30	Day	16/11/2013	N	N	N	N	Y	Y	N	N	N	N	Y	Y	N	N	N	N
31	Day	17/11/2013	N	N	N	N	N	N	N	N	Y	Y	N	N	N	N	N	N
32	Day	18/11/2013	N	N	N	N	N	N	N	N	N	N	Y	Y	N	N	N	N
33	Day	18/11/2013	N	N	N	N	N	N	N	N	N	N	Y	Y	N	N	N	N
34	Day	19/11/2013	N	N	N	N	N	N	N	N	N	N	N	N	N	N	N	N
35	Day	19/11/2013	N	N	N	N	N	N	N	N	N	N	N	N	N	N	N	N
Individual system totals			2	5	0	1	10	14	3	2	9	9	19	19	9	7	1	0
Radiosonde model totals			7		1		24		5		18		19	19	16		1	

Table 2: Metadata showing occurrences of phenomena discussed in report.

Annex 3 – Python generated overlaid standard deviation plots

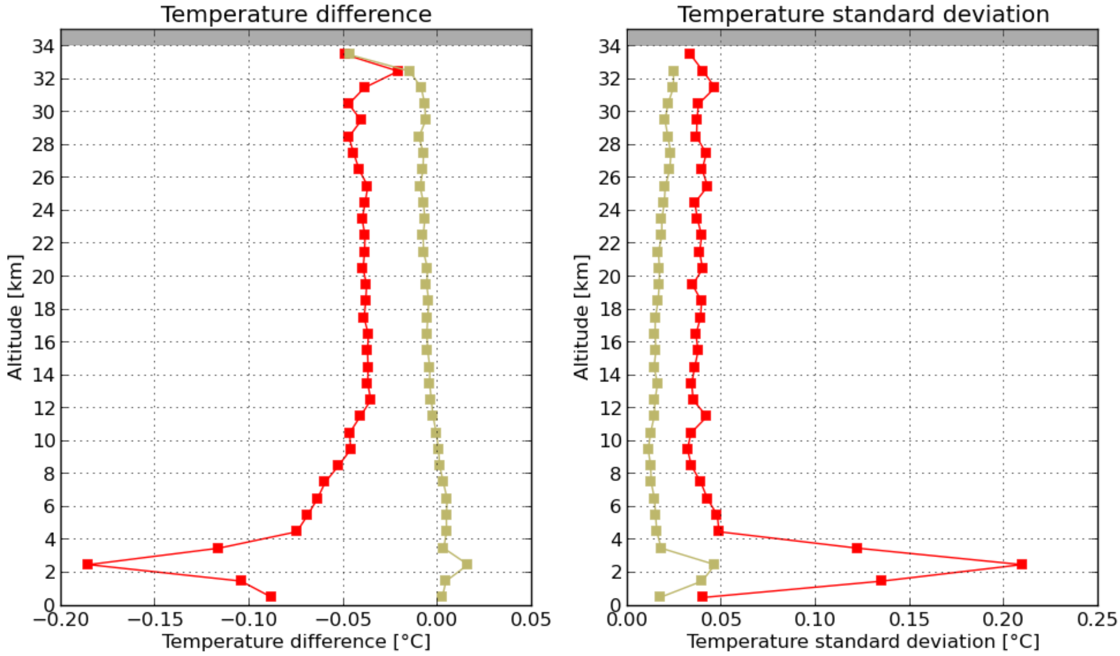

Figure 79 – Overlaid night-time temperature flight-by-flight differences (left) and standard deviations (right) of RS92_1 vs. RS92_2 and RS41_1 vs. RS41_2.

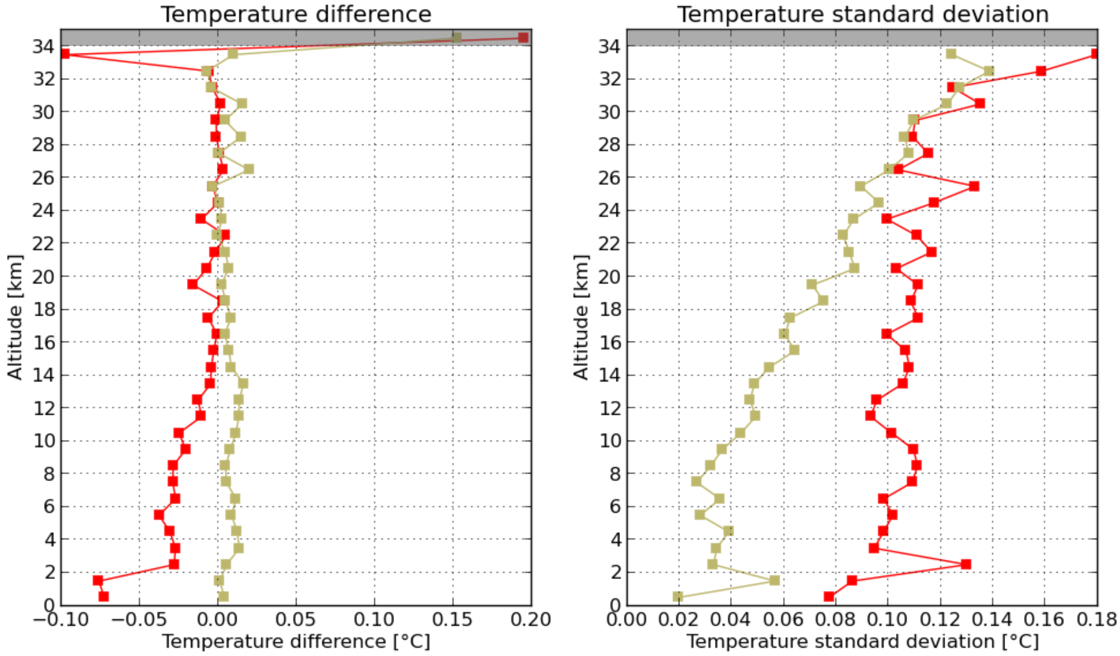

Figure 80 - Overlaid daytime temperature flight-by-flight differences (left) and standard deviations (right) of RS92_1 vs. RS92_2 and RS41_1 vs. RS41_2.

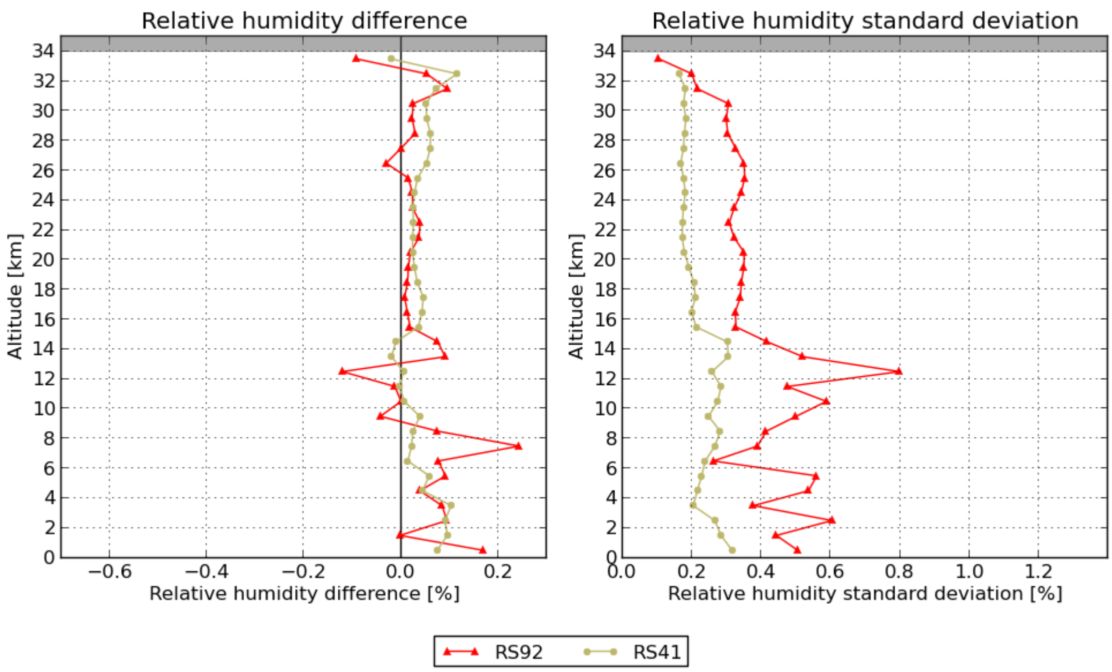

Figure 81 - Overlaid night-time relative humidity flight-by-flight differences (left) and standard deviations (right) of RS92_1 vs. RS92_2 and RS41_1 vs. RS41_2.

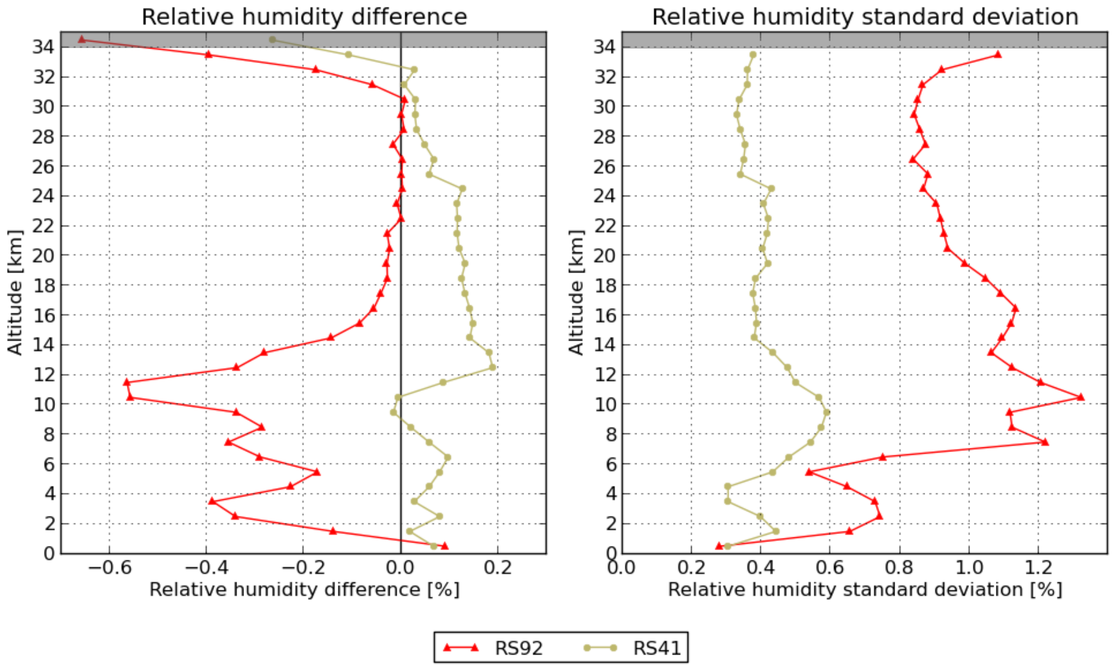

Figure 82 - Overlaid daytime relative humidity flight-by-flight differences (left) and standard deviations (right) of RS92_1 vs. RS92_2 and RS41_1 vs. RS41_2.

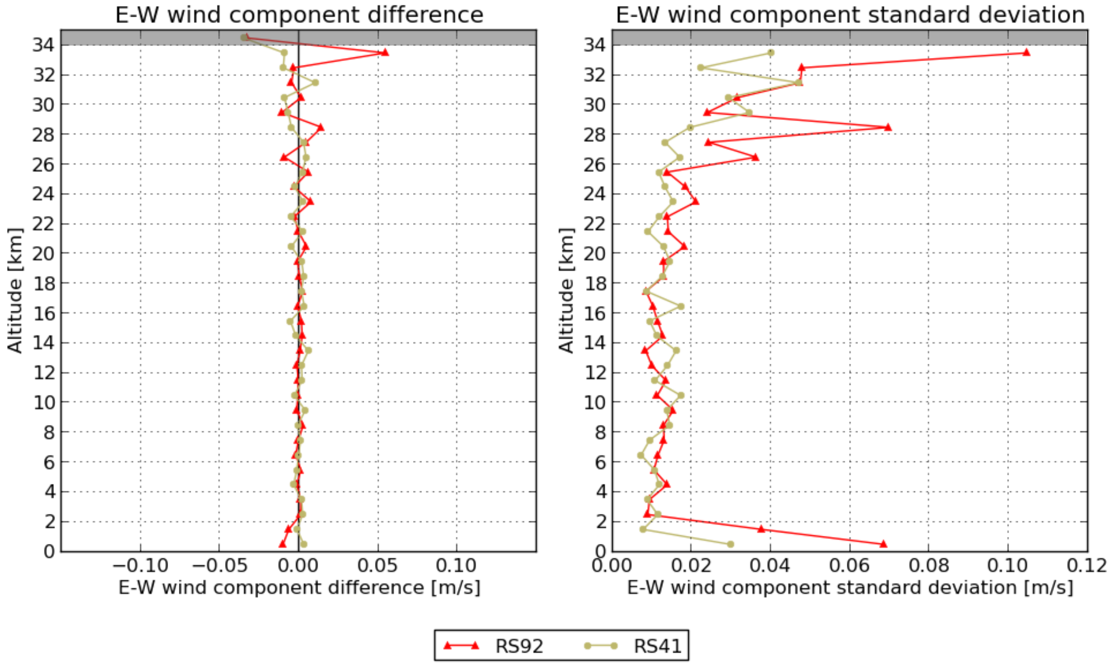

Figure 83 - Overlaid E-W wind component flight-by-flight differences (left) and standard deviations (right) of RS92_1 vs. RS92_2 and RS41_1 vs. RS41_2.

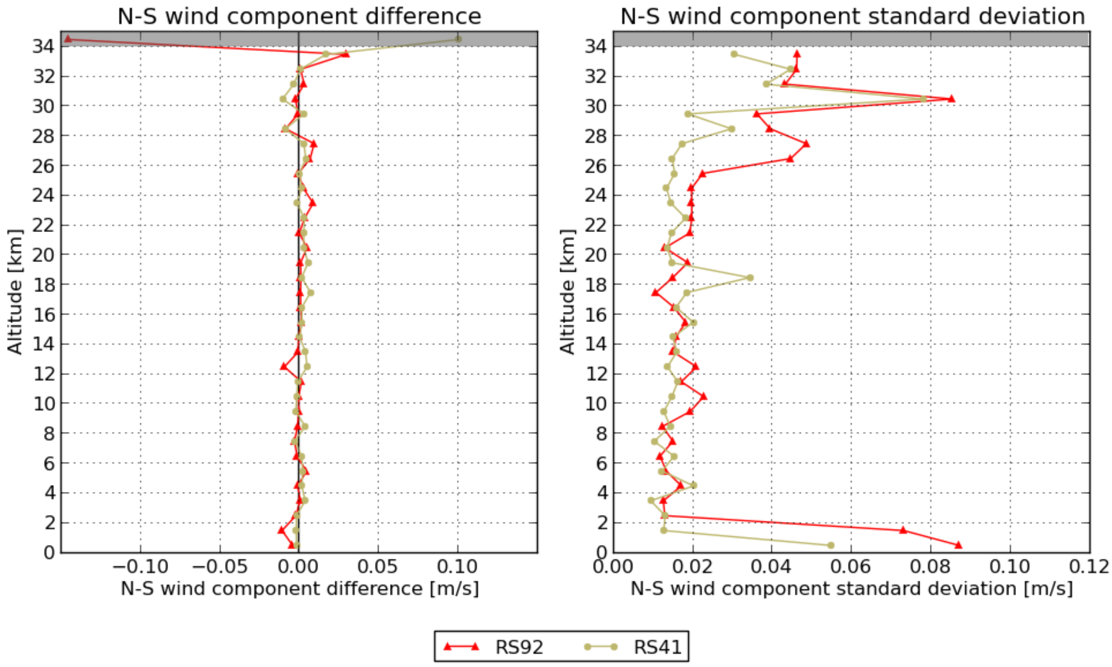

Figure 84 - Overlaid N-S wind component flight-by-flight differences (left) and standard deviations (right) of RS92_1 vs. RS92_2 and RS41_1 vs. RS41_2.

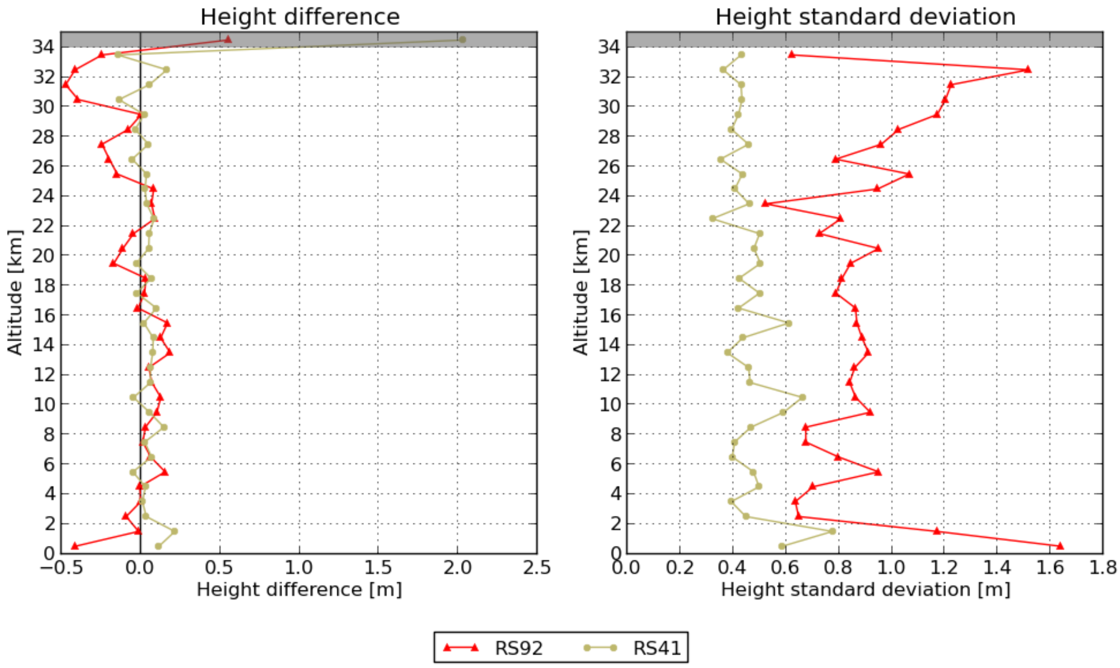

Figure 85 - Overlaid height flight-by-flight differences (left) and standard deviations (right) of RS92_1 vs. RS92_2 and RS41_1 vs. RS41_2.

Annex 4 – Sample sizes used in analysis

Daytime temperature

Height (km)	Radiosonde sample sizes (flights)			
	RS92_1	RS92_2	RS41_1	RS41_2
34-35	2	1	1	1
33-34	8	8	7	7
32-33	14	14	13	13
31-32	17	17	17	17
30-31	18	18	18	18
29-30	18	18	18	18
28-29	18	18	18	18
27-28	18	18	18	18
26-27	19	19	19	19
25-26	19	19	19	19
24-25	20	20	20	20
23-24	20	20	20	20
22-23	20	20	20	20
21-22	20	20	20	20
20-21	20	20	20	20
19-20	20	20	20	20
18-19	20	20	20	20
17-18	20	20	20	20
16-17	20	20	20	20
15-16	20	20	20	20
14-15	20	20	20	20
13-14	20	20	20	20
12-13	20	20	20	20
11-12	20	20	20	20
10-11	20	20	20	20
9-10	20	20	20	20
8-9	20	20	20	20
7-8	20	20	20	20
6-7	20	20	20	20
5-6	20	20	20	20
4-5	20	20	20	20
3-4	20	20	20	20
2-3	20	20	20	20
1-2	20	20	20	20
0-1	20	20	20	20

Night-time temperature

Height (km)	Radiosonde sample sizes (flights)			
	RS92_1	RS92_2	RS41_1	RS41_2
34-35	0	0	0	0
33-34	3	3	1	1
32-33	6	6	6	6
31-32	7	7	7	7
30-31	8	8	8	8
29-30	8	8	8	8
28-29	8	8	8	8
27-28	8	8	8	8
26-27	9	9	8	8
25-26	10	10	10	10
24-25	10	10	10	10
23-24	10	10	10	10
22-23	10	10	10	10
21-22	10	10	10	10
20-21	10	10	10	10
19-20	10	10	10	10
18-19	10	10	10	10
17-18	10	10	10	10
16-17	10	10	10	10
15-16	10	10	10	10
14-15	10	10	10	10
13-14	10	10	10	10
12-13	10	10	10	10
11-12	10	10	10	10
10-11	10	10	10	10
9-10	10	10	10	10
8-9	10	10	10	10
7-8	10	10	10	10
6-7	10	10	10	10
5-6	10	10	10	10
4-5	10	10	10	10
3-4	10	10	10	10
2-3	10	10	10	10
1-2	10	10	10	10
0-1	10	10	10	10

Daytime humidity and temperature vs. Temperature

Height (km)	Radiosonde sample sizes (flights)			
	RS92_1	RS92_2	RS41_1	RS41_2
10 → 20	10	10	10	10
0 → 10	20	20	20	20
-10 → 0	20	20	20	20
-20 → -10	20	20	20	20
-30 → -20	20	20	20	20
-40 → -30	20	20	20	20
-50 → -40	20	20	20	20
-60 → -50	20	20	20	20
-70 → -60	20	20	20	20

Night-time humidity and temperature vs. Temperature

Height (km)	Radiosonde sample sizes (flights)			
	RS92_1	RS92_2	RS41_1	RS41_2
10 → 20	7	7	7	7
0 → 10	10	10	10	10
-10 → 0	10	10	10	10
-20 → -10	10	10	10	10
-30 → -20	10	10	10	10
-40 → -30	10	10	10	10
-50 → -40	10	10	10	10
-60 → -50	10	10	10	10
-70 → -60	10	10	10	10

Pressure and GPS height comparison

Height (km)	Radiosonde sample sizes (flights)					
	RS92_1	RS92_2	RS41_1	RS41_2	RS92_1P	RS92_2P
34-35	1	1	1	1	1	1
33-34	10	9	8	8	10	9
32-33	18	18	18	18	18	18
31-32	24	24	24	24	24	24
30-31	26	26	26	26	26	26
29-30	26	26	26	26	26	26
28-29	26	26	26	26	26	26
27-28	26	26	26	26	26	26
26-27	26	26	26	26	26	26
25-26	26	26	26	26	26	26
24-25	26	26	26	26	26	26
23-24	26	26	26	26	26	26
22-23	26	26	26	26	26	26
21-22	26	26	26	26	26	26
20-21	26	26	26	26	26	26
19-20	26	26	26	26	26	26
18-19	26	26	26	26	26	26
17-18	26	26	26	26	26	26
16-17	26	26	26	26	26	26
15-16	26	26	26	26	26	26
14-15	26	26	26	26	26	26
13-14	26	26	26	26	26	26
12-13	26	26	26	26	26	26
11-12	26	26	26	26	26	26
10-11	26	26	26	26	26	26
9-10	26	26	26	26	26	26
8-9	26	26	26	26	26	26
7-8	26	26	26	26	26	26
6-7	26	26	26	26	26	26
5-6	26	26	26	26	26	26
4-5	26	26	26	26	26	26
3-4	26	26	26	26	26	26
2-3	26	26	26	26	26	26
1-2	26	26	26	26	26	26
0-1	26	26	26	26	26	26

GPS Height comparison

Height (km)	Radiosonde sample sizes (flights)			
	RS92_1	RS92_2	RS41_1	RS41_2
34-35	2	1	1	1
33-34	11	8	8	11
32-33	20	19	19	20
31-32	24	24	24	24
30-31	26	26	26	26
29-30	26	26	26	26
28-29	26	26	26	26
27-28	26	26	26	26
26-27	28	27	27	28
25-26	29	29	29	29
24-25	30	30	30	30
23-24	30	30	30	30
22-23	30	30	30	30
21-22	30	30	30	30
20-21	30	30	30	30
19-20	30	30	30	30
18-19	30	30	30	30
17-18	30	30	30	30
16-17	30	30	30	30
15-16	30	30	30	30
14-15	30	30	30	30
13-14	30	30	30	30
12-13	30	30	30	30
11-12	30	30	30	30
10-11	30	30	30	30
9-10	30	30	30	30
8-9	30	30	30	30
7-8	30	30	30	30
6-7	30	30	30	30
5-6	30	30	30	30
4-5	30	30	30	30
3-4	30	30	30	30
2-3	30	30	30	30
1-2	30	30	30	30
0-1	30	30	30	30

Page left intentionally blank

Met Office
FitzRoy Road, Exeter
Devon EX1 3PB
United Kingdom

Tel: 0870 900 0100
Fax: 0870 900 5050
enquiries@metoffice.gov.uk
www.metoffice.gov.uk